



# **Fiber Reinforcement in Prestressed Concrete Beams**

**Technical Report 0-4819-1**

**Performed in Cooperation with the  
Texas Department of Transportation  
and the Federal Highway Administration  
Project 0-4819**

**By**

**Hemant B. Dhonde  
Research Assistant**

**Y.L. Mo  
Professor**

**and**

**Thomas T.C. Hsu  
Moore's Professor**

**Department of Civil & Environmental Engineering  
University of Houston  
Houston, Texas**

**December 2005**

1. Report No. FHWA/TX-06/ 0-4819-1		2. Government Accession No.		3. Recipient's Catalog No.	
4. Title and Subtitle  Fiber Reinforcement in Prestressed Concrete Beams				5. Report Date December, 2005	
				6. Performing Organization Code	
7. Author(s) Hemant B. Dhonde, Y.L. Mo and Thomas T. C. Hsu				8. Performing Organization Report No. 0-4819-1	
9. Performing Organization Name and Address Department of Civil & Environmental Engineering Cullen College of Engineering University of Houston 4800 Calhoun Road Houston, TX 77204-4003				10. Work Unit No. (TRAIS)	
				11. Contract or Grant No. 0-4819	
12. Sponsoring Agency Name and Address Texas Department of Transportation Research and Technology Implementation Office P. O. Box 5080 Austin, Texas 78763-5080				13. Type of Report and Period Covered Technical Report September 2003 – August 2005	
				14. Sponsoring Agency Code	
15. Supplementary Notes					
16. Abstract  <p>Prestressed concrete I-beams are used extensively as the primary superstructure elements in Texas highway bridges. A commonly observed problem in these beams is the appearance of end zone cracking due to the prestressing forces, thermal effects of hydration, shrinkage and temperature variation. Even though a large quantity of transverse steel reinforcement is provided in the end zone, the cracking problem persists. The research described in this report was targeted to develop a workable steel fiber reinforced concrete mix that would be capable of partially or completely replacing the dense traditional reinforcement and eliminating cracking in the end zones.</p> <p>The research work was divided into three phases: <b>Phase One</b> consisted of developing TxDOT Traditional Fiber Reinforced Concrete (TTFRC) and Self-Consolidating Fiber Reinforced Concrete (SCFRC) mixes with steel fibers. Four TTFRC and three SCFRC mixes with two different types and variable amounts of hook-ended steel fibers were tested for their workability and hardened properties. Based on their performance, suitable TTFRC and SCFRC mixes with optimum fiber contents were selected to cast full-scale beams.</p> <p><b>Phase Two</b> research dealt with the casting and end zone monitoring of seven 25-ft.-long (AASHTO Type-A) I-beams using optimized TTFRC and SCFRC mixes. Conventionally used equipment and techniques were applied for mixing, transporting, placing and steam curing the beams at the precast plant. Strain gauges and temperature loggers installed inside the beams measured strains and temperatures, respectively, during steam curing and release of prestressing force. This instrumentation was aimed at finding the influence of steel fibers on controlling/eliminating the end zone cracks.</p> <p><b>Phase Three</b> research consisted of load testing the seven beams to failure to determine the effects of steel fibers on the structural performance of the beams. Both ends of the simply supported beams were tested to failure using four hydraulic actuators with strain controlled capability. For the first time, descending branches of load-deformation curves were obtained for the end zones of prestressed concrete beams to assess the ductility.</p> <p>The research findings proved that the end zone cracking would be eliminated by completely or partially replacing the traditional transverse steel reinforcement by steel fibers. Additionally, steel fibers enhanced the ductility and crack resistance of the prestressed TxDOT I-beams. This <b>report</b> also provides design guidelines and recommendations for producing, testing and casting steel fiber reinforced concrete mixes for successful application in the end zones of prestressed concrete I-beams.</p>					
17. Key Words Beams, concrete, cracking, ductility, full-scale tests, prestressed, self-consolidating concrete, shear, steel fibers.			18. Distribution Statement No restrictions. This document is available to the public through NTIS: National Technical Information Service 5285 Port Royal Road, Springfield, Virginia 22161. <a href="http://www.ntis.gov">www.ntis.gov</a> and University of Houston, Houston, Texas 77204 <a href="http://www.egr.uh.edu/structurallab/">www.egr.uh.edu/structurallab/</a>		
19. Security Classif.(of this report) Unclassified		20. Security Classif.(of this page) Unclassified		21. No. of Pages 156	22. Price

# **Fiber Reinforcement in Prestressed Concrete Beams**

by

Hemant B. Dhonde  
Research Assistant

Y.L. Mo  
Professor

and

Thomas T. C. Hsu  
Moore's Professor

## **Technical Report 0-4819-1**

Research Project Number 0-4819  
Project Title: Fiber Reinforcement in Prestressed Concrete Beams

Performed in cooperation with the  
Texas Department of Transportation  
and the  
Federal Highway Administration

**December 2005**

**Department of Civil and Environmental Engineering**

**University of Houston**

**Houston, Texas**

## *Disclaimer*

This research was performed in cooperation with the Texas Department of Transportation and the U.S. Department of Transportation, Federal Highway Administration. The contents of this report reflect the views of the authors, who are responsible for the facts and accuracy of the data presented herein. The contents do not necessarily reflect the official view or policies of the FHWA or TxDOT. This report does not constitute a standard, specification, or regulation, nor is it intended for construction, bidding, or permit purposes. Trade names were used solely for information and not product endorsement.

This page replaces an intentionally blank page in the original.

-- TxDOT Research Library Digitization Team

## **Acknowledgments**

This research, Project 0-4819, was conducted in cooperation with the Texas Department of Transportation and the U.S. Department of Transportation, Federal Highway Administration. The project monitoring committee consisted of Peter Chang (Program Coordinator), Andy Naranjo (Project Director), Dacio Marin (Project Advisor), Gilbert Sylva (Project Advisor), John Vogel (Project Advisor) and Stanley Yin (Project Advisor).

The researchers would like to thank the Texas Concrete Company, Victoria, Texas, for continued co-operation during this project. The researchers are grateful to Bekaert Corporation (USA) for supplying the steel fibers for this research. Master Builders Inc. (USA) and Engius (USA) are also appreciated for providing the chemical admixtures and temperature loggers, respectively, for this project.

This page replaces an intentionally blank page in the original.

-- TxDOT Research Library Digitization Team

# TABLE OF CONTENTS

	<b>Page</b>
<b>CHAPTER 1 Introduction</b>	<b>1</b>
1.1 Prestressed Concrete Beams	1
1.2 End Blocks of Prestressed-I-Beams	2
1.3 Problem Statement	3
1.4 Project Objectives	5
<b>CHAPTER 2 TxDOT Traditional Fiber Reinforced Concrete and Self-Consolidating Fiber Reinforced Concrete</b>	 <b>7</b>
2.1 Introduction	7
2.2 Fiber Reinforced Concrete	7
2.3 Self-Consolidating Concrete	11
2.4 Self-Consolidating Fiber Reinforced Concrete	22
2.5 Materials Used in the Research Project	23
2.6 Mixing Procedure	30
2.7 Results of Workability Tests of Concrete Mixes	30
2.8 SCC-Texas Workshop Demonstration	35
2.9 Results of Hardened Properties of Concrete Mixes	36
<b>CHAPTER 3 Early-Age Cracking in Prestressed Concrete I-Beams</b>	<b>47</b>
3.1 Analysis of End Zone Stresses Due to Prestress Forces	47
3.1.1 OpenSees Analytical Model	47
3.1.2 Results of End Zone Analysis under Prestress Forces	50
3.2 Analysis of End Zone Stresses Due to Thermal Load	53
3.2.1 SAP 2000 Analytical Model	53
3.2.2 Results of End Zone Analysis under Thermal Load	53
3.3 Summary of Stresses Due to Prestress and Thermal Loading	56
<b>CHAPTER 4 Prestressed Concrete Beams: Test Specimens and Early-Age Measurements</b>	 <b>57</b>
4.1 Test Specimens	57

4.2	Test Program	62
4.3	Casting of Test Specimens	64
4.4	Instrumentations for Early Age Measurements	66
4.5	Results of Early Age Measurements	71
<b>CHAPTER 5 Load Tests of Prestressed Concrete Beams</b>		<b>81</b>
5.1	Load Test Set-up	81
5.2	Load Test Variables	85
5.3	Load Test Results	86
5.3.1	Ultimate Shear Strengths	86
5.3.2	Ductility Observed in Shear Forces Vs. Deflection Curves	89
5.3.3	Ductility Observed in Shear Forces–Rebar Strains Curves (Strain Gauge)	93
5.3.4	Ductility Observed in Shear Forces–Rebar Strains Curves (LVDTs)	97
5.3.5	Cracking, Crack Widths and Failure of Beams	101
5.3.6	Comparison of Experimental and Analytical Shear Capacities	114
<b>CHAPTER 6 Conclusions and Guidelines</b>		<b>117</b>
6.1	Conclusions	117
6.2	Guidelines	119
6.2.1	End Zone Crack Control	119
6.2.2	Structural Performance of Beams	120
6.2.3	Overall Performance of Beams	121
<b>Draft Specifications for Using TxDOT Traditional Fiber Reinforced Concrete in Prestressed Concrete Beams</b>		<b>123</b>
<b>Draft Specifications for Using Self-Consolidating Fiber Reinforced Concrete in Prestressed Concrete Beams</b>		<b>129</b>
<b>References</b>		<b>135</b>

## LIST OF TABLES

	<b>Page</b>	
Table 2.5.1	Description of Various Mixes Tested	24
Table 2.5.2	Gradation Details of Aggregates	
	(a) Sieve Analysis for Coarse Aggregates	25
	(b) Sieve Analysis for Fine Aggregates	25
Table 2.5.3	Constituents of Various Mixes	26
Table 2.5.4	Mix Proportions of Various Normal-Slump Concrete Mixes	28
Table 2.5.5	Mix Proportions of Various SCC & SCFRC Concrete Mixes	29
Table 2.9.1	Hardened Properties of Various Mixes	39
Table 2.9.2	Normalized Hardened Properties of Various Mixes	45
Table 4.2.1	Test Program for Beams	63
Table 4.4.1	Temperature Loggers Installed in the Beams	67
Table 4.5.1	Tensile Strains measured by Strain Gauges Installed on Rebars for Various Beams in Phase Two	72
Table 5.2.1	Variables in Test Beams B0 to B6	86
Table 5.3.1	Ultimate Strengths of Beams B0 to B6 at North and South Ends	88
Table 5.3.3	Comparison of Shear Force at the Onset of Shear Crack for Various Beams	102
Table 5.3.4	Comparison of Shear Crack Width of Various Beams Measured Using Hand Held Microscope	103
Table 5.3.5	Comparison of End Zone Crack Width of Various Beams Measured Using Hand Held Microscope	106
Table 5.3.6	Comparison of Theoretical and Experimental Shear Strengths	115

## LIST OF FIGURES

		<b>Page</b>
Fig. 1.1.1	Prestressed Concrete I-Beam	1
Fig. 1.2.1	Stress Isobars in End Zone	2
Fig. 1.3.1	End Zone Cracking in a Prestressed I-Beam	4
Fig. 1.3.2	Typical End Zone Reinforcement Details of a Prestressed I-Beam	4
Fig. 2.2.1	Different Shapes of Steel Fibers	8
Fig. 2.2.2	‘Bridging’ Action of Fibers across Concrete Crack	9
Fig. 2.2.3	Load–Deflection Curves for Plain and Fibrous Concrete	9
Fig. 2.2.4	Effect of Steel Fiber Content on Compressive Stress-Strain Curve of FRC	10
Fig. 2.3.1	Slump Flow Test	13
Fig. 2.3.2	Visual Stability Index (VSI) Rating for SCC	15
Fig. 2.3.3	J-ring Apparatus	16
Fig. 2.3.4	J-ring Test Photos	17
Fig. 2.3.5	V-funnel Apparatus	18
Fig. 2.5.1	Steel Fiber RC80/60 BN	26
Fig. 2.5.2	Steel Fiber ZP305	26
Fig. 2.6.1	Concrete Mixer at the Precast Plant-Texas Concrete Co. Victoria, Texas	30
Fig. 2.7.1	Results of Slump and Slump Flow Test	32
Fig. 2.7.2	Results of T-20in. Time for Different Mixes	33
Fig. 2.7.3	V-funnel Time for Different Mixes	34
Fig. 2.7.4	J-ring Values for Different Mixes	35
Fig. 2.8.1	SCC-Texas Workshop Demonstration at University of Houston	36
Fig. 2.9.1	Cylinder Compression Test (a) Failed Cylinders (b) Measurement of Elastic Modulus and Poisson’s Ratio	37
Fig. 2.9.2	Split Cylinder Test Specimens	37
Fig. 2.9.3	Beam Flexure Test (Modulus of Rapture) Specimens	38
Fig. 2.9.4	Average Residual Stress Test	38

Fig. 2.9.5	Variation of Compressive Strength of Various Mixes with Age	40
Fig. 2.9.6	Variation of Split Tensile Strength of Various Mixes with Age	41
Fig. 2.9.7	Variation of Modulus of Rapture Strength of Various Mixes with Age	42
Fig. 2.9.8	Variation of Average Residual Strength of Various Mixes with Age	43
Fig. 2.9.9	Variation of Modulus of Elasticity of Various Mixes with Age	44
Fig. 2.9.10	Variation of Average Normalized Tensile Strength with Fiber Factor	46
Fig. 3.1.1	Schematic Modified Cross-Section of Beam for SRCS Analysis	48
Fig. 3.1.2	Finite Element Mesh for End Zone of Beam (OpenSees Analysis)	49
Fig. 3.1.3	Modeling of Prestress Load Distributi on along the Transfer Length	49
Fig. 3.1.4	End-Zone Stress Distribution for TTC1	51
Fig. 3.1.5	End-Zone Stress Distribution for SCFRC3 Mix	52
Fig. 3.2.1	Finite Element Model for Thermal Analysis of Beam Using SAP 2000	54
Fig. 3.2.2	Stresses Due to Thermal Loads in Type-A Beam Cross-Section	55
Fig. 4.1.1	Cross Section of Type-A beam	58
Fig. 4.1.2	Elevation and Reinforcement Details of Beams B1 and B6	59
Fig. 4.1.3	Elevation and Reinforcement Details of Beams B2, B3, B4 and B5	59
Fig. 4.1.4	Reinforcement and Instrumentation Details of Beam B1	
	(a) Beam B1-North (4.2 % steel)	60
	(b) Beam B1-Center (0.82 % steel)	60
	(c) Beam B1-South (1 % steel)	60
Fig. 4.1.5	Reinforcement and Instrumentation Details of Beams B2, B3, B4 & B5	
	(a) Beam North (1 % steel)	61
	(b) Beam-Center (0.42 % steel)	61
	(c) Beam-South (0.42 % steel)	61
Fig. 4.3.1	Casting of Beams	
	(a) Compaction using Vibrators in Beam B1	65
	(b) Concrete Placed in Beam B2 by a Hopper	65

Fig. 4.4.1	Location of temperature loggers in the beam	
	(a) For B1-South, B2-South, B3-South and B5-South Ends	68
	(b) For B1-Center, B4-South and B6-South.	68
Fig. 4.4.2	Position of Strain Gauges and LVDT Studs on R and S Rebars	69
Fig. 4.4.3	Position of Strain gauges and LVDT Studs on Y bar and V bar	70
Fig. 4.5.1	Variation of Rebar Strains measured by Strain Gauges with Time at the End Zone for Beam B1-North	73
Fig 4.5.2	Variation of Rebar Strains measured by Strain Gauges with Time at the End Zone for Beam B2-North	74
Fig. 4.5.3	Variation of Rebar Strains measured by Strain Gauges with Time at the End Zone for Beam B3-South	75
Fig. 4.5.4	Variation of Rebar Strains measured by Strain Gauges with Time at the End Zone for Beam B5-South	76
Fig. 4.5.5	Variation of Concrete Temperature with Age at Beam B1-South	78
Fig. 4.5.6	Variation of Concrete Temperature with Age at Beam B2-South	78
Fig. 4.5.7	Variation of Concrete Temperature with Age at Beam B5-South	79
Fig. 4.5.8	Variation of Concrete Temperature with Age at Beam B6-South	79
Fig. 5.1.1	Load Test Setup	81
Fig. 5.1.2	Plan View of Loading Frame	82
Fig. 5.1.3	Load Points on Test Beam	82
Fig. 5.1.4	Position of LVDTs on the Web of the Test Beam	84
Fig. 5.1.5	Tracking and Measuring Shear Cracks on the Web of Test Beam	85
Fig. 5.3.1	Shear Force–Deflection Curves for Beams B0 to B6	90
Fig. 5.3.2	Shear Force–Deflection Curves for South Ends of Beams B0 to B6	91
Fig. 5.3.3	Shear Force–Deflection Curves for North Ends of Beams B0 to B6	92
Fig. 5.3.4	Shear Force Vs. Rebar Tensile Strains Measured by Strain Gauge for Beams B1 to B5 at a Distance of H/2 from Support	94
Fig. 5.3.5	Shear Force Vs. Rebar Tensile Strains Measured by Strain Gauge for South Ends of Beams B1 to B5 at a Distance of H/2 from Support	95
Fig. 5.3.6	Shear Force Vs. Rebar Tensile Strains Measured by Strain Gauge for North Ends of Beams B1 to B5 at a Distance of H/2 from Support	96

Fig. 5.3.7	Shear Force Vs. Rebar Tensile Strains Measured by LVDT for Beams B0 to B5 at a Distance of H/2 from Support	98
Fig. 5.3.8	Shear Force Vs. Rebar Tensile Strains Measured by LVDT for South Ends of Beams B0 to B5 at a Distance of H/2 from Support	99
Fig. 5.3.9	Shear Force Vs. Rebar Tensile Strains Measured by LVDT for North Ends of Beams B0 to B5 at a Distance of H/2 from Support	100
Fig. 5.3.10	Variation of Shear Crack Width with Shear Force Measured Using Microscope for Beams B0 to B6	105
Fig. 5.3.11	Load Test Photographs of North and South Ends of Beam B1	
	(a) Cracking of Beam B1-North End	107
	(b) Flexure Failure of Beam B1-North End	107
	(c) Cracking of Beam B1-South End	107
	(d) Shear Failure of Beam B1-South End	107
Fig. 5.3.12	Load Test Photographs of North and South Ends of Beam B2	
	(a) Cracking of Beam B2-North End	108
	(b) Shear Failure of Beam B2-North End	108
	(c) Cracking of Beam B2-South End	108
	(d) Shear Failure of Beam B2-South End	108
Fig. 5.3.13	Load Test Photographs of North and South Ends of Beam B3	
	(a) Cracking of Beam B3-North End	109
	(b) Shear Failure of Beam B3-North End	109
	(c) Cracking of Beam B3-South End	109
	(d) Shear Failure of Beam B3-South End	109
Fig. 5.3.14	Load Test Photographs of North and South Ends of Beam B4	
	(a) Cracking of Beam B4-North End	110
	(b) Shear Failure of Beam B4-North End	110
	(c) Cracking of Beam B4-South End	110
	(d) Shear Failure of Beam B4-South End	110
Fig. 5.3.15	Load Test Photographs of North and South Ends of Beam B5	
	(a) Cracking of Beam B5-North End	111
	(b) Shear Failure of Beam B5-North End	111

	(c) Cracking of Beam B5-South End	111
	(d) Shear Failure of Beam B5-South End	111
Fig. 5.3.16	Load Test Photographs of North and South Ends of Beam B0	
	(a) Cracking of Beam B0-North End	112
	(b) Shear Failure of Beam B0-North End	112
	(c) Cracking of Beam B0-South End	112
	(d) Shear Failure of Beam B0-South End	112
Fig. 5.3.17	Load Test Photographs of North and South Ends of Beam B6	
	(a) Cracking of Beam B6-North End	113
	(b) Flexure Failure of Beam B6-North End	113
	(c) Cracking of Beam B6-South End	113
	(d) Shear Failure of Beam B6-South End	113

# CHAPTER 1

## INTRODUCTION

### 1.1 Prestressed Concrete Beams

In prestressed concrete construction, very high-strength steel (such as seven-wire strands of 270 ksi) are prestressed to reduce the cracking of concrete, to control the deflection and camber, to enhance the strength of the structures, and to lighten the dead weight. Because of these advantages, prestressed concrete has, in a short span of 50 years, become the predominant construction material. For example, 60 % of all the bridges built during the 1990-99 period in the United States are prestressed concrete bridges (others being reinforced concrete, steel and timber).

The developments in new materials and technology in recent years have made it possible to construct and assemble long-span prestressed concrete structural systems. Standardization in the design and manufacturing of the precast bridge components has optimized bridge design. Bridge superstructure elements such as the I-beams, double tee and box beams are generally plant-produced precast and prestressed concrete products inheriting the advantages of economy, durability, low maintenance and assured quality. The most commonly used precast/prestressed concrete beam for short-to-medium-spans is the I-beam (PCI 1999) as shown in Fig. 1.1.1.



**Fig. 1.1.1 Prestressed Concrete I-Beam**

An I-beam consists of a top and bottom flange with a slender web joining the flanges. The bottom flange and some portion of the web-bottom are reinforced with prestressing tendons; thus the bottom and top flanges build up the flexural strength. The web is reinforced with vertical/transverse deformed steel reinforcement bars (rebars) that contribute towards the shear strength of the beam.

## 1.2 End Blocks of Prestressed I-Beams

Before casting a precast, pretensioned beam, prestressing tendons are pulled and stressed to a designed prestress level. The tendons are then released after the concrete has matured to a required strength, which is usually 16 to 24 hours after casting. Thus, prestressing involves application of large concentrated tendon forces into the end regions of the beam called the “end block.” At these end blocks, prestress is gradually transferred to the concrete over a certain length of the beam known as the “transfer length.” The region affected by the concentrated force is called the “anchorage zone,” which encounters two critical tensile stresses as shown in Fig. 1.2.1; the spalling stress near the edges of the anchorage and the bursting stress along the transfer length (Breen *et al* 1994). Since the tensile strength of concrete is small in comparison to its compressive strength, cracks frequently occur due to the bursting and the spalling stresses. Large amounts of transverse deformed steel rebars are placed in the anchorage zone to arrest these cracks.

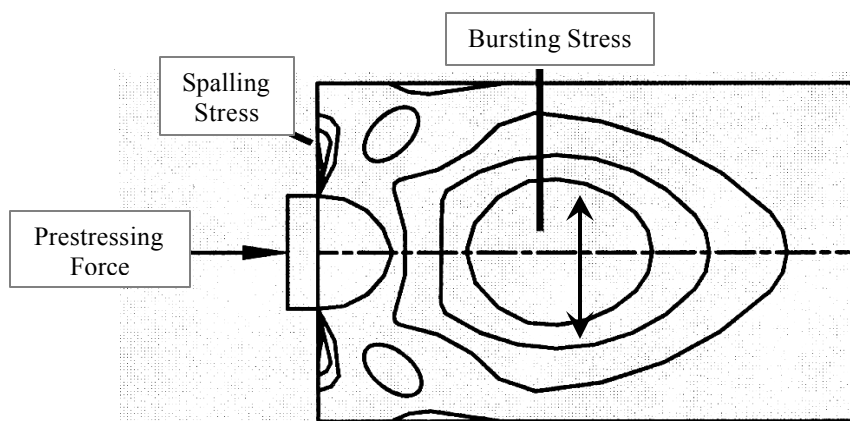


Fig. 1.2.1 Stress Isobars in End Zone (Breen *et al* 1994)

Adequate reinforcement should be present in the anchorage zone and placed in the vicinity of the expected cracks to retard or to eliminate the propagation and opening of the cracks. If, on the other hand, the anchorage zone reinforcement is inadequate or inappropriately located, the cracks will propagate in the structure until failure of the anchorage zone occurs. End zone cracking is commonly observed during the stressing of tendons (Breen *et al* 1994). The cracks occur as a result of the combination of residual stresses produced due to curing or hydration of the concrete and the transfer of the prestressing force (Earney 2000, Gopalaratnam *et al* 2001). Even if cracks do not appear after the tendons have been released, they may appear at a later stage due to creep, shrinkage, temperature effects and other such secondary causes.

In addition to giving the uncomfortable appearance of structural distress, excessive cracking can lead to the corrosion of reinforcement, thereby reducing the service life of bridges. Therefore, it is imperative to properly design and provide the end zone reinforcement in the anchorage zone.

### **1.3 Problem Statement**

The Texas Department of Transportation (TxDOT) and other such agencies throughout the United States extensively use the precast/prestressed concrete I-beams as the primary superstructure element in highway bridges. Various superimposed live, dead and vehicular loads are applied on the beams through an overlying deck-slab. A commonly observed problem in the prestressed concrete beams is the appearance of end zone cracking either just after the release of the prestressing force or after some time due to secondary effects of creep, shrinkage and temperature (Fig. 1.3.1). Typically, cracks occur at the intersection of the web and flange. The cracks usually begin at the end face, propagate horizontally along the length of the beam, and then incline towards the web region. Sometimes, the cracks initiate from the web center and horizontally extend towards the beam interior. To control this cracking, TxDOT provides a large quantity of transverse stirrups in the anchorage zone (Fig. 1.3.2). This end zone reinforcement amounts to a staggering 4.2 % by volume of concrete. Even with such a high percentage of reinforcing steel in the anchorage zone, cracking still occurs at the end zone and the problem persists.



**Fig. 1.3.1 End Zone Cracking in a Prestressed I-Beam**



**Fig. 1.3.2 Typical End Zone Reinforcement Details of a Prestressed I-Beam**

In general, prestressed concrete bridge beams are optimized in their cross-section dimensions to limit the dead weight of the structure. The slender web makes it even more difficult to place the large amount of rebars required for shear strength, confinement of concrete and anchorage zone reinforcement. Thus the anchorage zone reinforcement becomes quite congested, which leads to difficulty in consolidating the concrete properly. Hence, the quality of concrete degrades at the end zones, again making it susceptible to cracking. Moreover, it is also labor-intensive to produce and place the large amount of steel reinforcement in the end zone.

Highway bridges are exposed to potentially corrosive environments. The onset of any crack would initiate corrosion of the reinforcement and degrade the concrete structure. This problem becomes more critical at the beam ends. Therefore, it is desirable to reduce the end zone cracking by using unconventional means offered by the latest technological advancements.

#### **1.4 Project Objectives**

The large amount of the reinforcement (4.2 % by volume) in the anchorage zone makes the casting and vibration of concrete very difficult and tends to degrade the quality of concrete, yet the cracks still tend to appear. Thus, a solution must be developed which would not only control the end zone cracking, but would also help to enhance the quality of concrete and the ease of placement.

When steel fibers of high tensile strength are added to the concrete mix, the tensile and shear resistance of the composite system is enhanced. Fiber reinforced concrete is also known to possess better properties than traditional concrete. These properties include bond strength, residual flexural toughness, low shrinkage and ductility. It would be desirable to find out whether steel fibers could be used to enhance the properties of Texas traditional concrete.

Fibers are known to reduce the workability and the flow characteristics of plain concrete. To improve the workability, an idea was developed to place fibers in Self-Consolidating Concrete (SCC). Self-Consolidating Fiber Reinforced Concrete (SCFRC) appears to be a logical material for application to the end regions of prestressed concrete I-beams and is expected to control cracking as well as to improve casting performance.

The objectives of this research are:

- (a) To develop TxDOT Traditional Fiber Reinforced Concrete (TTFRC) and Self-Consolidating Fiber Reinforced Concrete (SCFRC) mixes having optimized performance with regard to its workability, fiber content, types of fibers and mechanical strengths suited to cast I-beams. The purpose is to control end zone cracking and to eliminate partially or completely the conventional transverse reinforcement in the anchorage zone.
- (b) To investigate and establish an effective construction procedure for casting full-scale I-beams with the optimized TTFRC and SCFRC mixes. To provide the

instrumentation necessary to collect data of concrete temperatures, stresses and strains that will help us to understand the mechanism of end zone cracking.

- (c) To conduct full-scale load tests of the I-beams to study the effect of steel fibers on their structural behavior with regards to ultimate shear strength, ductility and failure mechanisms.
- (d) To prescribe design recommendations for the end regions and construction guidelines for manufacturing and placing TTFRC and SCFRC mixes in the I beams.

## CHAPTER 2

# TXDOT TRADITIONAL FIBER REINFORCED CONCRETE AND SELF-CONSOLIDATING FIBER REINFORCED CONCRETE

### 2.1 Introduction

At the end regions of a prestressed concrete beam, prestress forces, concrete hydration-thermal loading and shrinkage are collectively responsible for generating end zone cracks. To prevent the occurrence of end zone cracks, dense and intricate reinforcement of steel deformed bars amounting to 4.2 % by volume of concrete is provided in the TxDOT I-beams. However, observations show that such a heavy reinforcement cannot completely eliminate the cracking in end regions. A potential alternative solution is to replace the conventional web reinforcement with steel fibers. This alternative solution could prevent the cracking at the end region, as well as allow easy placement of TxDOT traditional concrete.

Portland cement concrete is a relatively brittle material that is expected to crack under relatively small tensile stress. Fiber Reinforced Concrete (FRC) has the potential to increase the tensile and shear strengths of concrete and to reduce or eliminate traditional reinforcement (Noghabai 1998, 2000, Ashour *et al* 1992, Imam 1995, Casanova 1996). However, fibers are also known to impede the workability and the rheological characteristics of plain concrete. To enhance the workability of FRC, an idea was developed to place fibers in Self-Consolidating Concrete (SCC). Self-Consolidating Fiber Reinforced Concrete (SCFRC) appears to be an appropriate solution for application to the end regions of prestressed concrete I-beams to control cracking.

### 2.2 Fiber Reinforced Concrete

Fiber Reinforced Concrete (FRC) has gained world-wide popularity in the construction industry. It is widely used in manufacturing slabs, road pavements, machine foundations, seismic structures, precast concrete elements and shotcrete. In 1910, Porter first suggested the use of steel fibers in concrete (Naaman 1985). However, the first scientific investigation of FRC in United States was done in 1963 (Romualdi and Baston 1963). FRC is produced using the conventional hydraulic cements, fine and coarse aggregates, water and discrete discontinuous

reinforcing fibers. To enhance the workability and stability of FRC, superplasticizers (chemical admixtures) may also be added in the concrete. Fibers are commercially available and manufactured from steel, plastic, glass and other natural materials. Engineering specifications of fiber address its shape, material, length, diameter and type of cross-section (Fig. 2.2.1). Steel fibers can be defined as discrete, short lengths of steel having a ratio of its length to diameter (i.e. aspect ratio) in the range of 20 to 100 with any of the several cross-sections, and that are sufficiently small to be easily and randomly dispersed in fresh concrete mix using conventional mixing procedures (ACI 318 1996).

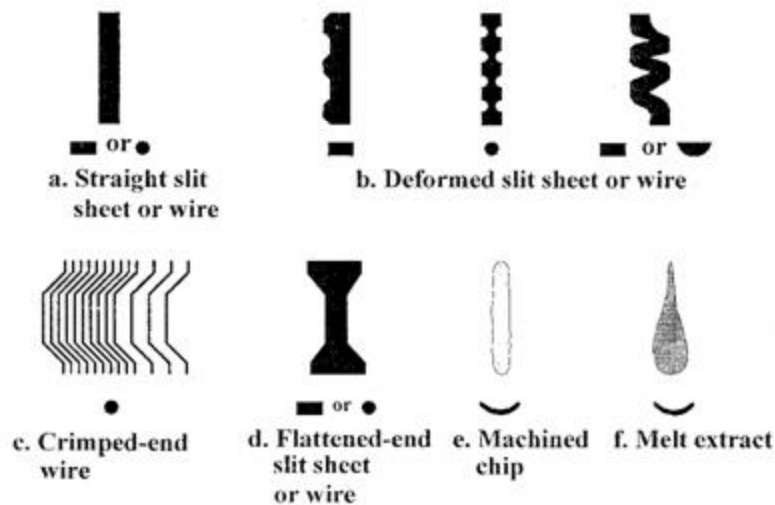


**Fig. 2.2.1 Different Shapes of Steel Fibers (ACI 544.1R 1996)**

Fibers act as multi-directional uniformly dispersed micro-reinforcement in the concrete matrix. As shown in Fig. 2.2.2, fibers bridge across a crack and prevent it from growing by transferring the tension across the crack. They help in carrying and redistributing the applied stresses in concrete by undergoing shear strains (Beaudoin 1990). Thus, shrinkage and thermal cracking during the plastic stage and micro-cracking in the concrete matrix during the loading stage are controlled by the presence of fibers in concrete. These characteristics of fiber impart post-cracking ductility to FRC. Fibers enhance the mechanical performance of concrete with regard to its tensile and shear strength, toughness, ductility, durability, fatigue and shrinkage resistance (Shah 1991). The beneficial influence of fibers in concrete depends on many factors such as type, shape, length and cross-section of fibers, strength and bond characteristics of fiber,

fiber content, matrix strength and mix design and mixing of concrete. Typical load-deflection curves for plain and fiber reinforced concrete are depicted in Fig. 2.2.3.

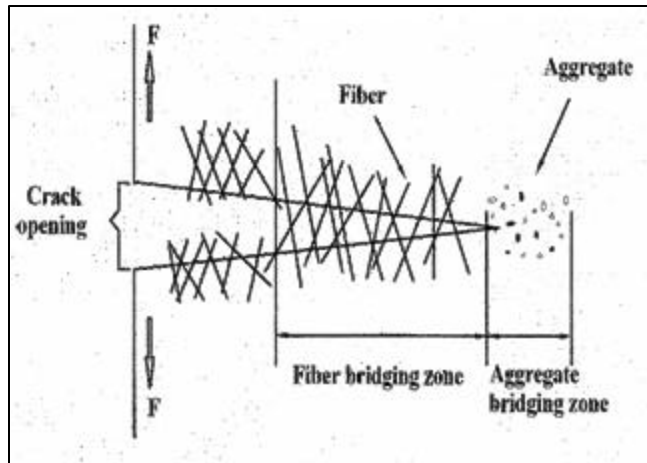


**Fig. 2.2.2 'Bridging' Action of Fibers across Concrete Crack (Beaudoin 1990)**

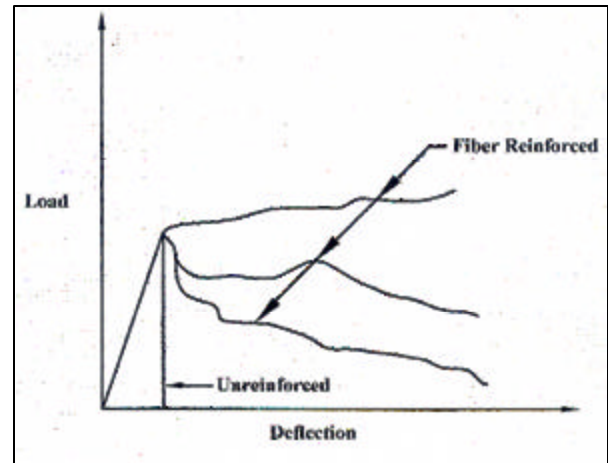


**Fig. 2.2.3 Load-Deflection Curves for Plain and Fibrous Concrete**

The replacement of traditional steel reinforcement with fibers has the following advantages:

- (a) Fibers increase the tensile strength of the matrix, thereby improving the flexural and shear strengths of concrete.
- (b) The bridging mechanism of fibers and its tendency to redistribute stress evenly throughout the matrix contribute to post-cracking resistance, restrain crack growth and impart ductility to concrete.
- (c) FRC is more durable and serviceable than conventional reinforced concrete (Grzybowski 1989, Rapoport *et al* 2001, Grzybowski and Shah 1990).
- (d) Producing and placing conventional reinforcement requires costly labor and time.

Thus, use of fibers in concrete saves labor costs and time.

Fibers have an effect on the mechanical performance of concrete in all failure modes (Gopalaratnam and Shah 1987). In FRC, an addition of up to 1.5 % of fibers by volume increases the compressive strength from 0 to 15 % (Johnston 1974, Dixon and Mayfield 1971). A gradual slope in the descending portion of the FRC stress-strain curve indicates improved spalling resistance, ductility and toughness as shown in Fig. 2.2.4 (Padmarajaiah and Ramaswamy 2002).

Hence, fibers marginally improve the compressive strength but significantly enhance the post-peak strain and ductility of FRC. Fibers have the ability to improve the direct tensile strength of concrete up to 40 % when 1.5 % volume of fibers is used in FRC (Williamson 1974). Previous research has shown that fibers substantially increase the shear strength of concrete (Narayanan and Darwish 1987, Barr 1987, Oh et al 1999, Noghabai 2000). FRC having 1 % volume of fibers can increase up to 170 % of the ultimate shear strength (Narayanan and Darwish 1987). Steel fibers have been shown to be an effective mean to completely replace traditional transverse shear reinforcement (Williamson 1978, Noghabai 2000). Rather than using a single type of fiber, a combination of fibers with various aspect ratios can prove to be more efficient in improving the mechanical performance of FRC (Noghabai 2000). The enhanced performance of FRC over its unreinforced counterpart comes from its improved capacity to absorb energy during and after fracture.

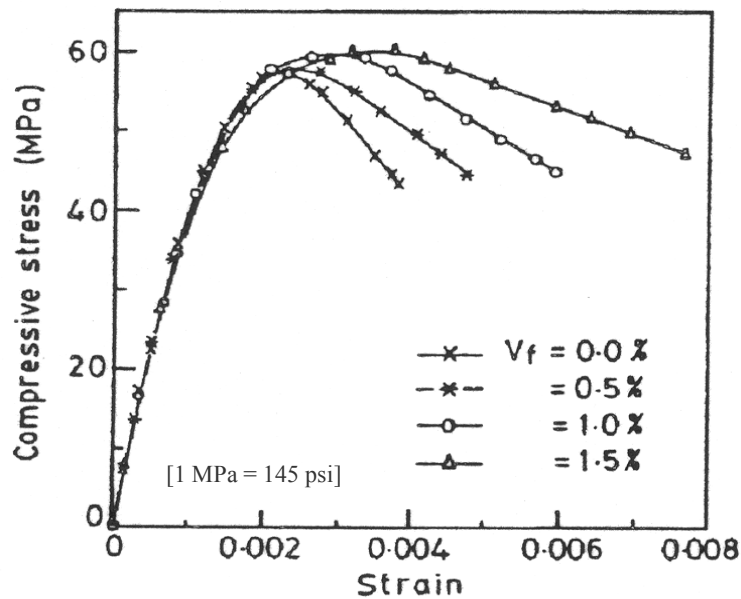


**Fig. 2.2.4 Effect of Steel Fiber Content on Compressive Stress-Strain Curve of FRC (Padmarajaiah and Ramaswamy 2002)**

The following advantages of FRC were reported by Narayanan and Darwish (1987);

- (a) The spacing of cracks in FRC beams was reduced to a fifth of that in the control beams with or without conventional stirrups.

- (b) The mode of failure changed from shear to flexure type when the volume of fibers ( $V_f$ ) was increased beyond an optimum value of  $V_f = 1.0\%$ .
- (c) More uniform redistribution of stresses was observed in the fiber concrete beams in comparison to the traditional beams.

The only disadvantages of FRC would be its decreased workability and accelerated stiffening of fresh concrete due to the addition of fibers. This increases construction labor and time due to the excess vibration that is required to make the FRC workable. The problem could be partially overcome with the use of newly developed high range superplasticizers that not only enhance the workability of FRC but also maintain the plasticity of the mix for a longer time.

The influence of steel fibers on the flexural strength of concrete is much greater than for direct tension and compression (Hannant 1978). The flexural strength of FRC is increased by about 55% with a  $V_f = 2\%$  as reported by Oh *et al* (1999). The presence of coarse aggregate in the concrete coupled with mixing and placing constraints, limits the maximum fiber content to 1.5%. It has been determined that balling of fibers in concrete during mixing and placing increases as the aspect ratio increases. An aspect ratio of 100 for steel fibers was found to be optimum. Fibers aligned in the longitudinal direction of a beam produce improved flexural strengths of up to 150% (Johnston 1974, Snyder and Lankard 1972, Watrehouse and Luke 1972, Johnston 1989). The influence of a particular fiber on the hardened properties of FRC depends on the product of volume of fiber (fiber content) and its aspect ratio (length/diameter). This parameter is termed the 'fiber factor.' If the fiber factor is less than 25, the fibers would not significantly effect the mechanical properties of FRC (Johnston 1980).

Concrete is prone to shrinkage when subjected to a drying environment. During shrinkage, if concrete is restrained, tensile stresses are induced leading to cracking. Short and randomly distributed fibers can reduce shrinkage cracking in concrete (Hoff 1987). Research has shown that a well compacted FRC will limit the corrosion of fibers close to the surface skin of the concrete even when concrete is highly saturated with chloride ions (Schupack 1985).

### 2.3 Self-Consolidating Concrete

Self-Consolidating Concrete (SCC), also referred to as self-compacting concrete, is a highly workable concrete that can flow through densely reinforced or complex structural elements under its own weight and adequately fill voids without segregation or excessive

bleeding, without the need of vibration (PCI 2003). SCC is not only designed to consolidate but also flow under its own weight. It provides slick finished surfaces without vibration. SCC has substantial commercial benefits because of ease of placement in complex forms with congested reinforcement. This is in contrast to traditional concrete, where the difficulties in compaction could cause entrapped air voids, which could severely reduce the strength and durability of concrete (Gaimster and Foord 2000, Khayat *et al* 1999). SCC has gained widespread attention in the United States in the last few years for its obvious advantages of savings in labor costs, shortened construction time, better finish and improved work environment (Gaimster and Foord 2000, Khayat *et al* 1999).

SCC, which does not need vibration to achieve full consolidation, necessitates it to be a high-performance concrete that demonstrates high fluidity and possesses good cohesiveness at the same time, in a plastic state. SCC mix constituents and their proportions are to be carefully selected so as to achieve a concrete with lower rheological shear stress and viscosity that would remain homogenous during its use. Thus, rheological properties, i.e. properties dealing with the deformation and flow characteristics of fresh concrete, are important for successful production and use of SCC. Advancement in SCC technology was primarily possible due to the introduction of a new generation of chemical admixtures that improved and controlled the rheological properties of SCC. Better performing SCC mixes were produced on the advent of melamine, naphthalene and acrylic based High Range Water Reducing superplasticizers (HRWR) and Viscosity Modifying Agents (VMA).

SCC must satisfy the following workability criteria stipulated by the PCI guidelines (PCI 2003):

- (a) Filling ability – The property which determines how fast SCC flows under its own weight and completely fills intricate spaces with obstacles, such as reinforcement, without losing its stability.
- (b) Passing ability – the ability of SCC to pass through congested reinforcement and adhere to it without application of external energy.
- (c) Stability – the ability of SCC to remain homogenous by resisting segregation, bleeding and air popping during transport and placing as well as after placement.

These properties provide SCC with a unique rheology that distinguishes it from conventional concrete. Producing such a special concrete requires an improved work environment and strict

quality control measures. The quality of SCC can be ascertained with the aid of numerous workability tests.

All workability tests should preferably be conducted near the mixer, after about 60 seconds of mixing. This allows the SCC mix to stabilize after the agitation of mixing. Visual inspection of SCC mix in the mixer would help to gauge the probable degree of workability. Both quantitative and qualitative measurements should be taken to judge the workability of the mixes in accordance with the PCI guidelines (PCI 2003). Mentioned below are some of the important workability tests for SCC:

(a) **Slump flow test** – Filling ability and flowability of the mix can be tested using the slump flow test, which is similar to the conventional slump test used for traditional concretes with regards to the testing apparatus. The ‘slump flow’ is the mean diameter of the horizontal spread of the concrete mass, after lifting Abram’s cone (Fig. 2.3.1). As a ‘rule of thumb,’ any concrete having a slump flow value greater than 25 inches can be classified as SCC. A slump flow test is simple, rapid and can easily be performed on site. It is therefore the most commonly used test. The test gives a good assessment of filling ability, and may give some indication of resistance to segregation. The test can be used effectively to control the consistency of SCC on site from batch-to-batch (PCI 2003).

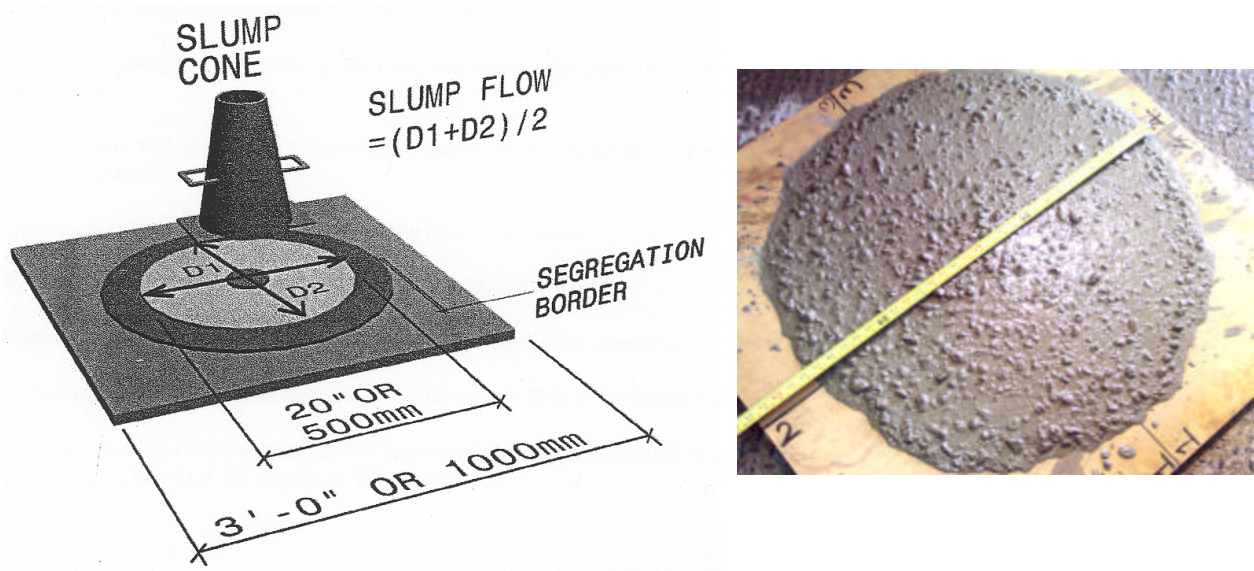


**Fig. 2.3.1 Slump Flow Test (PCI 2003)**

SCC having satisfactory slump flow could be produced easily with high coarse aggregate content suitable for large depths of casting. The slump cone test can also be performed by inverting the cone, i.e. up-side down, with almost the same results. But only one of the two types of slump flow tests shall be used to control and compare the SCC mixes; switching between the two tests is not recommended (PCI 2003). T-20in is the time required by the concrete mass to spread to 20 inches diameter, indicating the filling ability of the mix. Slump flow is the static measure of the extent of flowability of SCC, while T-20in time is the dynamic part that depicts how fast the SCC would flow and fill the form.

Visual Stability Index (VSI) is a qualitative test performed by observing the SCC in the mixer, in the wheelbarrow and during other tests and is also to be recorded during the slump flow test. It rates the quality of SCC in terms of segregation and bleeding. Fig. 2.3.2 shows the detailed description of VSI ratings along with photos for SCC mix. 0-VSI rating suggests a stable SCC, whereas 3-VSI rating means severe segregation and bleeding indicating a very poor quality of SCC. The VSI ratings could be done in increments of 0.5 of the stability of the mix (Daczko 2002). VSI is quite useful for quality control and consistency testing of SCC. During the slump flow test, there is no restriction offered to the freely flowing SCC. Hence, the flow spread and T-20in time recorded during this test will be referred to as unrestricted slump flow and unrestricted T-20in time. A T-20in time between 3 to 7 seconds and a VSI rating of zero is recommended (PCI 2003).

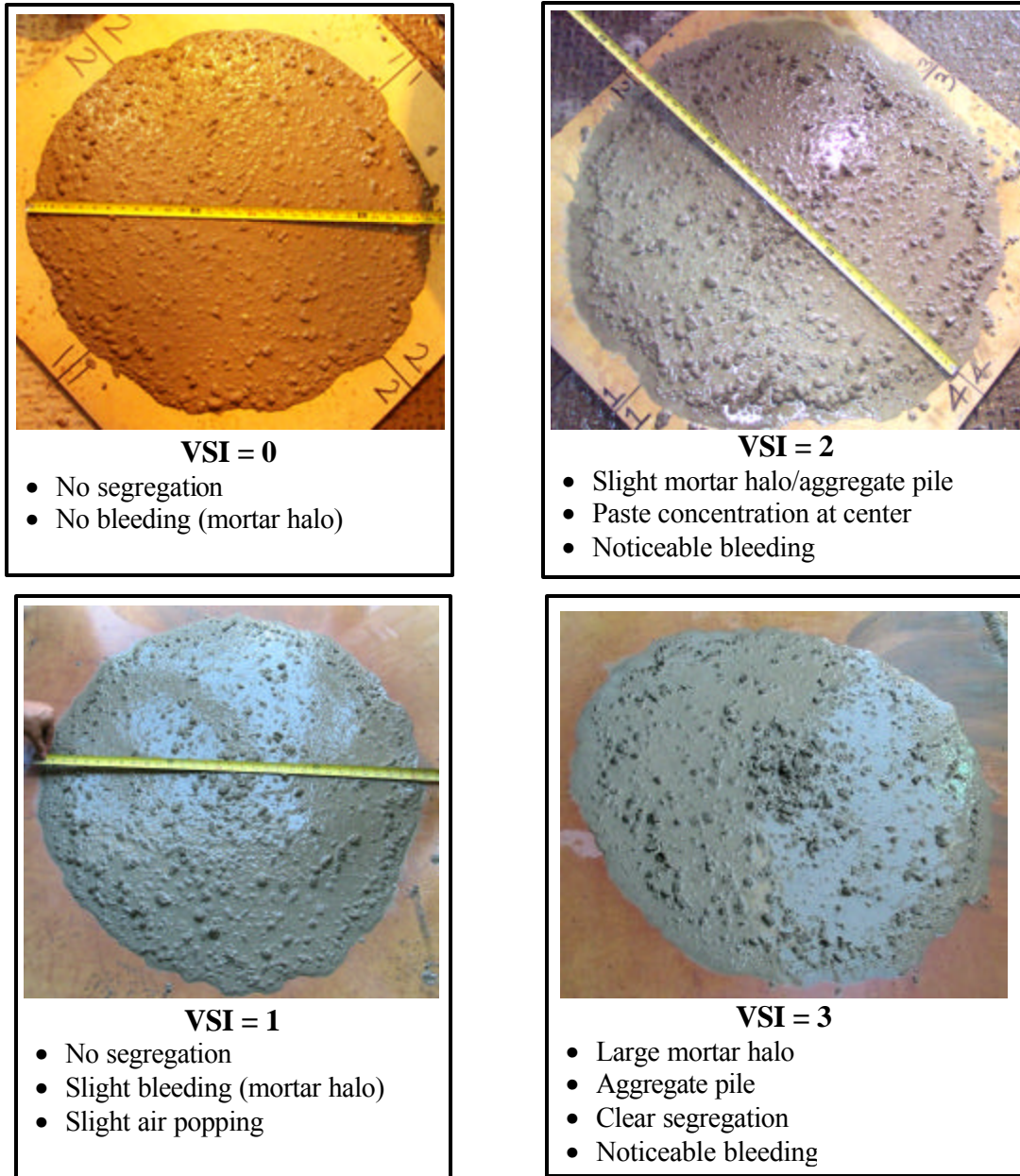


**Fig. 2.3.2 Visual Stability Index (VSI) Rating for SCC**

**(b) J-ring test** – The passing ability of SCC mix is tested using a J-ring apparatus. J-ring tests are performed by lifting Abram’s cone and allowing SCC to flow radially outward through the J-ring. The flow of SCC is obstructed by the bars, thereby creating a difference of level in the SCC (quantified as the J-ring value) that is inside the J-ring and the SCC that has passed through it. A J-ring apparatus is shown in Fig. 2.3.3. A J-ring consists of an open steel circular ring to which reinforcement bars are attached. These bars can be of different diameters

and spaced at different intervals, depending on the actual reinforcement spacing and size used at the site. Generally, a spacing of three times the maximum aggregate size will be satisfactory (PCI 2003).

The J-ring attempts to simulate the congestion of reinforcement in an actual structure. Desired J-ring values for a good SCC mix lie within the vertical offset of 0.4 to 0.6 inch. Slump flow and T-20in time can also be measured during the J-ring test, which indicates the restricted slump flow and restricted T-20in time. It should be noted that flowability and passing ability are interdependent. The restricted slump flow is affected by the degree to which the concrete movement is blocked by the reinforcing bars. The extent of blocking is much less affected by the flow characteristics. Hence, it can be stated that the greater the difference in height, i.e. the higher the J-ring value, the lower the passing ability of the SCC (EFNARC 2002). The J-ring value is the difference between the heights of the SCC inside and outside the ring. The J-ring value is calculated by measuring the heights of the SCC from the top of the J-ring at various points orthogonal to each other, as shown in Fig. 2.3.3, and then averaging out the measured difference in height. Fig. 2.3.4 shows the J-ring apparatus used in this project and the measurements taken during one of the tests. Blocking can best be detected visually, which is often more reliable than calculations.

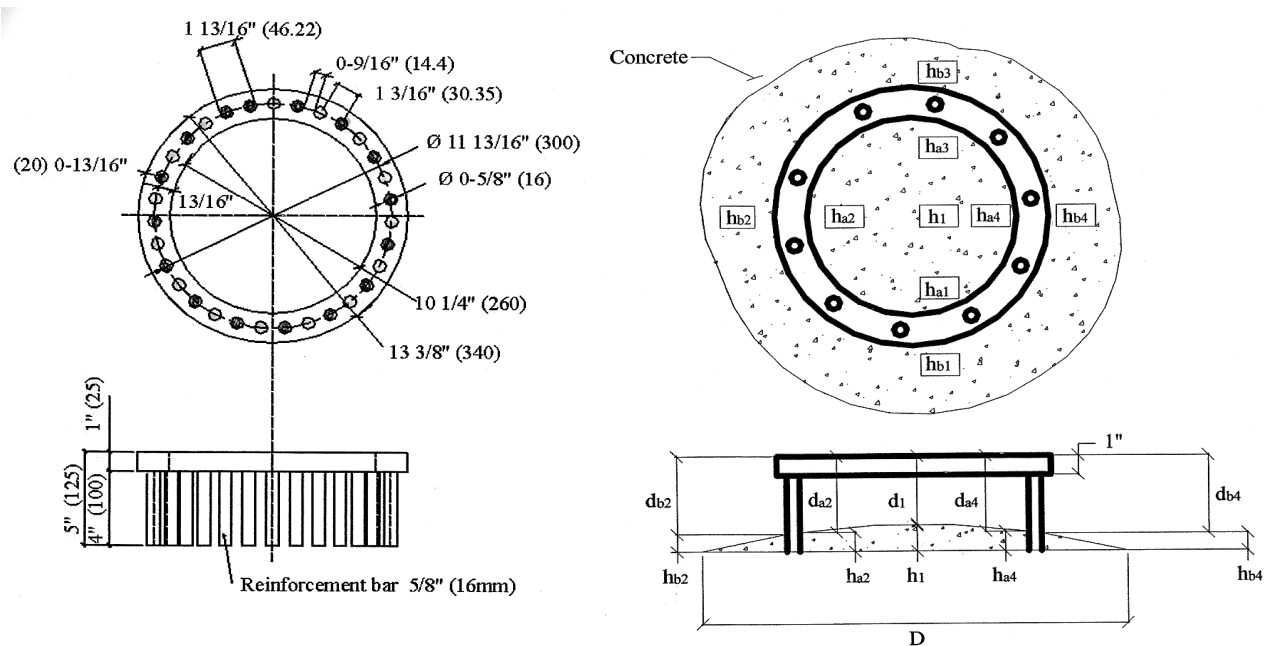
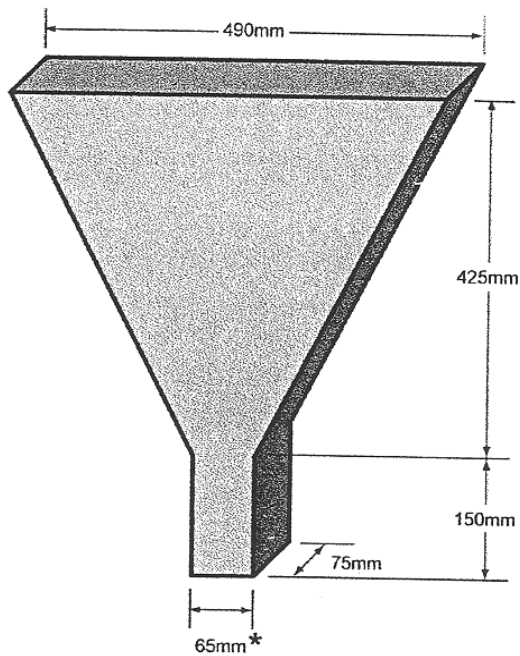


Fig. 2.3.3 J-ring Apparatus (PCI 2003)



**Fig. 2.3.4 J-ring Test Photos**

(c) **V-funnel test** – The filling ability of SCC is measured using the V-funnel test. This is performed by measuring the time ( $T$  in seconds) taken for the mix to completely empty-out through the funnel, which has a rectangular opening of 3 x 2.5 inches as shown in [Fig. 2.3.5](#). V-funnel time recorded after 5 minutes of standing the mix, is termed the T-5 time. The difference between the T-5 time and the V-funnel time ( $T$ ) indicates the segregation potential and thixotropic properties of the SCC. The property of SCC to temporarily lose its flowability by momentary increase in viscosity on standing and regaining the flowability on application of external energy is called the thixotropic behavior of SCC. The V-funnel time indicates the filling ability of SCC. Shorter flow times indicate greater flowability. For a satisfactory SCC, the V-funnel time can be 7 to 10 seconds.



\* In some V funnels, this dimension is 75mm (1 in = 25.4 mm)

**Fig. 2.3.5 V-funnel Apparatus (PCI 2003)**

The basic ingredients used to make SCC are the same as those used in making conventional concrete. The only difference is that SCC has a comparatively high fine-to-coarse aggregate ratio, a low water-cement ratio and good aggregate grading. The addition of High Range Water Reducing agents (HRWR) is required to impart flowability and passing ability to the mix. But excessive HRWR may result in segregation and bleeding. To alienate segregation and bleeding, a viscosity modifying agent (VMA) is added to the concrete (Okamura and Ozawa 1995). Numerous research findings have shown that it is no longer a dream to make a flowable yet stable SCC, tailored for any application.

SCC uses a higher proportion of ultra-fine materials and effective admixtures. Unlike the normal vibrated concrete, SCC has a ratio of fine aggregate to coarse aggregates slightly above unity. Normal vibrated concrete has a coarse to fine aggregate ratio generally in the range of 1.6 to 2.5 (Holschemacher *et al* 2002). SCC is a special concrete and hence requires new mix design procedures. Various mix design methods are proposed for SCC. To understand the design principles, the workability concepts and mechanisms of SCC should first be studied. SCC requires high flowability and a low yield value of the rheological characteristics. High

flowability can be obtained by decreasing the yield value of the mortar paste and increasing the plastic viscosity of the concrete to resist segregation. Superplasticizers reduce the yield value of the mortar paste by a pronounced dispersion effect. It is also known that the plastic viscosity of mortar governs the compactibility of concrete. There is an optimum value of plastic viscosity for which there exists maximum flowability and stability.

If the powder content is increased, the viscosity increases while the yield value decreases, resulting in a highly flowable SCC (Toyoharu *et al* 1998). The flowability of SCC is affected by the degree of dispersion of the cement particles due to the physiochemical effect of the admixtures. Belite (C2S) rich cement brings out the dispersing action of superplasticizers quite effectively (Nawa *et al* 1993). High early strength cement and ordinary Portland cement produce high yield values in SCC, whereas moderate heat cement and belite (C2S) cement are best for SCC. Mechanically stabilized cements using fly ash, silica fume, slag and limestone powder having high-fineness are best suited for SCC (Nawa *et al* 1989 and Edamatsu *et al* 1997).

The effects of coarse and fine aggregates on the rheological, static and kinetic properties of SCC are critical. When the amount of coarse aggregate is increased, the flowability and compactibility of SCC decreases as the internal friction between aggregates increases. Flowability falls as the maximum size of coarse aggregate increases. Fine aggregates help in lowering the yield value of concrete to a certain point. Large amounts of fine aggregates lower the compactibility of SCC as the thickness of the mortar paste covering the fines decreases (Toyoharu *et al* 1998).

Based on the method of preventing segregation, i.e. by increasing the plastic viscosity of paste, SCC may be classified into three groups:

- (a) Powder-based SCC in which a large amount of powder is added.
- (b) Chemical-based SCC in which VMA is used to resist segregation.
- (c) Combination types of SCC in which a combination of the above-mentioned types is used.

Powder-based SCC is the first generation of SCC which has generally high strength and good durability. Chemical-based SCC was an extension of the anti-washout underwater concrete. The advantage of this type of SCC is that it develops high flowability even with low powder contents and offers a better quality control of the mix. The new generation of combination types of SCC

benefits from the advantages of the previous two types. Combination types of SCC have a wide range of flowability along with a better control on the stability of the mix (Toyoharu *et al* 1998).

SCC mix design procedures proposed by the Japan Society of Civil Engineers (JSCE 1998), Prof. Okamura and others, aim at determining the proportions of various ingredients to fulfill the performance requirements of self-consolidation, flowability, stability, strength and durability. The mix design procedure consists of three stages: consideration of mix proportion, mix proportion design and verification of mix proportions.

The first step determines the target performance requirements of SCC, considering the structural, constructional and environmental conditions. A preliminary mix design is developed in the second step based on the various empirical mix design charts and guidelines. The final step involves verifying the preliminary mix design by actually preparing a trial mix and checking its performance at all levels. If the trial mix does not work, it is modified and again tested, until success is achieved (Toyoharu *et al* 1998).

SCC is gaining popularity in the United States for its obvious advantages of savings in labor costs, shortened construction time, better finish and improved work environment. Following are the advantages of SCC:

- (a) SCC can be placed efficiently without the need of any mechanical vibration, since SCC can flow and fill the form on virtue of its self-weight.
- (b) SCC can save considerable construction labor and time involved in concrete placement and finishing work. Hence, SCC creates opportunities to reallocate labor and time for other jobs.
- (c) SCC eliminates vibration and hence the associated machinery noise at the work place.
- (d) Concreting in intricately shaped structural forms and dense reinforcement is effectively possible with SCC. The filling capacity of SCC is high, making the placement easy and fast.
- (e) The self-consolidating nature of SCC ensures that the concrete is more homogenous and uniform, thereby reducing permeability and improving durability of the concrete.
- (f) SCC has an improved interfacial transition zone between the cement paste and aggregate or reinforcement. This increases the bond characteristics of the

aggregates and reinforcement with the matrix, resulting in better strengths and durability.

SCC has the following disadvantages:

- (a) Special and expensive admixtures such as HRWR and VMA are required to produce SCC.
- (b) Considerable experience and skill is essential to manufacture SCC successfully.
- (c) Strict quality control is to be maintained during the production, testing and placing of SCC.
- (d) SCC has a relatively high cement paste content generating more heat of hydration which may result in excess drying shrinkage. The fact that SCC has a lower aggregate content makes it even more susceptible to drying shrinkage.
- (e) Forms are required to be relatively tight and stronger for SCC (Bury et al 2002).

Many of the above mentioned drawbacks of SCC could be reduced or eliminated. The cost of expensive admixtures could be counter-balanced with the savings in construction labor and time. An appropriate SCC mix design method that blends optimum amounts of admixtures and powder will eventually control the excess use of admixtures. SCC awareness programs, workshops, seminars and demonstrations would help the construction industry gain confidence, skills and expertise in manufacturing and using SCC.

In SCC, cement could be partially replaced by various supplementary powders such as fly ash, silica fume, lime fines, finely ground slag, etc. (Toyoharu et al 1998). This would reduce the cost as well as the problem of drying shrinkage. The use of expansive additives such as belite (C2S) in cement is very effective in compensating the shrinkage of SCC (Akihiro et al 1998). Moreover, SCC with high aggregate contents, almost approaching that used in conventional concretes, has been successfully produced (Grünewald and Walraven 2001). Studies have shown that the relatively viscous SCC mix does not require leak-proof forms (Bury et al 2002).

## 2.4 Self-Consolidating Fiber Reinforced Concrete

Fiber Reinforced Concrete (FRC) requires a high degree of vibration to get good compactness. This increases the labor costs and noise pollution at the work site. Moreover, if the reinforcement is dense or the form is intricate in shape, it becomes even more difficult to place and vibrate the concrete. Unfortunately, when one tries to enhance the workability of FRC by adding more superplasticizers or intensifying the degree of vibration, segregation invariably occurs. Hence, the development of a Self-Consolidating Fiber Reinforced Concrete (SCFRC) should make for easier placement of concrete, save labor and avoid noise pollution. Self-Consolidating Concrete (SCC) offers several economic and technical benefits; the use of steel fibers extends its possibilities ([Grünewald and Walraven 2001](#)).

SCFRC appears to be a logical material for application to the end region of prestressed concrete I-beams. When steel fibers are added to the concrete mix, the tensile and shear resistance of the composite material is enhanced. However, fibers are also known to impede the workability of plain concrete. Moreover, the end zones are densely reinforced, making it necessary to use a highly workable concrete with steel fibers that would not only reduce or completely eliminate the conventional reinforcement but also make it easier to place concrete. The use of SCFRC for the end zone of prestressed girders would guarantee the following advantages:

- (a) Fibers in SCFRC are expected to partially or fully replace the dense reinforcement of the end region and also control the end zone cracking.
- (b) SCFRC would be easier to place and finish than the conventional FRC when used in the prestressed girders.
- (c) The shear and flexural strength of prestressed girders is expected to be improved with the use of SCFRC mixes. Additionally, the ductility of prestressed girders will also increase if SCFRC is utilized.
- (d) SCFRC might prove to be more economical in the long run, owing to the fact that both labor and time are saved with the use of SCFRC.

Some research experiments as well as field applications have been successfully carried out on SCFRC. The mix design of SCFRC could be based on the mix design of an existing SCC mix ([Pettersson 1998](#)). The workability of SCFRC is affected by fibers as they possess high

surface area. The degree to which workability decreases depends on the type and content of fibers, the matrix composition and the properties of the constituents of the matrix on their own. The higher the fiber content in SCFRC, more difficult it becomes to uniformly distribute the fibers in the matrix (Grünwald and Walraven 2001). Concrete with satisfactory workability could be made self-consolidating even with a large fiber content of up to 1.3 % by volume (Ambroise *et al* 2001).

## 2.5 Materials Used in the Research Project

Phase One of this research project involved the development of Self-Consolidating Concrete (SCC), TxDOT Traditional Fiber Reinforced Concrete (TTFRC) and Self-Consolidating Fiber Reinforced Concrete (SCFRC). In Phase Two of this research work, full scale I-girders were cast using suitable mixes from Phase One. All the mixes were produced and tested for their fresh properties at the Texas Concrete Company precast plant in Victoria, Texas. Thus, traditionally available construction materials that were used to manufacture the TxDOT girders had been utilized to develop the various mixes. As shown in Table 2.5.1, a total of ten different mixes were tested for their fresh and hardened properties. The table also states the nomenclature and importance of various mixes that were tested. The purpose of testing these mixes was to arrive at an optimized fiber content that would yield maximum workability and strengths.

(a) *Cement* – High early strength cement was used in all the mixes, since it was necessary to develop high release strengths at an early age in the beams. Portland cement (Type-III) conforming to ASTM C150-2002 and fly ash (Type-C) conforming to ASTM C618-2003 were the only powder materials used for the experiments. Fly ash was added to the mix to enhance workability, curtail rise in temperature and reduce cost. The weight ratios of cement to fly ash were 68:32 for TTC1 and TTFRC mixes and 69:31 and 70:30 for SCC and SCFRC mixes, respectively. The corresponding cementitious contents were 767 lb/yd<sup>3</sup> for TTC1 and TTFRC mixes and 808 lb/yd<sup>3</sup> and 837 lb/yd<sup>3</sup> for SCC and SCFRC mixes. A relatively high cementitious content was necessary in SCC to maintain its yield value and viscosity, thus imparting stability to the fresh mixes (Khayat *et al* 1997, Sonebi and Bartos 2002).

**Table 2.5.1 Description of Various Mixes Tested**

<b>Description of Mix</b>	<b>Mix Nomenclature</b>	<b>Significance</b>
Texas department of transportation Traditional Concrete mix	<b>TTC1</b>	This mix is traditionally used by TxDOT to cast I-girders. This mix served as a ‘control-mix’ for the TTFRC mixes.
TxDOT Traditional Fiber Reinforced Concrete mix	<b>TTFRC1</b>	These were the FRC mixes with TTC1 as the base mix, using various lengths and contents of steel fibers (i.e. variable fiber factor).
	<b>TTFRC2</b>	
	<b>TTFRC3</b>	
	<b>TTFRC4*</b>	
Self-Consolidating Concrete	<b>SCC2-3</b>	These SCC mixes were tested to provide guidelines for the development of satisfactory SCFRC mixes.
	<b>SCC4</b>	
Self-Consolidating Fiber Reinforced Concrete	<b>SCFRC1</b>	These were the SCFRC mixes with different lengths and contents of steel fibers (i.e. variable fiber factor).
	<b>SCFRC2</b>	
	<b>SCFRC3</b>	

\* - Mix not tested for hardened properties.

(b) *Coarse and Fine Aggregates* –The mixes utilized uniformly-graded, rounded, river-bed, coarse aggregates of 3/4 inch nominal size (AASHTO T27 1996) and well-graded, river-bed sand with a fineness modulus of 2.55 (AASHTO M43 1998). The specific gravity of the coarse aggregates was 2.6 and that of the fine aggregates was 2.63. Sieve analysis details for the coarse and fine aggregates are shown in Table 2.5.2.

**Table 2.5.2 Gradation Details of Aggregates (a) Coarse Aggregates (b) Fine Aggregates**

(a) Sieve Analysis for Coarse Aggregates

Sieve Size (in.)	% Retained	Specified -AASHTO T27 1996
1	0	0
0.75	3	0-10
0.375	62	45-80
0.187	95	90-100
0.093	99	95-100

(b) Sieve Analysis for Fine Aggregates

Sieve Size (in.)	% Retained	Specified -AASHTO M43 1998
0.375	0	0
0.187	1.4	0-5
0.093	15	0-20
0.046	25.4	15-50
#30	44.4	35-75
#50	74.4	65-90
#100	94.8	90-100
#200	99.4	97-100

(c) *Admixtures* - A Polycarboxylate-based HRWR (Master Builders-Glenium-3200HES) conforming to ASTM C 494-1999, Type F was used to achieve a flowable and cohesive SCC and SCFRC mix. An organic modified cellulose ether-based VMA (Master Builders-Rheomac-450) was used as required to improve the stability of the mix. A retarder conforming to ASTM C 494-1999, Type-B was added to the mixes as required to delay the initial setting of the mix.

(d) *Steel fibers* – Two types of steel fibers manufactured by Bekaert-Dramix<sup>®</sup> were used. RC80/60BN (Fig. 2.5.1) and ZP305, (Fig. 2.5.2) having a ‘trough’ shape with hooks at both ends, were used in the TTFRC and SCFRC mixes. The RC80/60BN fibers had a length of 2.4 inch, a diameter of 0.03 inch (aspect ratio of 80) and possessed a tensile strength of 150 ksi. The ZP305 fibers were 1.2 inches long and 0.022 inch in diameter (aspect ratio of 55) and possessed a tensile strength of 160 ksi. The fibers were relatively stiff and glued into bundles. The glue dissolved in the water during mixing, thus dispersing the fibers in the mix.



**Fig. 2.5.1 Steel Fiber RC80/60BN**  
(Bekaert-Dramix®)



**Fig. 2.5.2 Steel Fiber ZP305**  
(Bekaert-Dramix®)

**Table 2.5.3 Constituents of Various Mixes**

Components	Description	Reference Code
<b>Portland Cement</b>	Type-III	ASTM C150
<b>Fly Ash</b>	Type-C	ASTM C618
<b>Coarse Aggregates</b>	¾ in. Rounded River-bed gravel	AASHTO T27
<b>Fine Aggregates</b>	FM = 2.55, Well Graded, River-bed	ASHTO M 43
<b>HRWR</b> Glenium3200HES & Rheobuild1000	Type-F (Polycarboxylate based)	ASTM- C494
<b>VMA</b> Rheomac450	Organic Modified Cellulose Ether	-
<b>Retarder</b>	Type-B	ASTM - C494
<b>Steel Fibers</b> * Bekaert Dramix® * Hooked Ends 	RC80/60BN ↓ L = 2.4 in., D = 0.030 in. L/D = 80	ZP305 ↓ L = 1.2 in., D = 0.022 in. L/D = 55

Table 2.5.3 shows the details of various constituents used in the mixes. Table 2.5.4 and Table 2.5.5 present the mix proportions of various mixes. Table 2.5.4 shows the mix proportions of the traditionally used normal-slump concretes: TTC1 and various TTFRC mixes. The TTC1

mix was the control mix for the different TTFRC mixes. Four TTFRC mixes were tested with different types and amounts of fibers. The hardened properties of the TTFRC4 mix were not tested as this mix was not planned in the initial stages, but was decided by the Texas Concrete Company to be used to cast a beam in the final stage of the research. [Table 2.5.5](#) shows the mix proportions of various SCC and SCFRC mixes. Two SCC mixes were cast. SCC4 differed from the SCC2-3 mix only in the proportions of coarse aggregates (CA) and fine aggregates (FA). Because of the higher CA/FA ratio, SCC4 required the addition of VMA to maintain its stability. Three SCFRC mixes were essentially the same apart from the use of different types and amounts of steel fibers used. Besides the added fibers, the basic proportions of SCFRC mixes were very similar to the control SCC2-3 mix. Slightly higher cement and fine aggregate contents were used in the SCFRC mixes to stabilize the mixes due to the addition of fibers.

**Table 2.5.4 Mix Proportions of Various Normal-Slump Concrete Mixes**

<b>Component</b> (lb/yd <sup>3</sup> )	<b>TTC1</b>	<b>TTFRC1</b>	<b>TTFRC2</b>	<b>TTFRC3</b>	<b>TTFRC4*</b>
<b>Cement</b>	519	519	519	519	519
<b>Fly ash</b>	248	248	248	248	248
<b>Cementitious materials</b>	767	767	767	767	767
<b>Water/Cement ratio (w/c)</b>	0.43	0.43	0.43	0.43	0.43
<b>Water/Cementitious ratio</b>	0.3	0.3	0.3	0.3	0.3
<b>Coarse aggregate (CA)</b>	1899	1899	1899	1899	1899
<b>Fine aggregate (FA)</b>	1156	1156	1156	1156	1156
<b>CA / FA ratio</b>	1.64	1.64	1.64	1.64	1.64
<b>HRWR / Superplastizer</b> (fl.oz./cwt)	9.6 (R) (20)	14 (R) (30)	12 (R) (24)	9.6 (R) (20)	9.6 (R) (20)
<b>VMA</b> (fl.oz./cwt)	0	0	0	0	0
<b>RC80/60BN</b> Long Fiber [LF]	0	0	132 (1 %) <b>V<sub>f</sub> = 80</b>	66 (0.5 %) <b>V<sub>f</sub> = 40</b>	0
<b>ZP305</b> Short Fiber [SF]	0	132 (1 %) <b>V<sub>f</sub> = 55</b>	0	0	198 (1.5 %) <b>V<sub>f</sub> = 82.5</b>
<b>Retarder</b> (fl.oz./cwt)	1.0 (3)	1.0 (3)	1.0 (3)	1.0 (3)	1.0 (3)

**NOTE:** R=Rheobuild-1000 V<sub>f</sub>= Fiber Factor = (Vol. of fiber) x (Aspect ratio of fiber)

\* - Hardened properties of this mix were not tested.

**Table 2.5.5 Mix Proportions of Various SCC and SCFRC Concrete Mixes**

<b>Component</b> (lb/yd <sup>3</sup> )	<b>SCC2-3*</b>	<b>SCC4</b>	<b>SCFRC1</b>	<b>SCFRC2</b>	<b>SCFRC3</b>
<b>Cement</b>	555	555	587	587	587
<b>Fly ash</b>	253	253	250	250	250
<b>Cementitious materials</b>	808	808	837	837	837
<b>Water/Cement ratio (w/c)</b>	0.43	0.43	0.43	0.43	0.43
<b>Water/Cementitious ratio</b>	0.3	0.3	0.3	0.3	0.3
<b>Coarse aggregate (CA)</b>	1501	1794	1540	1540	1540
<b>Fine aggregate (FA)</b>	1514	1196	1580	1580	1580
<b>CA / FA ratio</b>	0.99	1.5	0.97	0.97	0.97
<b>HRWR / Superplastizer</b> (fl.oz./cwt)	7.2 (GL) (14)	7.2 (GL) (14)	10.5 (GL) (20)	10.5 (GL) (20)	10.5 (GL) (20)
<b>VMA</b> (fl.oz./cwt)	0	0.3 (2)	0	0	0
<b>RC80/60BN</b> Long Fiber [LF]	0	0	66 (0.5 %) <b>V<sub>f</sub> = 40</b>	0	0
<b>ZP305</b> Short Fiber [SF]	0	0	0	66 (0.5 %) <b>V<sub>f</sub> = 28</b>	132 (1 %) <b>V<sub>f</sub> = 55</b>
<b>Retarder</b> (fl.oz./cwt)	1.5 (4.4)	1.5 (4.4)	1.6 (4.4)	1.6 (4.4)	1.6 (4.4)

**NOTE:** GL = Glenium 3200 HES    V<sub>f</sub> = Fiber Factor = (Vol. of fiber) x (Aspect ratio of fiber)

\* - SCC2 & SCC3 mixes were identical; hence the combination mix was represented as SCC2-3.

## 2.6 Mixing Procedure

All concrete mixes were mixed in a 6 yd<sup>3</sup> drum mixer at the Texas Concrete Company's Victoria, Texas, precast plant (Fig. 2.6.1). The yield for each mix was 2 yd<sup>3</sup>. The following step-by-step procedure was adopted to mix the concrete:

1. Fine and coarse aggregates were first fed into the mixer-drum using a conveyor belt.
2. Cement and fly ash were then added to the aggregates inside the drum and initial dry mixing was carried out for 30 seconds.
3. Premixed water with HRWR was then introduced into the mix and mixed for 120 seconds.
4. SCC4 was mixed following steps 1 to 3 without any VMA dose. Preliminary workability tests indicated SCC4 to be flowable but highly unstable. To rectify this instability, VMA was separately introduced into the fresh SCC4 and mixed for an extra 60 seconds.
5. In the case of TTFRC and SCFRC mixes, fibers in the form of bundles were uniformly fed along with the fine and coarse aggregates on the conveyor belt.



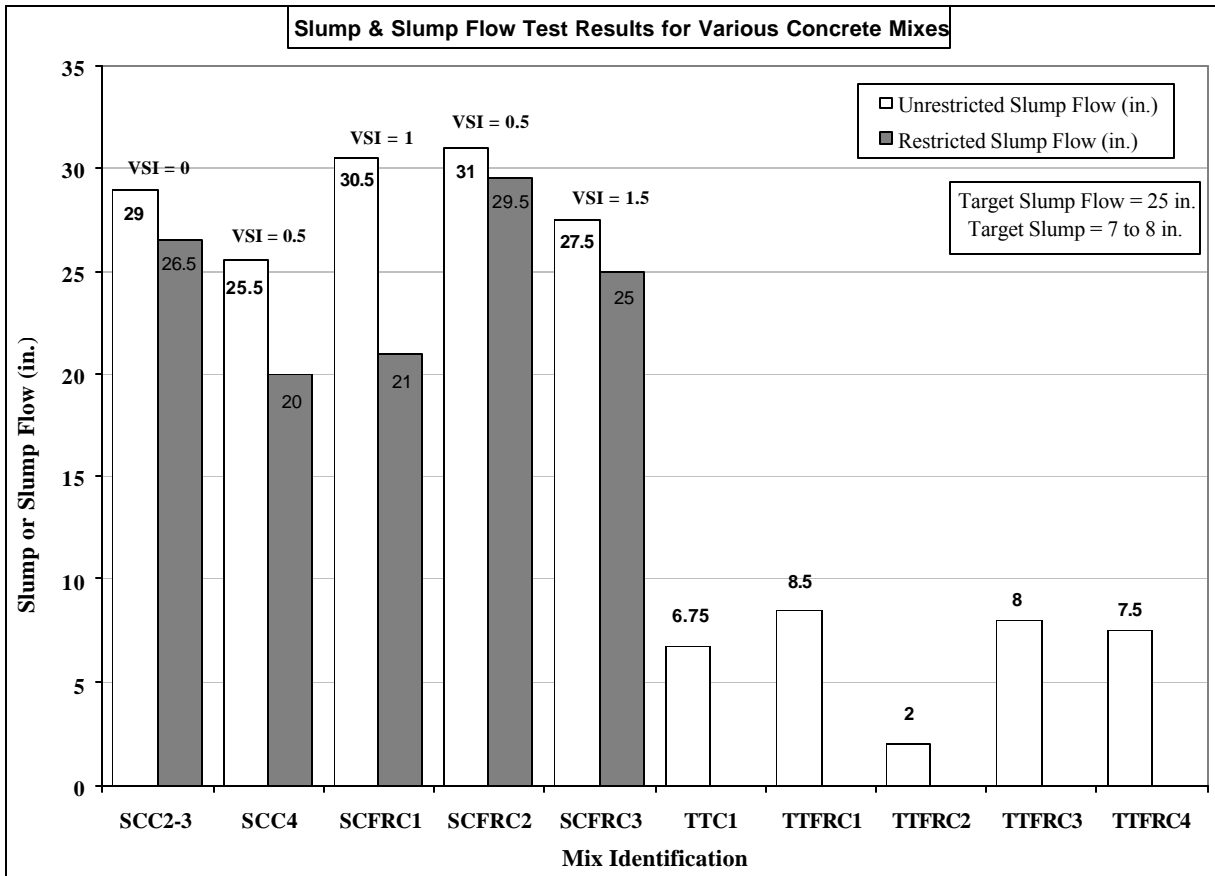
**Fig. 2.6.1 Concrete Mixer at the Precast Plant-Texas Concrete Co., Victoria, Texas**

## 2.7 Results of Workability Tests of Concrete Mixes

All workability tests were conducted near the mixer, after waiting for 60 seconds of mixing, unless otherwise stated. Both quantitative and qualitative measurements were taken to judge the workability of the mixes in accordance with the PCI-2003 guidelines. Slump tests were conducted for traditional normal-slump concretes, TCC1 and various TTFRC mixes in

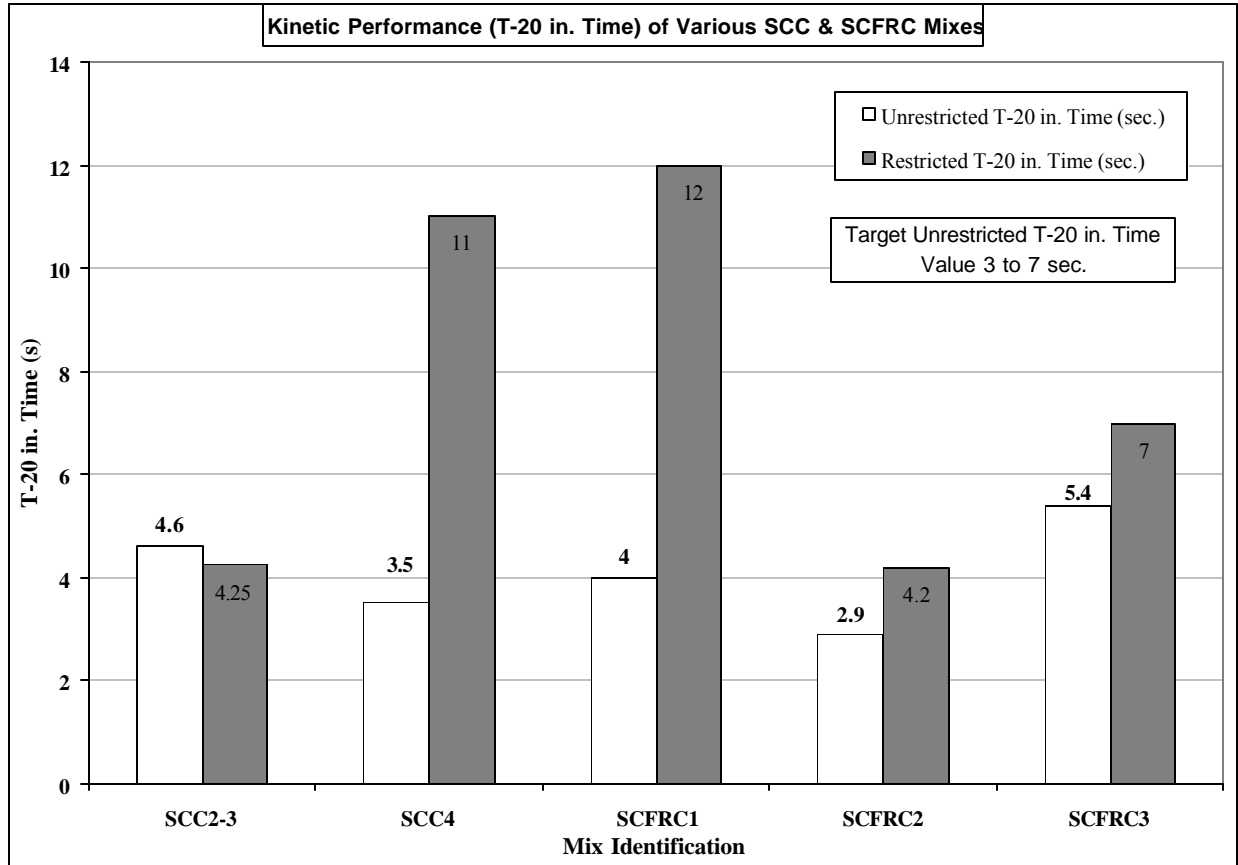
accordance with ASTM C143/C143-2003. A slump flow test, T-20in time measurement and VSI rating were carried out for all the SCC/SCFRC mixes. The targeted minimum slump flow for the research was 25 inches. The targeted T-20in and VSI for the research project were 3 to 7 seconds and 0 to 1, respectively. During the slump flow test, there was no restriction offered to the freely flowing SCC/SCFRC. Hence, the flow spread and T-20in time recorded during this test were referred to as the unrestricted slump flow and unrestricted T-20in time.

Fig. 2.7.1 shows the results of slump and slump flow tests for various mixes. The figure also depicts the values of unrestricted and restricted (with J-ring) slump flow for all the mixes. All the mixes achieved the minimum target level of unrestricted slump flow, i.e. 25 inches. None of the mixes showed segregation, bleeding or halo-formation, giving a satisfactory VSI, within the targeted value of 0 to 1. The unrestricted slump flow for SCC4 was less than that for SCC2-3. This was because SCC4 had a relatively higher CA/FA ratio, which made the mix harsher, and also because VMA reduced the slump flow, as it increased the viscosity of the mix. Moreover, SCC4 had a larger coarse aggregate content, which made the SCC4 mix more difficult to pass through the J-ring. The unrestricted slump flows of SCFRC mixes were as good as that of the SCC mixes. Comparatively larger slump flow could be attributed to the slightly more cementitious material content in the SCFRC mixes. Apparently, fibers did not affect the unrestricted slump flow. Restricted slump flow for SCFRC1 mix was considerably lower than its unrestricted slump flow. Long fibers hindered the flow of SCFRC through the J-ring and thus lowered the slump flow. TTFRC mixes in general had satisfactory workability. TTFRC2 with 1 % by volume of long fibers had low workability due to a large quantity of fibers.



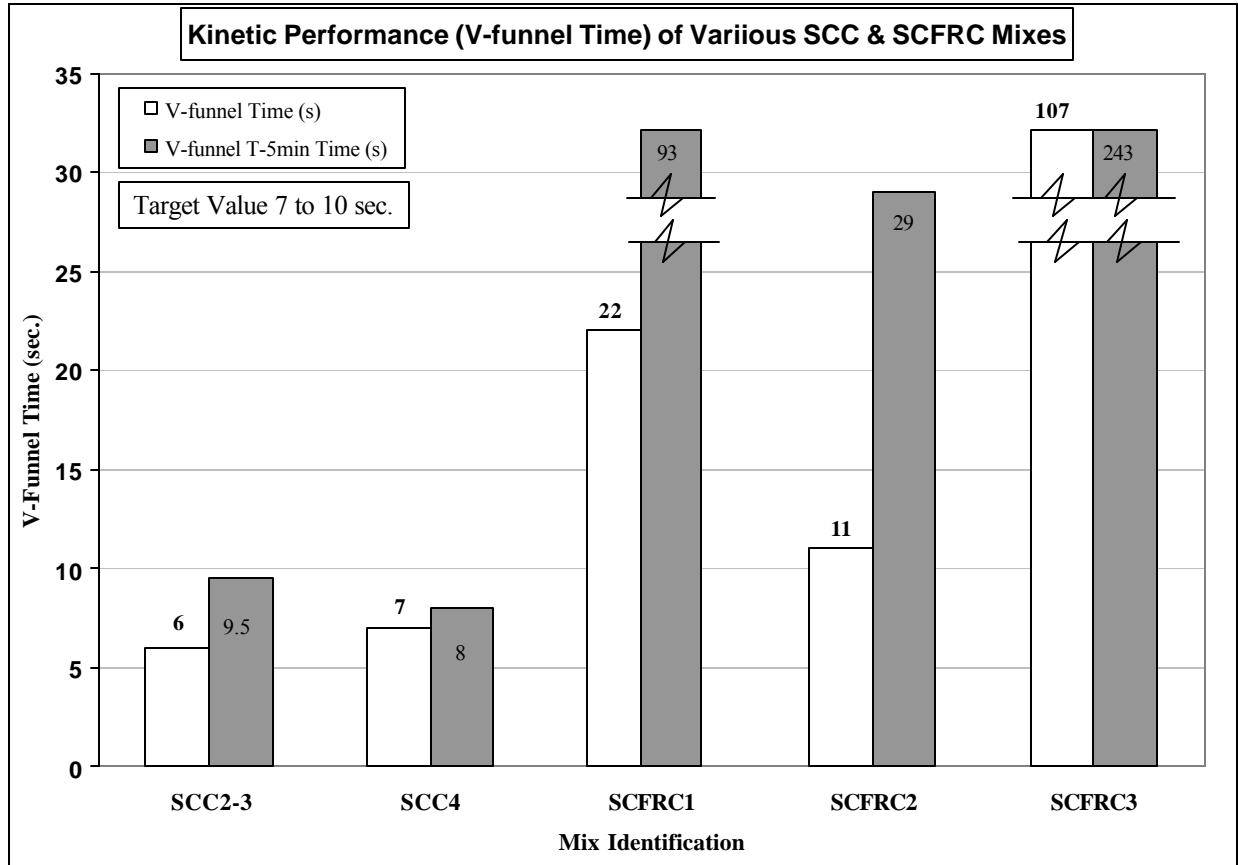
**Fig. 2.7.1 Results of Slump and Slump Flow Test**

Fig. 2.7.2 shows the kinetic performance, i.e. T-20in time, measured during the slump flow and J-ring tests for various mixes. All the SCC/SCFRC mixes performed satisfactorily with regards to the T-20in time as they were within the targeted values. The restricted T-20in time for SCC4 and SCFRC1 mix was considerably high. This was due to a high aggregate content in SCC4 and the use of long fibers in SCFRC1. The SCFRC mixes with short fibers did not show escalated values of restricted T-20in time, since the short fibers passed readily through the J-ring.



**Fig. 2.7.2 Results of T-20in Time for Different Mixes**

The filling ability of various mixes was measured using the V-funnel by noting the time (T sec) taken for the mix to completely empty-out through the funnel, which had a rectangular opening of 3 x 2.5 inches. The targeted V-funnel time was between 7 and 10 seconds. After this, the funnel was refilled with the recently tested mix and left standing for 5 minutes. The V-funnel time recorded after 5 minutes of standing was the T-5 time. The SCC mixes showed good filling ability, whereas the SCFRC mixes had comparatively lower filling abilities as shown in Fig. 2.7.3. Fibers blocked the opening of the V-funnel causing extended time delays in emptying the V-funnel.



**Fig. 2.7.3 V-funnel Time for Different Mixes**

The passing ability of various SCC/SCFRC mixes was evaluated using the J-ring apparatus with a clear bar spacing of 1.75 inches, to simulate actual congestion of reinforcement in beams. The desired J-ring value was the vertical offset of 0.4 to 0.6 inch. Slump flow and T-20in time was also measured during the J-ring test, which indicated the restricted slump flow and restricted T-20in time which were already discussed. SCC2-3 mix was the only mix that measured a J-ring value within the targeted range of 0.4 to 0.6 in. as seen in Fig. 2.7.4. Thus, large amounts of aggregates or fibers were found to be detrimental to the passing ability of SCC/SCFRC. Long fibers drastically reduced the passing ability of SCFRC due to the blocking effect.

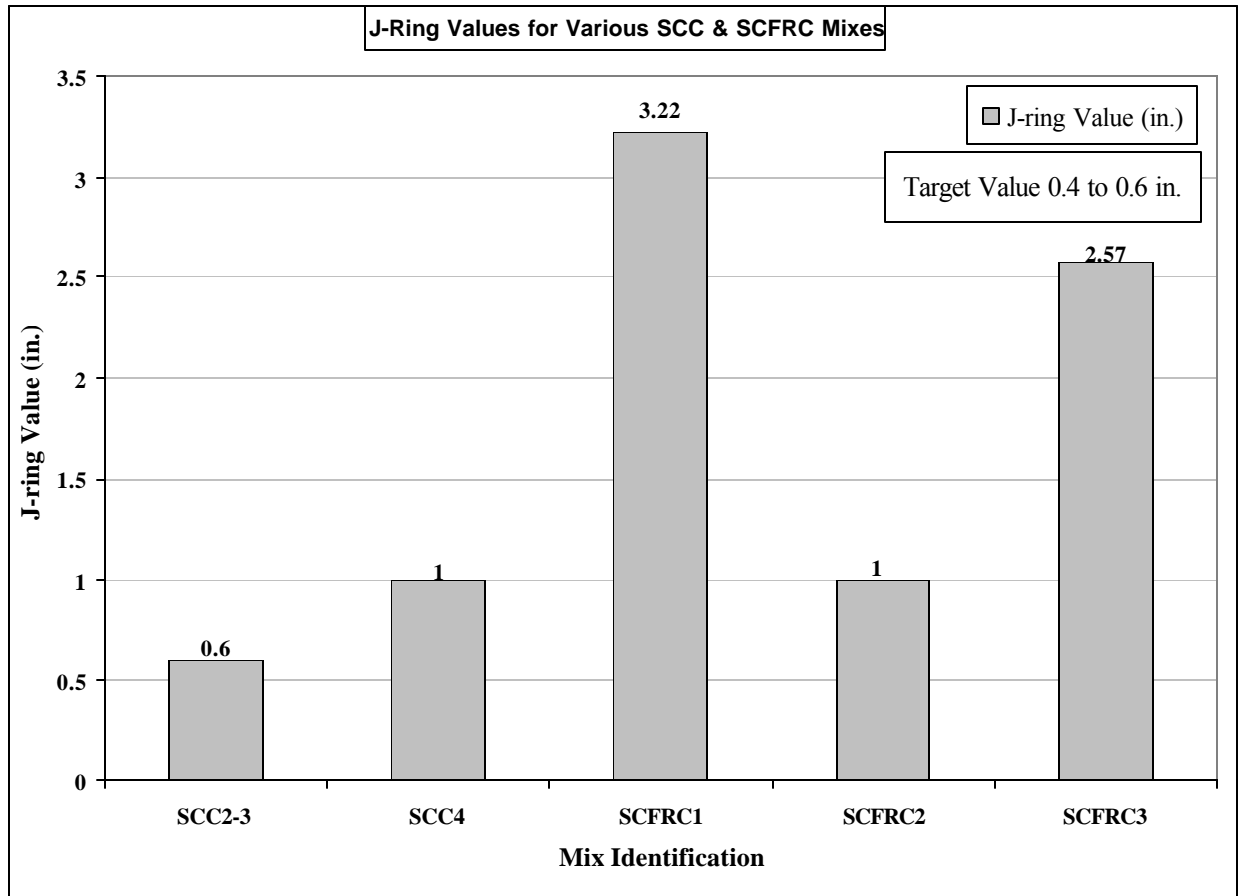


**Fig. 2.7.4 J-ring Values for Different Mixes**

## 2.8 SCC-Texas Workshop Demonstration

The SCC-Texas Workshop took place at University of Houston on March 11, 2004. A total of 175 participants attended the workshop. In addition to the eight presentations and two panel discussions, the casting of the end region of a Type-A beam using a plexiglass mold (Fig. 2.8.1) and SCFRC2 mix was demonstrated to the participants. It is also to be noted that vibration was not used in this demonstration. The demonstration revealed that the SCFRC mix flowed and filled the mould quite efficiently without any signs of instability or fiber blocking. The passing ability of SCFRC2 mix measured by the J-ring was much lower than the actual passing ability of the mix observed in the demonstration. Hence, it was decided to disregard the passing ability values measured by the J-ring during the preliminary workability tests of SCFRC1 and SCFRC3 mixes, as being too conservative, and select these SCFRC mixes to cast the I-beams. It can be

seen from Fig. 2.8.1 that the application of SCFRC to the end region with dense reinforcements is promising due to the enhanced workability.



**Fig. 2.8.1 SCC-Texas Workshop Demonstration at University of Houston**

## **2.9 Results of Hardened Properties of Concrete Mixes**

Hardened properties of the mixes were tested at 1, 3, 7 and 28 days after casting. The specimens were air cured and tested at the University of Houston testing laboratory. Cylinder compressive strength, split tensile strength, beam flexure-Modulus Of Rapture (MOR) strength and Average Residual Strength (ARS) tests were conducted to determine the hardened properties of the mixes. The density of the concrete was also measured during these tests. Along with the compressive strength tests, the stress-strain curve, modulus of elasticity and Poisson's ratio were also experimentally determined.



(a)



(b)

**Fig. 2.9.1 (a) & (b) Cylinder Compression Test: (a) Failed Cylinders (b) Measurement of Elastic Modulus and Poisson's Ratio**



**Fig. 2.9.2 Split Cylinder Test Specimens**

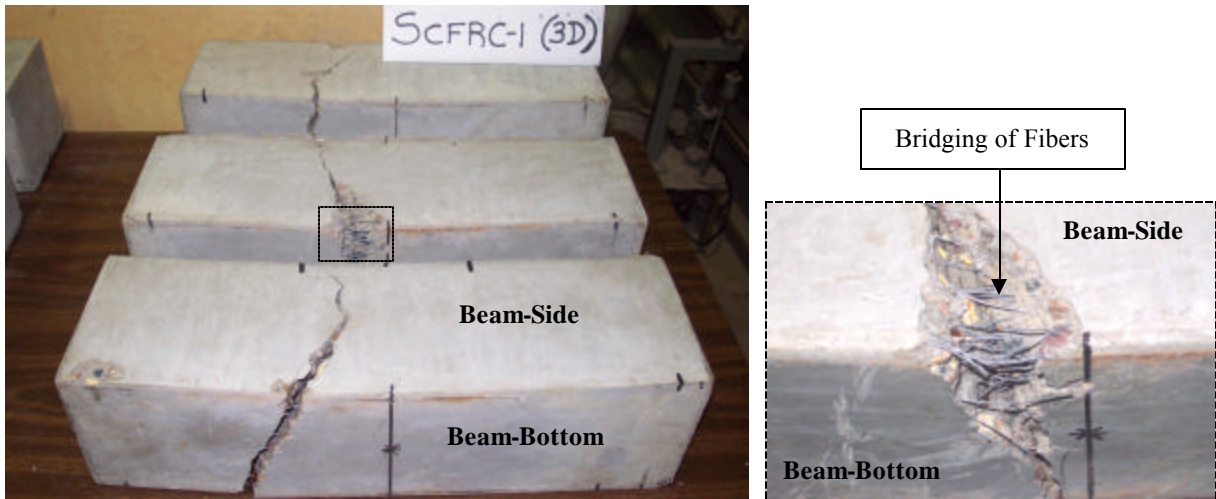


**Fig. 2.9.3 Beam Flexure Test (Modulus of Rapture) Specimens**

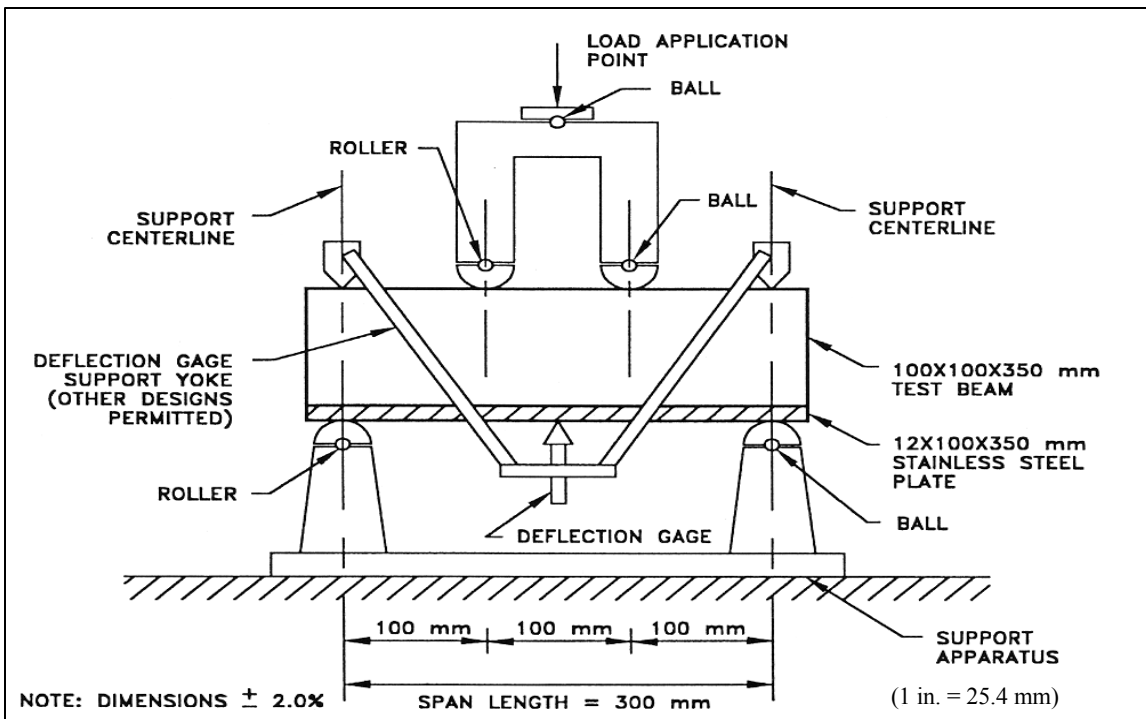


**Fig. 2.9.4 Average Residual Stress Test (ASTM C1399-1999)**

As shown in Fig. 2.9.1 (a), 6 x 12 in. cylinder specimens were tested for compressive strengths as per ASTM C39/39M-2003 procedure. Cylinder specimens of 4 x 8 in. size were also tested for compressive and split tensile strengths. The modulus of elasticity and Poisson's ratio were determined in accordance with the ASTM C469-2002 guidelines. Split cylinder tests were

carried out as per ASTM C496-1996. Fig. 2.9.2 shows the failed split cylinder specimens. ASTM C78-2002 procedures were followed to conduct the MOR test, and the failed specimens are shown in Fig. 2.9.3. ARS (Fig.2.9.4) tests were carried out in accordance with ASTM C1399-1999. Table 2.9.1 presents the hardened properties of the mixes in detail.

**Table 2.9.1 Hardened Properties of Various Mixes**

Properties	Days	TTC1	TTFRC1	TTFRC2	TTFRC3	SCC2-3	SCC4	SCFRC1	SCFRC2	SCFRC3
Compressive Strength (psi)	1	6405	6601	4383	5562	4916	6162	6950	6691	7500
	3	7648	8608	7002	7747	5771	8154	8884	8553	9056
	7	9321	9703	8420	9109	6525	10298	9455	9724	10223
	28	11550	11883	10294	11337	8367	12346	12021	12271	13070
Split Tensile Strength (psi)	1	446	668	727	497	383	377	733	711	878
	3	561	787	900	629	479	436	898	866	977
	7	695	878	1015	680	566	529	935	1100	1139
	28	918	1050	1120	748	667	631	1082	1154	1226
Modulus of Rupture (psi)	1	845	976	1492	1175	580	754	1250	1190	1588
	3	933	1278	2338	1500	769	840	1558	1412	1867
	7	1009	1424	2742	1640	911	967	1649	1547	1944
	28	1181	1563	3294	1814	1146	1069	1801	1664	2225
Avg. Residual Strength (psi)	1	0	959	1417	864	0	0	1055	756	1368
	3	0	1092	1660	920	0	0	1330	1110	1713
	7	0	1171	1918	1002	0	0	1621	1339	2061
	28	0	1286	2265	1150	0	0	1809	1490	2240
Elastic Modulus (ksi)	1	5693	4967	4381	5801	3105	3576	5650	5453	5731
	3	6050	5752	5236	5933	3700	4300	5995	5810	6100
	7	6488	6090	5681	6074	4730	5448	6225	6030	6377
	28	6909	6641	6086	6598	5800	6600	6550	6317	6750
Poisson's Ratio	1	0.170	0.166	0.180	0.180	0.175	0.180	0.170	0.186	0.173
	3	0.168	0.182	0.190	0.190	0.180	0.130	0.176	0.182	0.179
	7	0.190	0.174	0.195	0.195	0.182	0.140	0.190	0.175	0.206
	28	0.188	0.205	0.200	0.200	0.200	0.230	0.196	0.173	0.191
Release $f_c$ (psi)	0.75	6790	6860	5000	5800	6175	6900	7020	6950	7850
Density (pcf)	1	154	156	156	156	149	155	154	152	154

**Note:** Release  $f_c$  was the compressive strength of cylinders at release of prestress, about 18-hours after casting.

The cylinders under compression failed mostly in the “shear-type” failure mode for all mixes. As depicted in Fig.2.9.5, there was a steady increase in the compressive strength for all the mixes as each mix aged. SCC4, which had a higher CA/FA ratio, was much stronger than the SCC2-3 mix. In general, the compressive strength at various ages for SCC2-3 was about 43 % less than SCC4, but the 18-hour compressive strength of steam cured cylinders for SCC4 was only about 12 % more than SCC2-3. The steel fibers seem to have improved the compressive strength of TTFRC and SCFRC, in comparison with SCC2-3. Release strengths tested about 18

hours after casting of all the mixes were satisfactory, i.e. at least equal to the targeted value of 5600 psi.

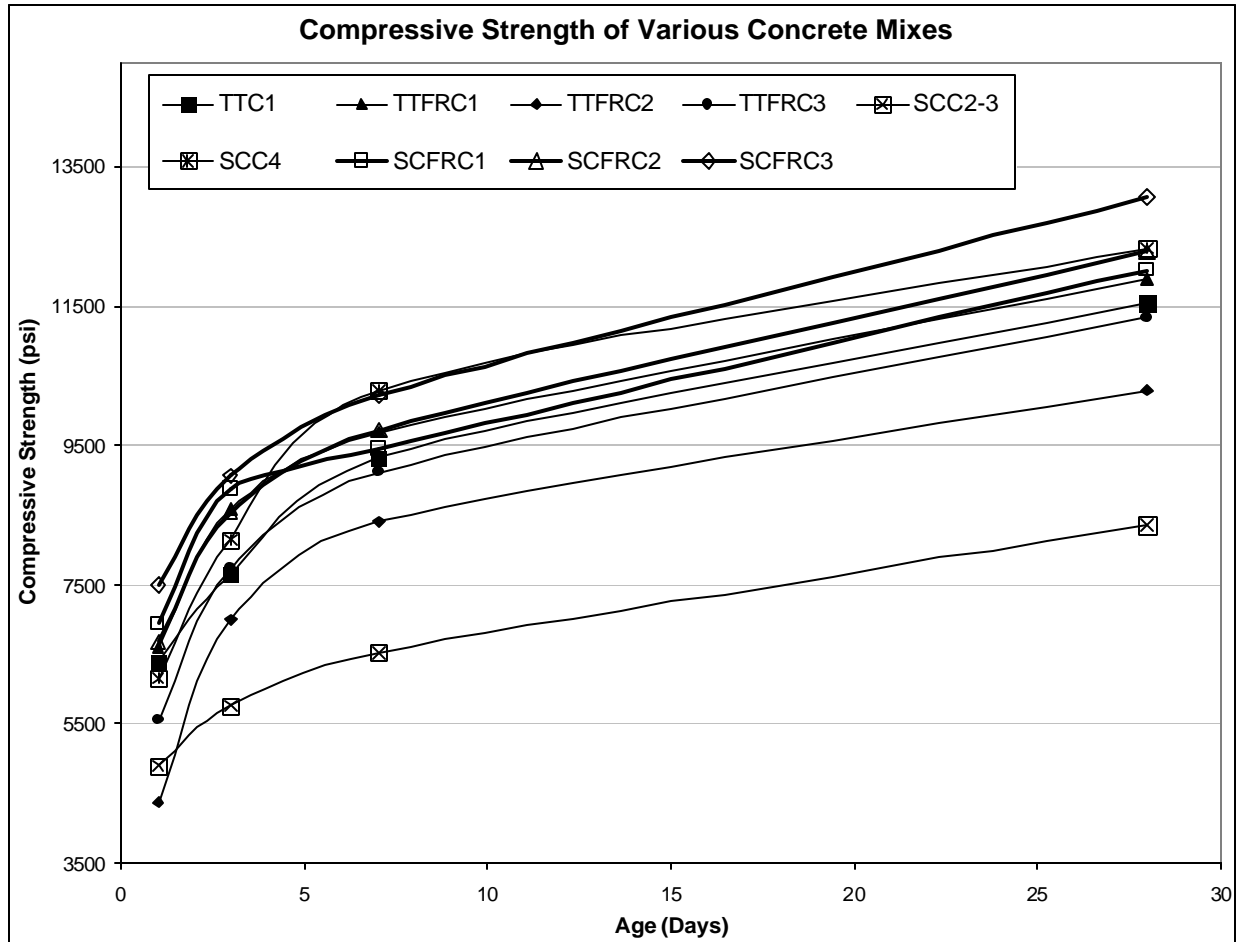


**Fig. 2.9.5** Variation of Compressive Strength of Various Mixes with Age

Fig. 2.9.6 shows the variation of split tensile strength at different ages for the mixes. There was a steady increase in the split tensile strength with age. On average, the split tensile strength of TTC1 and TTFRC mixes was about 7.5 % and 10.1 % of their compressive strength, respectively. Also the average split tensile strength of SCC2-3 and SCFRC mixes was 8.2 % and 10.4 % of their compressive strength, respectively. Hence, nearly the same compressive strength was observed for SCC and SCFRC, while the split-tensile strengths for SCFRC were observed to be 50 % higher than those for SCC2-3. Also, TTFRC mixes had an average of 25 % more split

tensile strength than the control TTC1 mix. Thus, clearly fibers substantially increased the tensile strength of concrete.

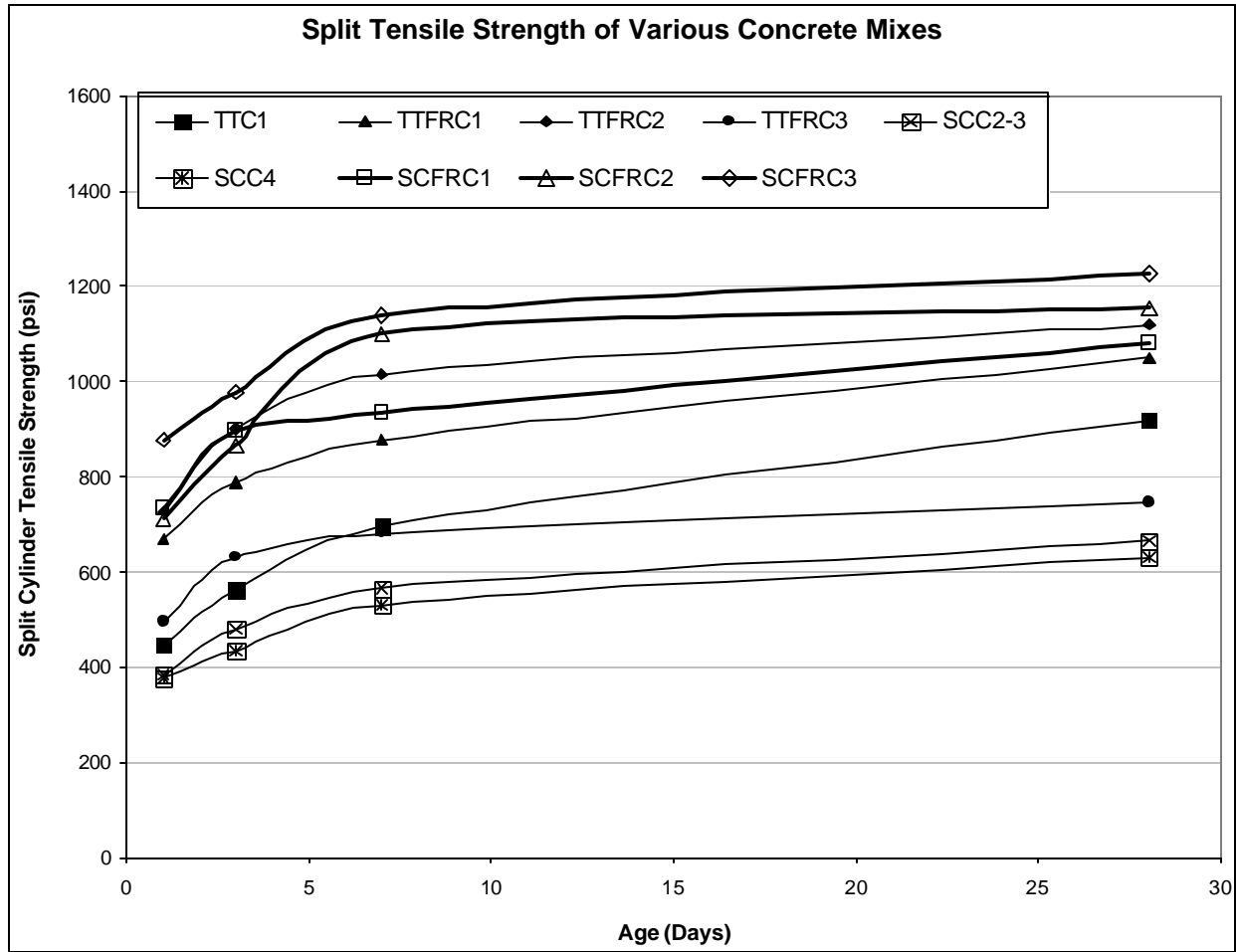


**Fig. 2.9.6 Variation of Split Tensile Strength of Various Mixes with Age**

Fig. 2.9.7 shows the variation of MOR values for various concrete mixes with age. The TTFRC and SCFRC beams demonstrated more ductility with fibers that bridged the cracks (Fig. 2.9.3) and failed in bond. The fibers were rarely broken. The TTFRC2 mix had the greatest MOR value. This was due to the use of 1 % long fibers having a maximum fiber factor of 80. Equivalent TTFRC and SCFRC mixes had almost the same MOR value. For SCFRC the MOR value was about 18 % of its compressive strength. MOR values for SCFRC were almost twice as large as those for SCC2-3. This proves that the fibers do increase the tensile strength of

concrete. MOR values for SCFRC2 were slightly less than that of SCFRC1, as the fiber factor of the former was comparatively less.

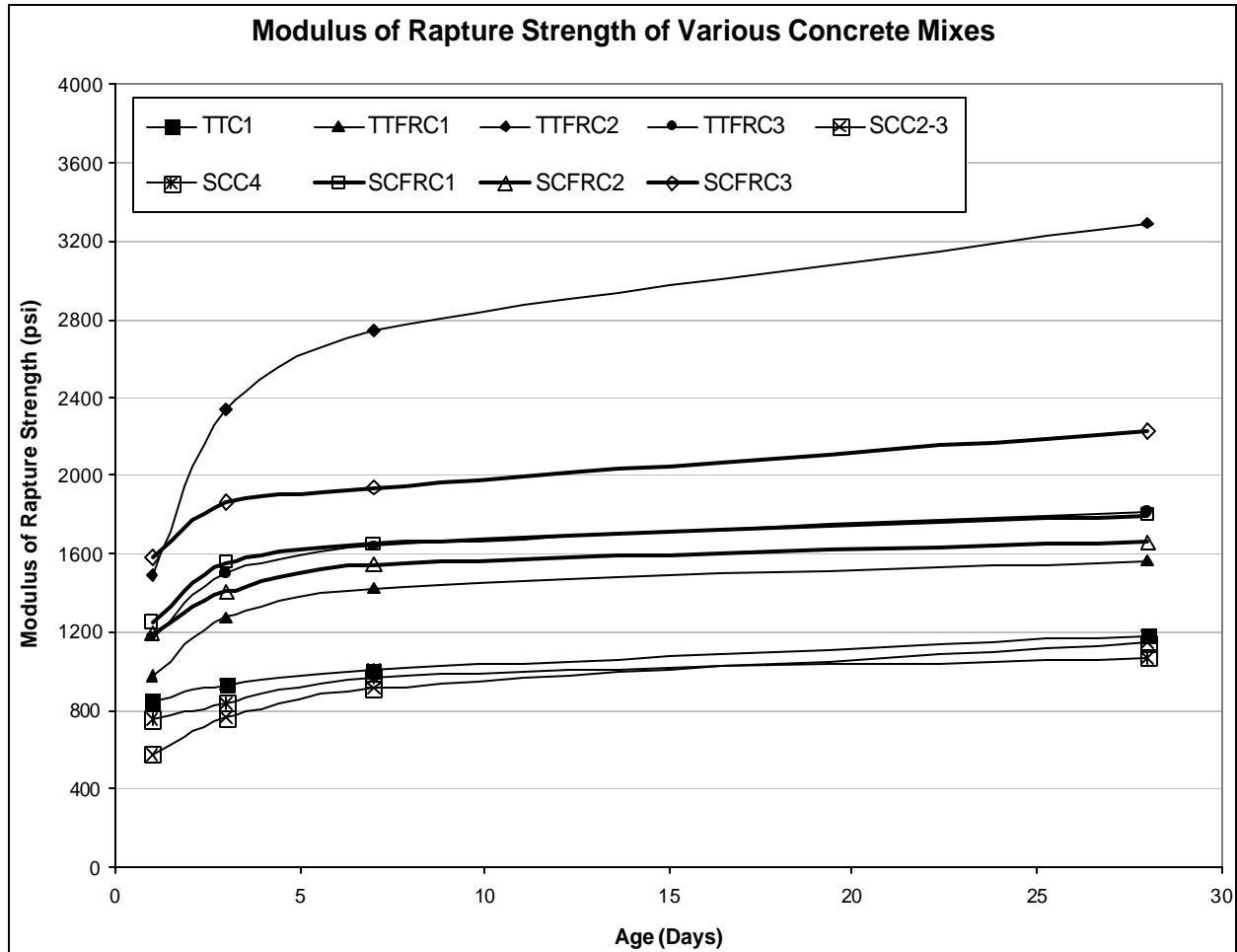


**Fig. 2.9.7** Variation of Modulus of Rapture Strength of Various Mixes with Age

ARS test results (Fig. 2.9.8) show the residual strength in the fiber reinforced beams after the first crack. ARS values for all the fiber mixes continued to increase steadily with age. SCFRC3 and TTFRC2 mixes had the maximum and almost the same residual strength. The least ARS strength was for TTFRC3 and TTFRC1 mixes as they had comparatively smaller fiber factors.

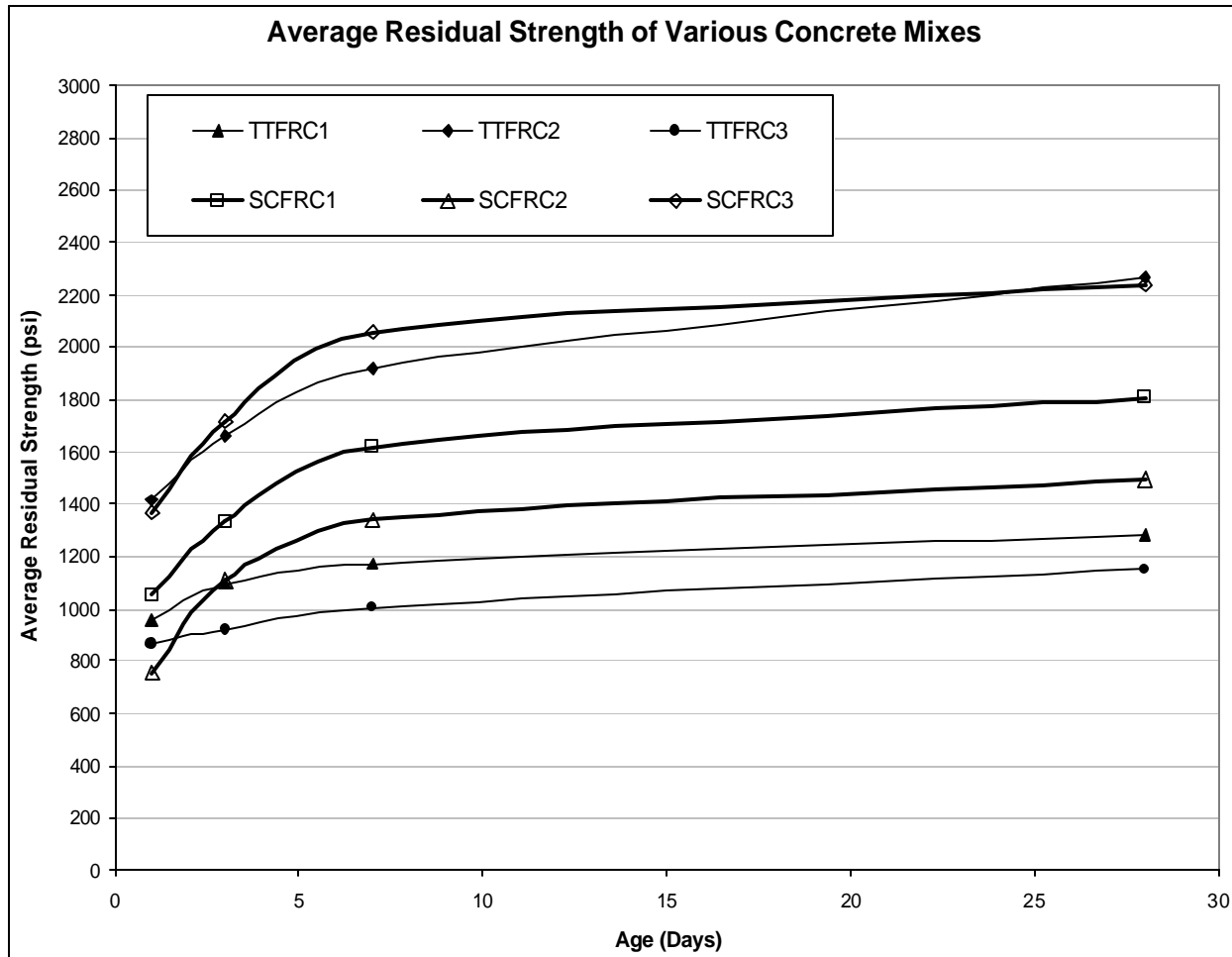


**Fig. 2.9.8** Variation of Average Residual Strength of Various Mixes with Age

The modulus of elasticity gradually increased for the concrete mixes as shown in Fig. 2.9.9. Fibers considerably enhanced the modulus of elasticity in the case of the SCFRC mixes. The TTFRC mixes had slightly smaller values for the modulus of elasticity than the non-fiber TTC1 mix. This may be due to the decreased workability and stability of the TTFRC mixes. SCC mixes had the smallest modulus of elasticity of all the mixes.

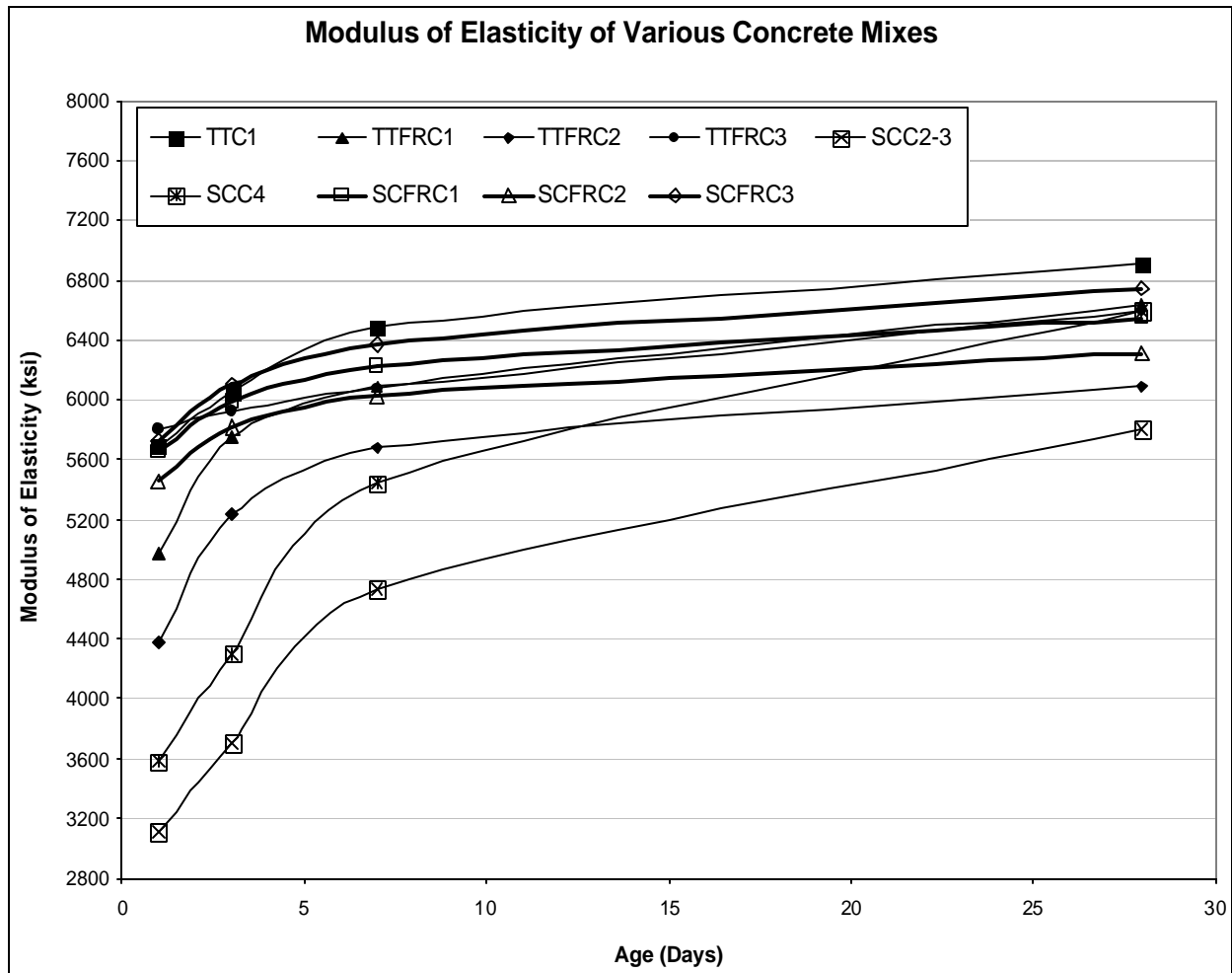


**Fig. 2.9.9 Variation of Modulus of Elasticity of Various Mixes with Age**

To get a better idea and to compare the mixes for their mechanical strengths, normalized hardened property values were calculated. The normalized value of a mix at a particular age is the ratio of its individual hardened property value and its respective compressive strength. [Table 2.9.2](#) presents the normalized strength values for various mixes at different ages.

**Table 2.9.2: Normalized Hardened Properties of Various Mixes**

Properties	Days	TTC1	TTFRC1	TTFRC2	TTFRC3	SCC2-3	SCC4	SCFRC1	SCFRC2	SCFRC3
<b>Split Tensile Strength (%)</b>	<b>1</b>	7.0	10.1	16.6	8.9	7.8	6.1	10.6	10.6	11.7
	<b>3</b>	7.3	9.1	12.9	8.1	8.3	5.4	10.1	10.1	10.8
	<b>7</b>	7.5	9.0	12.0	7.5	8.7	5.1	9.9	11.3	11.1
	<b>28</b>	8.0	8.8	10.9	6.6	8.0	5.1	9.0	9.4	9.4
<b>Average</b>		<b>7.5</b>	<b>9.3</b>	<b>13.1</b>	<b>7.8</b>	<b>8.2</b>	<b>5.4</b>	<b>10.0</b>	<b>10.4</b>	<b>10.8</b>
<b>Modulus of Rupture (%)</b>	<b>1</b>	13.2	14.8	34.0	21.1	11.8	12.2	18.0	17.8	21.2
	<b>3</b>	12.2	14.9	33.4	19.4	13.3	10.3	17.5	16.5	20.6
	<b>7</b>	10.8	14.7	32.6	18.0	14.0	9.4	17.4	16.0	19.0
	<b>28</b>	10.2	13.2	32.0	16.0	13.7	8.7	15.0	13.6	17.0
<b>Average</b>		<b>11.6</b>	<b>14.4</b>	<b>33.0</b>	<b>18.6</b>	<b>13.2</b>	<b>10.2</b>	<b>17.0</b>	<b>16.0</b>	<b>19.5</b>
<b>Avg. Residual Strength (%)</b>	<b>1</b>	0.0	14.5	32.3	15.5	0.0	0.0	15.2	11.3	18.2
	<b>3</b>	0.0	12.7	23.7	11.9	0.0	0.0	15.0	13.0	19.0
	<b>7</b>	0.0	12.1	22.8	11.0	0.0	0.0	17.1	13.8	20.2
	<b>28</b>	0.0	10.8	22.0	10.1	0.0	0.0	15.0	12.1	17.1
<b>Average</b>		<b>0.0</b>	<b>12.5</b>	<b>25.2</b>	<b>12.1</b>	<b>0.0</b>	<b>0.0</b>	<b>15.6</b>	<b>12.6</b>	<b>18.6</b>

TTFRC2 mix had exceptional tensile strength, but the mix had poor workability and caused problems in mixing due to a high fiber content. Hence, the mix was discarded and was not to be used in casting of the beams. The normalized hardened property values suggest that the tensile strength of TTFRC (excluding TTFRC2) was increased by about 31 % with the use of fibers, if compared to the control non-fibrous TTC1 mix. Similarly, on average the tensile strength of SCFRC was increased by about 30 % with the use of fibers, in comparison to the

control SCC2-3 mix. Fig. 2.9.10 presents the variation of average normalized tensile strength with fiber factor for the fiber reinforced mixes. The average normalized tensile strength for fiber mixes with fiber factors of 40 (0.5 % by volume long fibers) and 55 (1 % by volume short fibers) were almost the same. As the fiber factor increases from 30 to 55, the average normalized tensile strength increased slightly; but significant increase in the average normalized tensile strength was observed when the fiber factor reached 80. Nevertheless, the workability of the mix with such a high fiber content was unsatisfactory. Hence, the optimum fiber contents selected to be used to cast the beams in the later part of this research project were:

- (1) Short Fibers – 1 % by volume (Fiber Factor = 55)
- and (2) Long Fibers – 0.5 % by volume (Fiber Factor = 40)

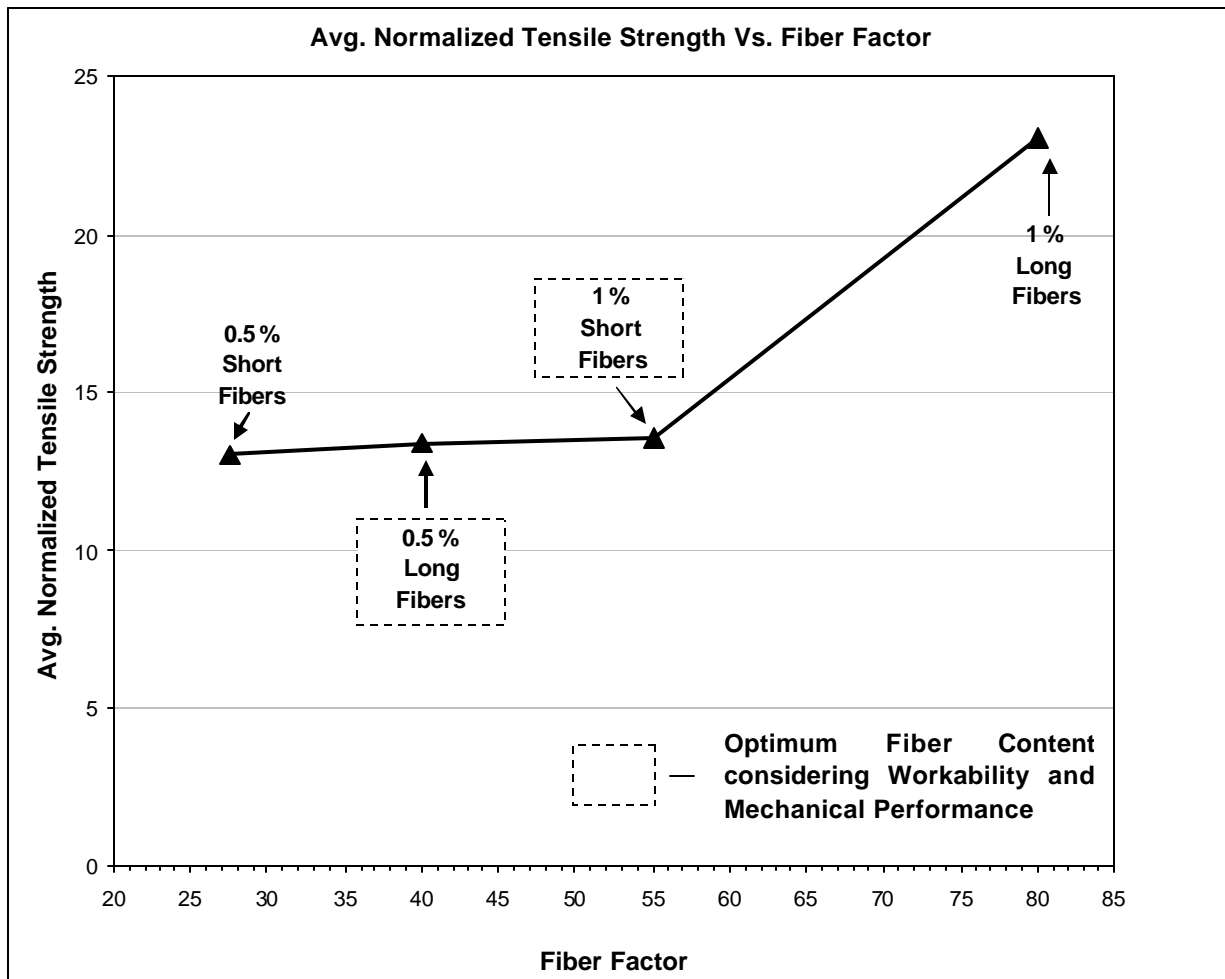


**Fig. 2.9.10 Variation of Average Normalized Tensile Strength with Fiber Factor**

## CHAPTER 3

### EARLY-AGE CRACKING IN PRESTRESSED CONCRETE I-BEAMS

In this chapter, an analysis was performed to study the cracking of the end zone in the I-beams caused by the prestress and the thermal loadings. First, the stresses developed under prestress were analyzed in [Section 3.1](#) by a nonlinear finite element program SRCS based on the OpenSees framework ([Fenves 2001](#)). Second, the stresses developed under thermal loading were analyzed in [Section 3.2](#) by performing a finite element analysis using SAP 2000. Finally, the total stresses due to prestress and thermal loading were added together in [Section 3.3](#).

#### 3.1 Analysis of End Zone Stresses Due to Prestress Forces

##### 3.1.1 OpenSees Analytical Model

OpenSees stands for Open System for Earthquake Engineering Simulation ([Fenves 2001](#)). OpenSees has been developed in the Pacific Earthquake Engineering Center at UC Berkeley (PEER) and is an object-oriented framework for simulation applications in earthquake engineering using finite element methods. An object-oriented framework is a set of cooperating classes that can be used to generate software for a specific class of problem, such as finite element analysis. The framework dictates the overall program structure by defining the abstract classes, their responsibilities, and how these classes interact. OpenSees is a communication mechanism for exchanging and building upon research accomplishments, and has the potential for a community code for earthquake engineering because it is open source.

Using OpenSees as the finite element framework, a nonlinear finite element program titled Simulation of Reinforced Concrete Structures (SRCS) was developed at the University of Houston for the simulation of reinforced concrete structures subjected to monotonic and reversed cyclic loading. Two material modules, SteelZ01 and ConcreteZ01, have been developed and incorporated into OpenSees to model the materials required for the analysis of the reinforced concrete plane stress elements. The program SRCS has been validated by Zhong ([2005](#)) with full-scale structural tests.

Each end zone of a test beam was modeled by two-dimensional reinforced concrete plane stress elements. The end zone lengths of 36 inches from the ends of the beams were modeled by 9 columns and 7 rows of plane stress elements as shown in Fig. 3.1.2. The idealized schematic cross-section of the beam is shown in Fig 3.1.1. The longitudinal and transverse reinforcements of the beam at the location of the elements were smeared over the area of the elements. The nodes at the bottom and the inner edges of the beam were restrained against movement in both the vertical as well as horizontal directions. The prestress loads have been applied at the nodes corresponding to the level of application of the prestress. The loads have been distributed among the nodes over the transfer length of the beam as shown in Fig 3.1.3.

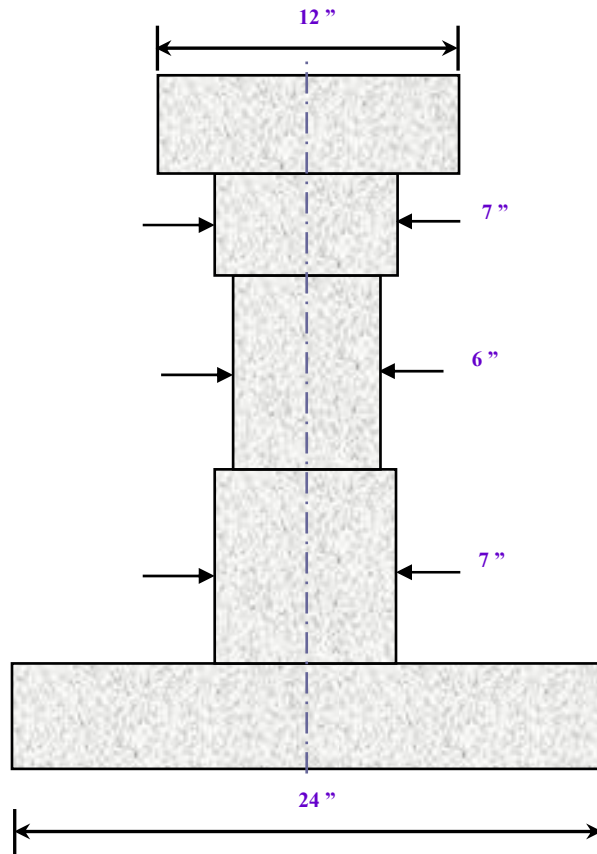


**Fig 3.1.1 Schematic Modified Cross-Section of Beam for SRCS Analysis**

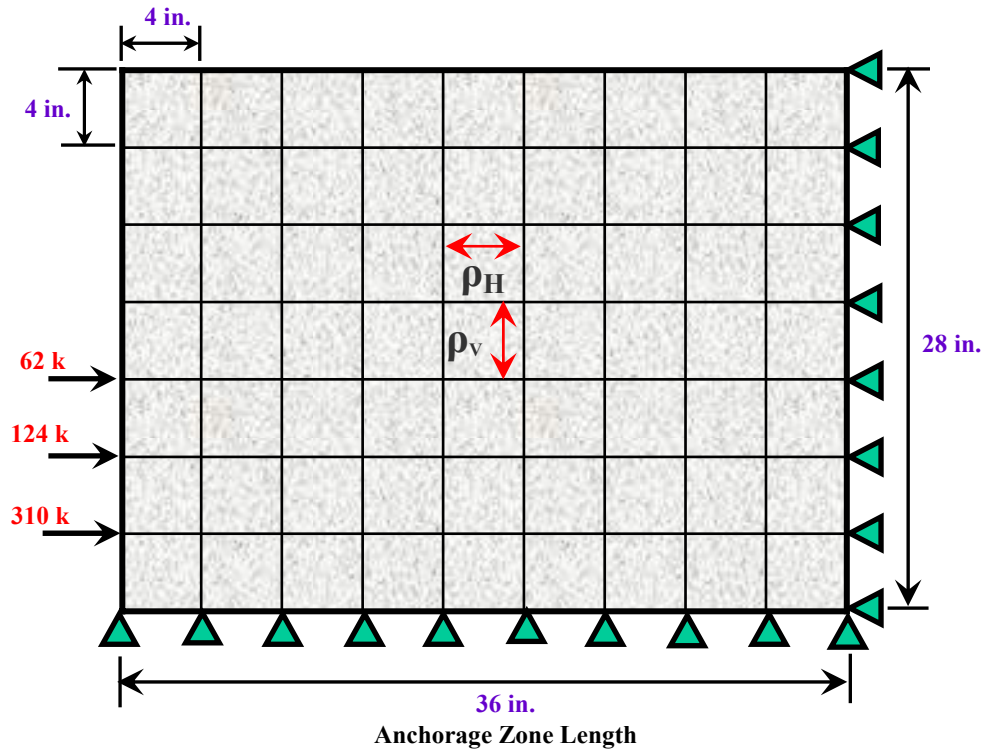


Fig 3.1.2 Finite Element Mesh for End Zone of Beam (OpenSees Analysis)

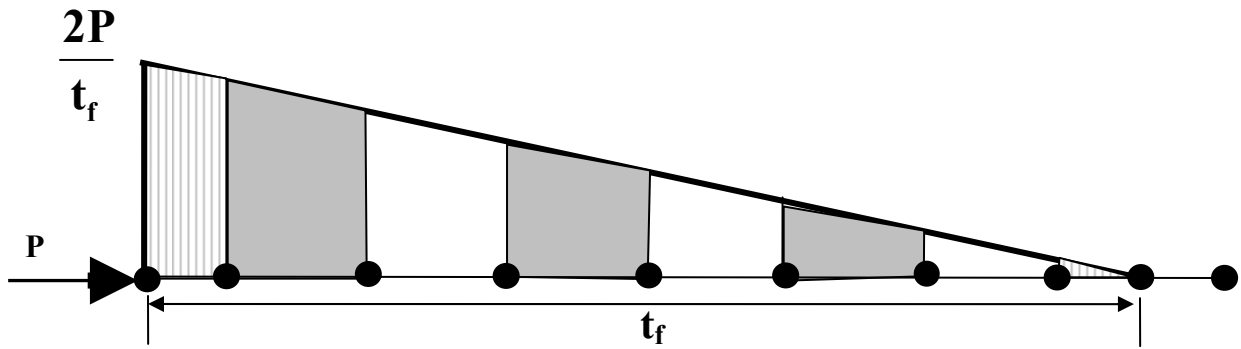


Fig 3.1.3 Modeling of Prestress Load Distribution along the Transfer Length

### 3.1.2 Results of End Zone Analysis under Prestress Forces

The stress distribution under prestress loads for beams with TxDOT Traditional Concrete (TTC1) and Self Consolidating Fiber Reinforced Concrete (SCFRC3) is shown in Figures 3.1.4 and 3.1.5, respectively. Different colors have been used to shade the different regions having stresses with certain ranges. It was observed that the maximum stresses occur at regions immediately surrounding the location of the prestressing strands at the end of the beams. The stresses at distances greater than 20 inches from the end of the beams were found to be within safe limits.

Fig. 3.1.4 shows that an end zone with TTC1 mix is subjected to a maximum tensile stress of about 800 psi. This tensile stress is very close to the tensile strength of 895 psi for TTC1 mix. That means that the possibility of cracking is quite large in this case. In contrast, Fig. 3.1.5 shows that an end zone with SCFRC3 mix is subjected to a maximum tensile stress of about 700 psi. This tensile stress is much smaller than the tensile strength of 1662 psi for SCFRC3 mix. In other words, the possibility of cracking is very small.

**Case (I): TTC1**

 $f_t = 800$ psi	 $f_t = 500$ psi	 $f_t = 300$ psi	 $f_c = 1296$ psi
$f_{cr} = 895$ psi	$f_c^{18 \text{ hrs}} = 6790$ psi	$\epsilon_{cr} = 8 \times 10^{-5}$	

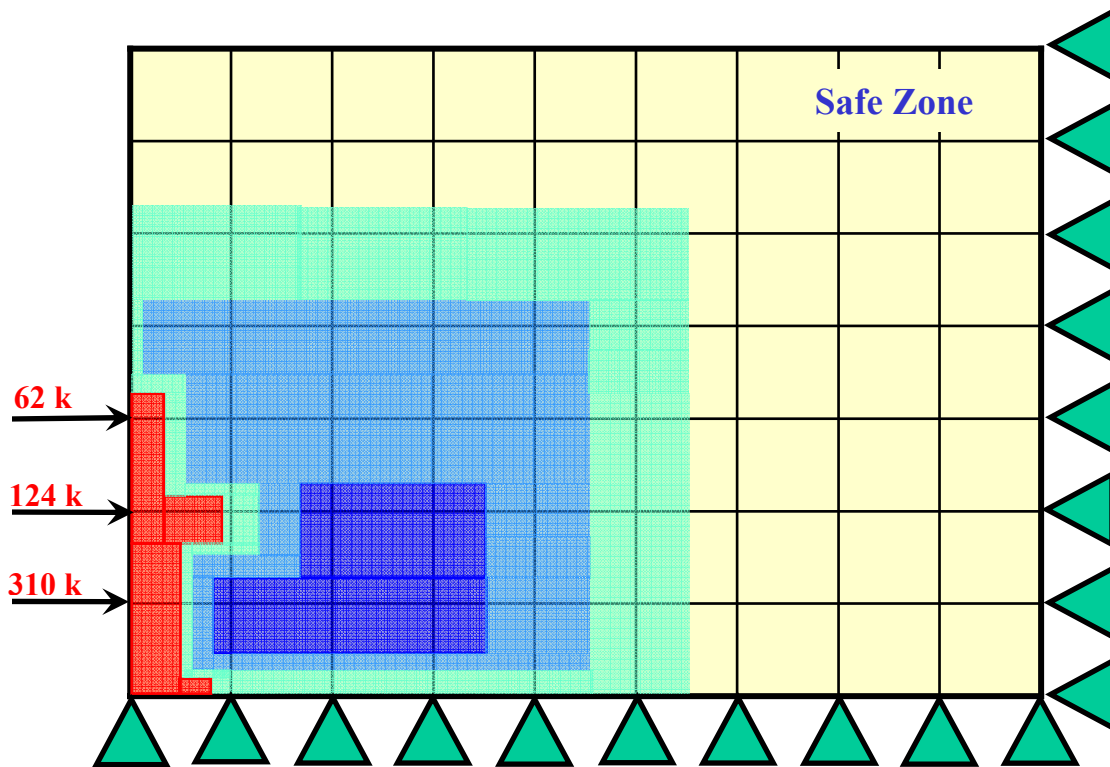


**Fig 3.1.4 End-Zone Stress Distribution for TTC1 mix**

**Case (II): SCFRC3**

■  $f_t = 700$  psi     
 ■  $f_t = 400$  psi     
 ■  $f_c = 905$  psi

$f_{cr} = 1662$  psi     
  $f_c^{18 \text{ hrs}} = 7850$  psi     
  $\epsilon_{cr} = 8 \times 10^{-5}$

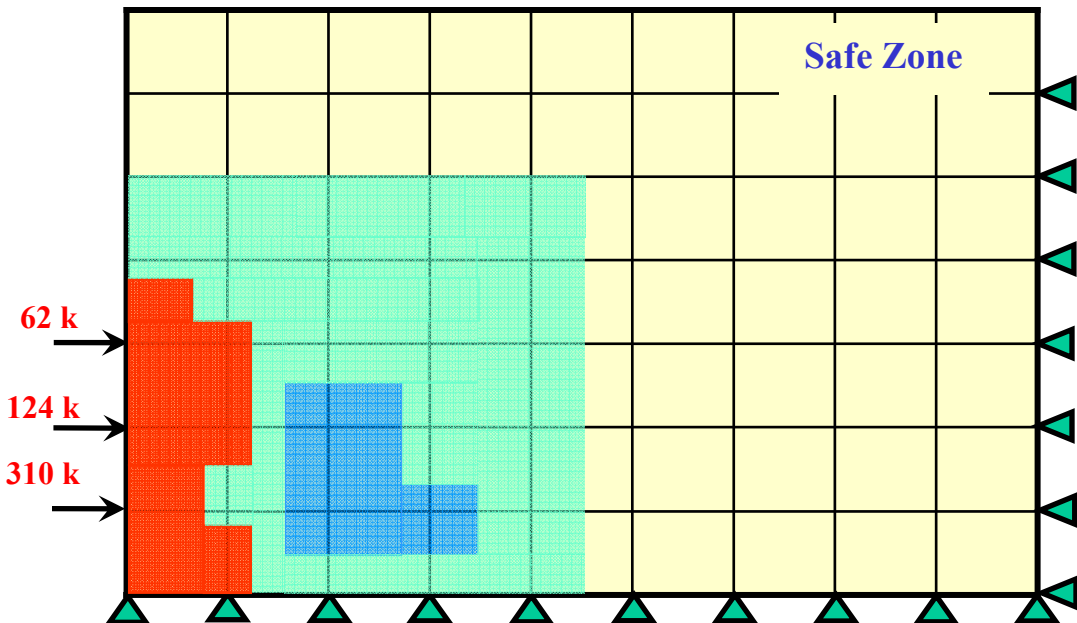


**Fig 3.1.5 End-Zone Stress Distribution for SCFRC3 Mix**

## **3.2 Analysis of End Zone Stresses Due to Thermal Load**

### **3.2.1 SAP 2000 Analytical Model**

A three-dimensional model of the beam was analyzed by the well-known computer program SAP 2000. 3-D solid concrete elements were used in this case to model the entire length of the beam. The lower surface of the beam was restrained against any motion. A typical developed model of the beam is shown in [Fig.3.2.1](#). For thermal analysis, a temperature increment of 60 °F was applied to the beam.

### **3.2.2 Results of End Zone Analysis under Thermal Load**

The vertical stress distributions at the end face and at the critical sections (2.5 ft from the face) of the beam are shown in [Fig 3.2.2](#). The stress contours show that the critical stress regions on a cross-section occur at the inclined portion of the flange corresponding to the crack locations observed in the field. The maximum thermal stress at this location is 210 psi due to a conventionally assumed temperature increment of 60 °F. This thermal stress is unlikely to cause cracking by itself, but will help to cause cracking when added to stresses from other sources such as prestress. It should also be mentioned here that the actual temperature increments measured and reported in [chapter 4](#) were much higher than the 60 °F assumed.

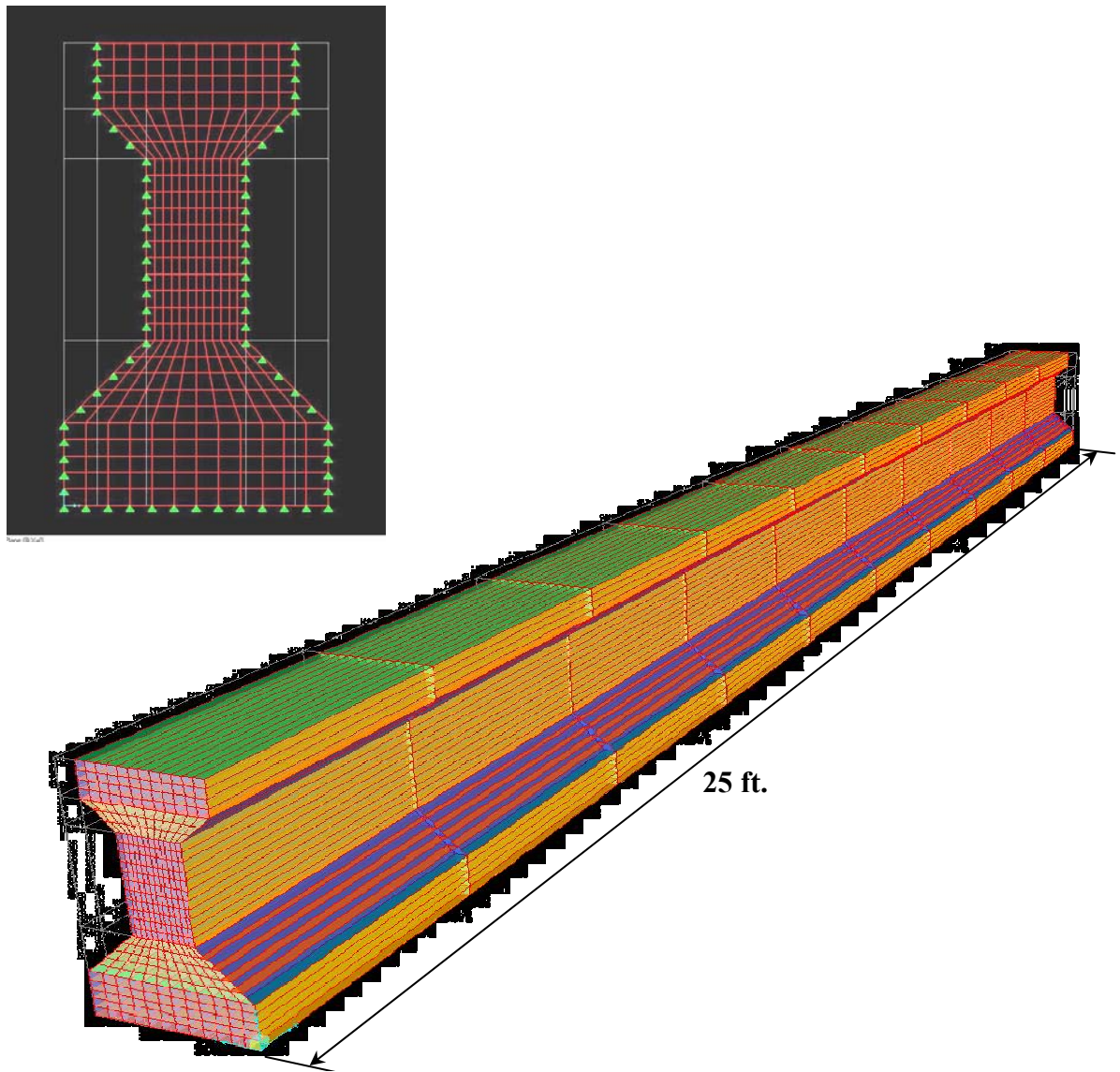


**Fig. 3.2.1 Finite Element Model for Thermal Analysis of Beam Using SAP 2000**

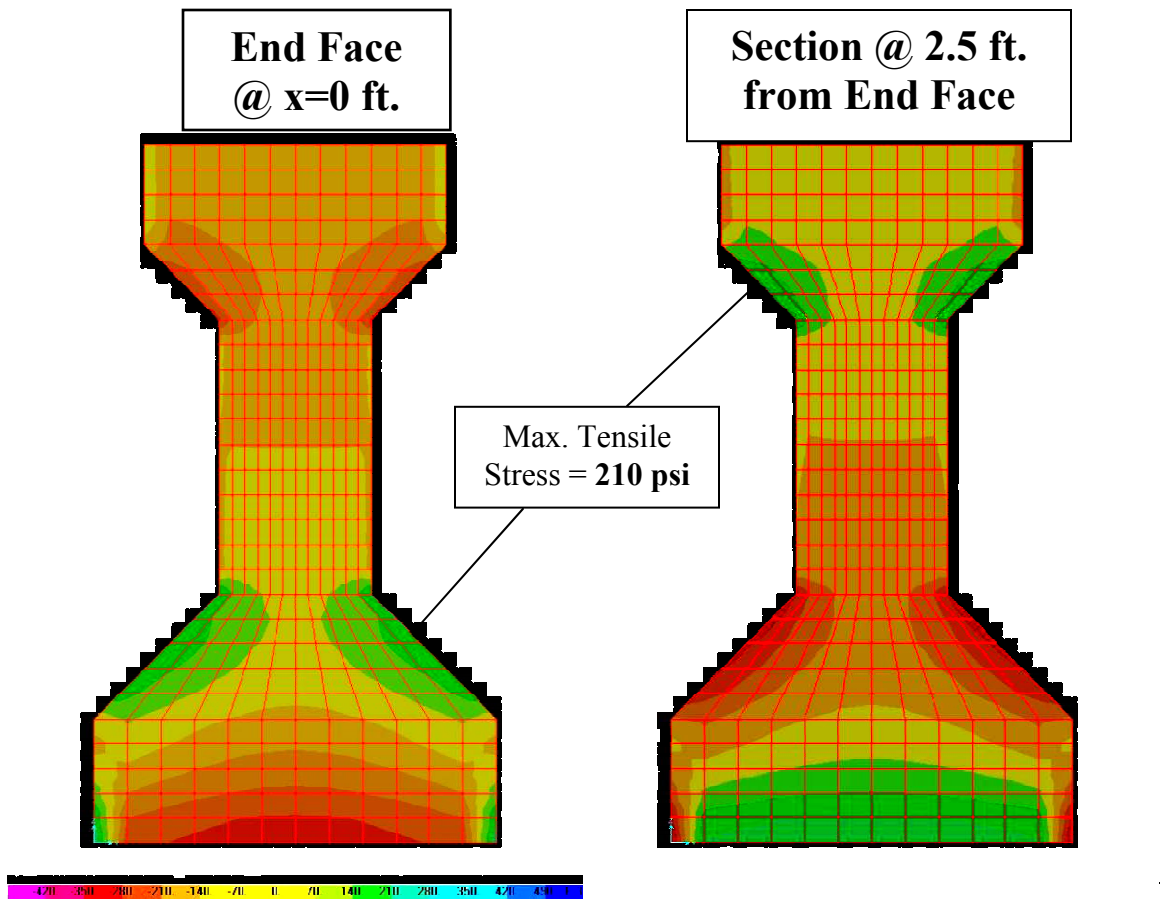


**Fig. 3.2.2 Stresses Due to Thermal Loads in Type-A Beam Cross-Section**

### **3.3 Summary of Stresses Due to Prestress and Thermal Loading**

From the above two analyses of stresses caused by prestress and thermal loading, the total tensile stress due to prestress force and thermal loading can be calculated. In the case of TTC1 beams, the total maximum tensile stress in the end region was 800 psi (prestress) + 210 psi (thermal) = 1010 psi. This total stress was greater than the cracking strength of 895 psi for TTC1 mix. This means that the end zone was very likely to crack. The locations with the greatest total stresses were also found to match the crack locations observed in the beams on-site.

In the case of SCFRC3 mix, the total maximum tensile stress in the end region was 700 psi (prestress) + 210 psi (thermal) = 910 psi. This total stress was much less than the cracking strength of 1662 psi for SCFRC3 mix. This means that the end zone was unlikely to crack.

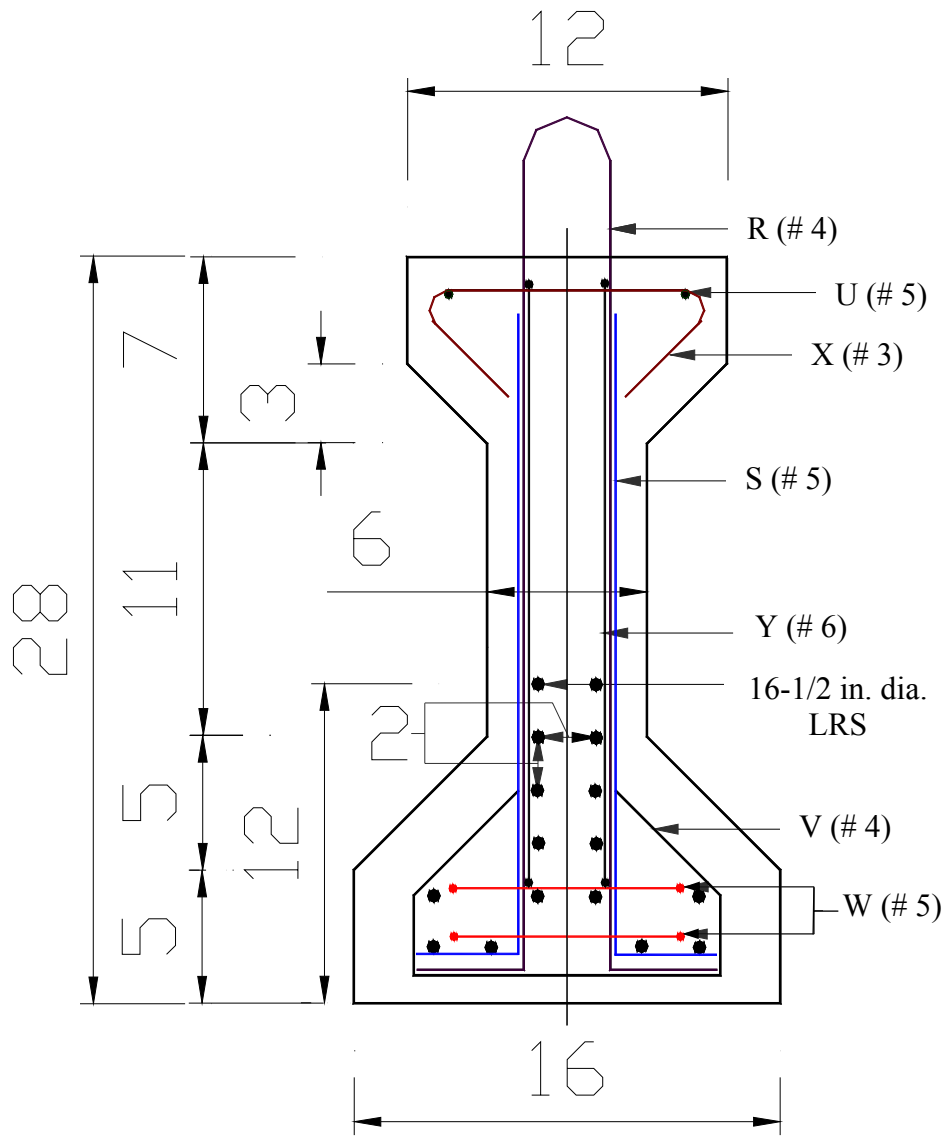
## CHAPTER 4

### PRESTRESSED CONCRETE BEAMS: TEST SPECIMENS AND EARLY-AGE MEASUREMENTS

#### 4.1 Test Specimens

TxDOT Type-A beams were selected, cast and tested to study the behavior of prestressed concrete beams reinforced with steel fibers. The cross-section of the TxDOT Type-A beams used in this research is shown in [Fig. 4.1.1](#). The total height of the beam was 28 inches and the widths of the top and bottom flange were 12 inches and 16 inches, respectively. The width of the web was 6 inches. The position of the prestressing tendons and the type of the reinforcing bars are also shown. # 3 rebars were used for X rebars, # 4 rebars were used for R and V rebars, # 5 rebars were used for U , W and S rebars, and # 6 rebars were used for Y rebars. X and V rebars were designed to confine the concrete and act as secondary reinforcements in the top and bottom flange, respectively. R and S rebars served as transverse reinforcement for shear strength. The W and Y bars were installed to resist the end zone bearing, spalling and bursting stresses, whereas the U rebars ran all along the beam to support the R, S, X, W and Y rebars. Sixteen 0.5 inch diameter-7 wire low relaxation strands were used as the prestressing steel. The prestressing strands had ultimate strength of 270 ksi.

The elevation of the TxDOT Type-A beams is shown in [Fig. 4.1.2](#) and [Fig. 4.1.3](#). The total length of the beams tested was 25 feet. [Fig. 4.1.4](#) and [Fig. 4.1.5](#) show the reinforcement and instrumentation details of Beam B1 and Beams B2, B3, B4 and B5, respectively. It should be noted that two additional Type-A beams (Beams B0 and B6), sponsored by the Texas Concrete Company, were also studied in this research project. In Beam B0, transverse reinforcement had been completely replaced by 1.5 % by volume of short steel fibers and the concrete mix design used was TTFRC4. The reinforcement of Beam B6 was the same as that of Beam B1, but the mix design used was SCC2-3 instead of TxDOT traditional concrete.



(All dimensions are in inches)

**Fig. 4.1.1 Cross-section of Type-A Beam**

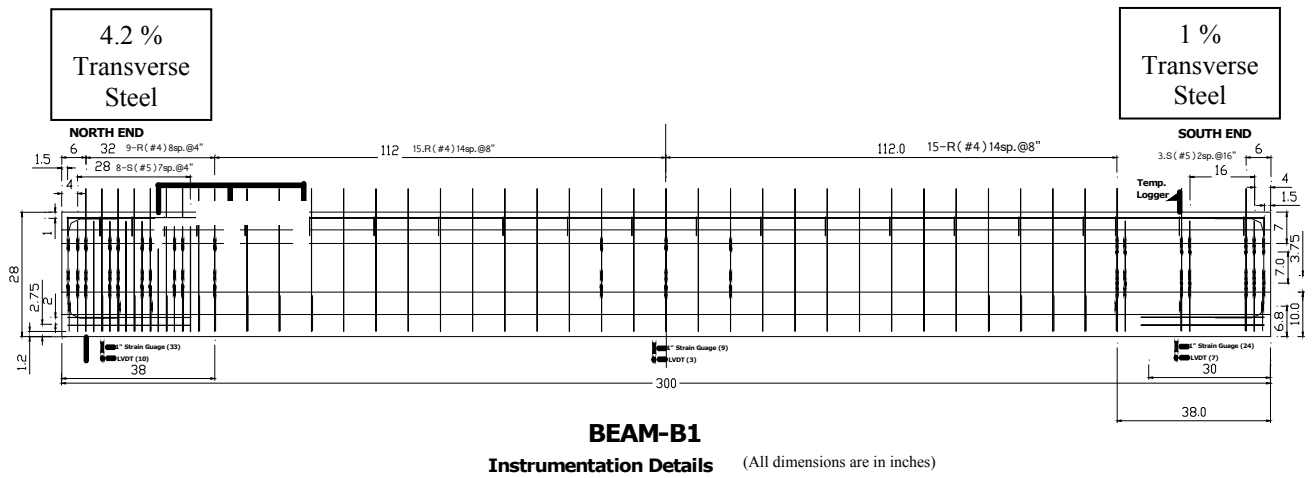


**Fig.4.1.2 Elevation and Reinforcement Details of Beams B1 and B6**

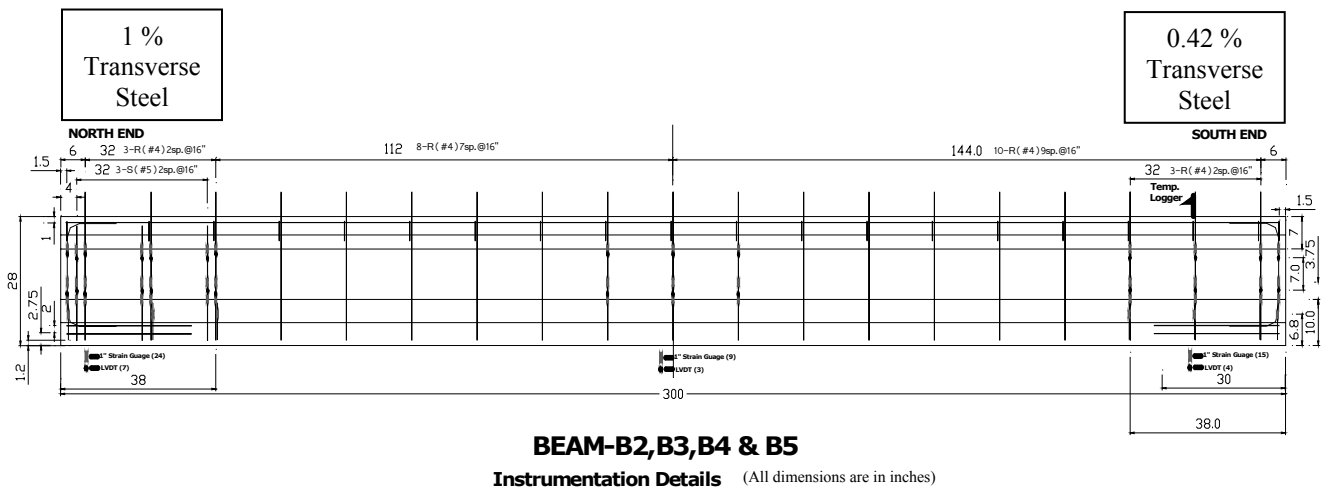


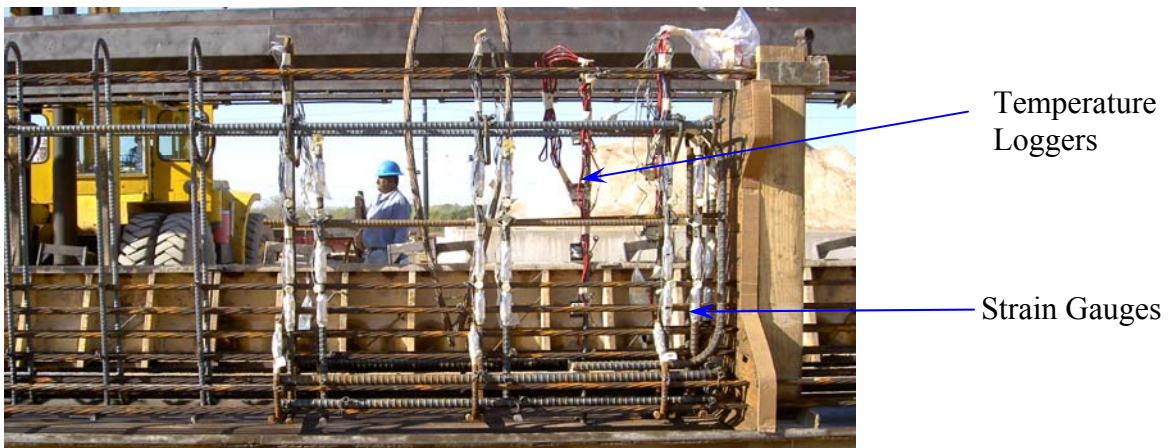
**Fig. 4.1.3 Elevation and Reinforcement Details of Beams B2, B3, B4 and B5**



(a) Beam B1-North (4.2 % steel)



(b) Beam B1-Center (0.82 % steel)



(c) Beam B1-South (1 % steel)

**Fig. 4.1.4 Reinforcement and Instrumentation Details of Beam B1**



(a) Beam-North (1 % steel)



(b) Beam-Center (0.42 % steel)



(c) Beam-South (0.42 % steel)

**Fig. 4.1.5 Reinforcement and Instrumentation Details of Beams B2, B3, B4 and B5**

## 4.2 Test Program

As mentioned previously, seven TxDOT Type-A beams were designed to study the following variables: the type of concrete mix, the type and volume of steel fibers and the amount of transverse reinforcement. The aim was to evaluate the effects of steel fibers on the casting procedure, the control of the end region cracking and the increase in shear strength and ductility of the beams.

Table 4.2.1 shows the test program for all of the five beams. Beam B1 was designed as the conventional TxDOT Type-A beam which served as a reference specimen. A TxDOT traditional concrete mix (TTC1) was used in this beam. The reinforcement details of the beam followed the standard design from TxDOT except at the south end where the reinforcement was reduced to 1 % (about 25 % of the traditional value of 4.2 %). This reduction can be observed from the spacing of R and S rebar, which was 4 inches at the north end and 16 inches at the south end. The transverse steel at midspan was R rebars @ 8 in. spacing, the same as used in the midspans of the conventional TxDOT beams.

Beams B2 and B3 were designed with the same concrete mix as beam B1 but with an addition of 1 % of ZP305 short fibers for Beam B2 and 0.5 % of RC80/60BN long fibers for Beam B3. Beams B4 and B5 were designed with a self-consolidating concrete (SCC2-3) mix with an addition of 0.5 % of RC80/60BN long fibers for Beam B4 and 1 % of ZP305 short fibers for Beam B5. Beam B0 was designed without any transverse reinforcement; instead, a 1.5 % volume of ZP305 short steel fibers was used with TTFRC4 concrete mix. Beam B6 had the same design as beam B1, but the mix used was self-consolidating concrete (SCC2-3) instead of TxDOT traditional concrete (TTC1).

**Table 4.2.1 Test Program for Beams**

Beam I.D.	Mix	Transverse Steel*			Casting Schedule
		North End	Center	South End	
<b>B0</b>	<b>TTFRC4</b> 1.5% ZP305 Fibers	0	0	0	18 <sup>th</sup> March 2005
<b>B1</b>	<b>TTC1</b> Control Mix: TXDOT Traditional Concrete	<b>100%</b> R & S rebar @ 4 in. $\rho_v = 4.2\%$	<b>100%</b> R rebar @ 8 in. $\rho_v = 0.84\%$	<b>25%</b> R & S rebar @ 16 in. $\rho_v = 1.0\%$	18 <sup>th</sup> March 2005
<b>B2</b>	<b>TTFRC1</b> 1% ZP305 Fibers	<b>25%</b> R & S rebar @ 16 in. $\rho_v = 1.0\%$	<b>50%</b> R rebar @ 16 in. $\rho_v = 0.42\%$	<b>10%</b> R rebar @ 16 in. $\rho_v = 0.42\%$	18 <sup>th</sup> March 2005
<b>B3</b>	<b>TTFRC3</b> 0.5% RC80/60BN Fibers	<b>25%</b> R & S rebar @ 16 in. $\rho_v = 1.0\%$	<b>50%</b> R rebar @ 16 in. $\rho_v = 0.42\%$	<b>10%</b> R rebar @ 16 in. $\rho_v = 0.42\%$	18 <sup>th</sup> March 2005
<b>B4</b>	<b>SCFRC1</b> 0.5% RC80/60BN Fibers	<b>25%</b> R & S rebar @ 16 in. $\rho_v = 1.0\%$	<b>50%</b> R rebar @ 16 in. $\rho_v = 0.42\%$	<b>10%</b> R rebar @ 16 in. $\rho_v = 0.42\%$	23 <sup>th</sup> March 2005
<b>B5</b>	<b>SCFRC3</b> 1% ZP305 Fibers	<b>25%</b> R & S rebar @ 16 in. $\rho_v = 1.0\%$	<b>50%</b> R rebar @ 16 in. $\rho_v = 0.42\%$	<b>10%</b> R rebar @ 16 in. $\rho_v = 0.42\%$	23 <sup>th</sup> March 2005
<b>B6</b>	<b>SCC2-3</b> Control Mix: Self- Consolidating Concrete	<b>100%</b> R & S rebar @ 4 in. $\rho_v = 4.2\%$	<b>100%</b> R rebar @ 8 in. $\rho_v = 0.84\%$	<b>25%</b> R & S rebar @ 16 in. $\rho_v = 1.0\%$	23 <sup>th</sup> March 2005

**Notes:** \* - Represents percentage of the traditional reinforcement in Type-A beam at respective locations.

The transverse reinforcement of Beams B2, B3, B4 and B5 was reduced from the standard design of the TxDOT Type-A beam. At the north end, the transverse reinforcement was reduced to 25 %. As shown in [Table 4.2.1](#), R & S rebar spacing was reduced from 4 inches to 16 inches. At the south end of the beam, the transverse reinforcement was reduced to 10 % (from R & S rebar spacing of 4 inches to only R rebar with the spacing of 16 inches). Transverse steel at midspan for these beams was reduced to 50 % of the conventional beam, i.e. R rebar @ 16 in. spacing. The reductions in transverse reinforcement were done to determine the effect of adding steel fibers on the properties of beams such as end zone cracking, shear and flexural strength, ductility and workability of concrete mixes during casting. Beam B6 had similar reinforcement

details as beam B1. Beams B1 and B6 served as control beams for TTFRC and SCFRC beams, respectively.

The beam design and test plan (Table 4.2.1) were made such that the test results of Beams B0 and Beam B6 could be compared to the conventional TxDOT Beam B1, serving as a reference beam.. The test results of Beam B0 can be compared to those of Beam B1 to study how much transverse reinforcement can be replaced by the steel fibers. Also, the test results of Beam B6 can be compared to those of Beam B1 to study the effects of using SCC2-3 as the replacement to traditional concrete.

In order to study the effect of the different types of concrete mixes (traditional concrete and self consolidating concrete), test results of Beam B2 can be compared to those of Beam B5, and Beam B3 can be compared to Beam B4. In order to study the effect of the different types of steel fibers (ZP305 and RC80/60BN steel fibers), the test results of Beam B2 can be compared with those of Beams B3, B4 and B5.

### 4.3 Casting of Test Specimens

The general procedure for mixing the respective concrete mixes for all the beam specimens was similar to the one discussed in Chapter 2 (Section 2.6) of this report. Two cubic yards of concrete was mixed for each beam. Just after mixing, normal slump tests were carried out for TTC1/TTFRC mixes and slump flow tests were done for SCC/SCFRC mixes. The workability test results were similar to the results obtained in the material testing research phase as shown in Fig. 2.7.1 and Fig. 2.7.2.

The seven beams were cast in two groups on two different days. The four beams, B0 to B3 with TTC1/TTFRC mixes, were cast together, with beam B1-North end placed nearest to the prestressing jack, followed by B2, B3 and B0. The second group of three beams, B4, B5 and B6 with SCC/SCFRC mixes, were cast after a few days with B4-North end placed closest to the prestressing jack, followed by B5 and B6. Fig. 4.3.1 (a) shows the casting and compaction of beams. Concrete was transported from the plant mixer and delivered into the beams using a mobile hopper as shown in Fig. 4.3.1 (b). The rate of casting concrete was about 5 ft<sup>3</sup> per min. for both groups of beams.

Beams were cast from south end to north end. Three needle vibrators were used for TTC1 and TTFRC mixes, i.e. for beams B1, B2 and B3. The vibration energy required for beams B2

and B3 was slightly more than that for beam B1, because the presence of fibers along with the beam transverse reinforcement made the concrete harsher and hard to work with.

Casting and compaction of beam B0 was relatively fast and easy even if the mix used the largest amount (1.5 % by volume) of fibers. This was because transverse reinforcement in beam B0 was totally absent, causing no hindrance to the compaction of the fiber reinforced mix. Thus, fiber reinforced concretes would be relatively easy to compact in the absence of any conventional reinforcement.

In the second group of SCC/SCFRC beams, B4 to B6, concrete mixes were deposited in the beams and allowed to flow. To achieve a satisfactory workability of the SCC mix, beam B6 with SCC was cast first with the fastest time and least effort. SCC flowed from the south end to the north end of beam B6, and filled the form without any vibration. With the successful SCC mix as the base mix, SCFRC mixes were prepared for the casting of beams B4 and B5.

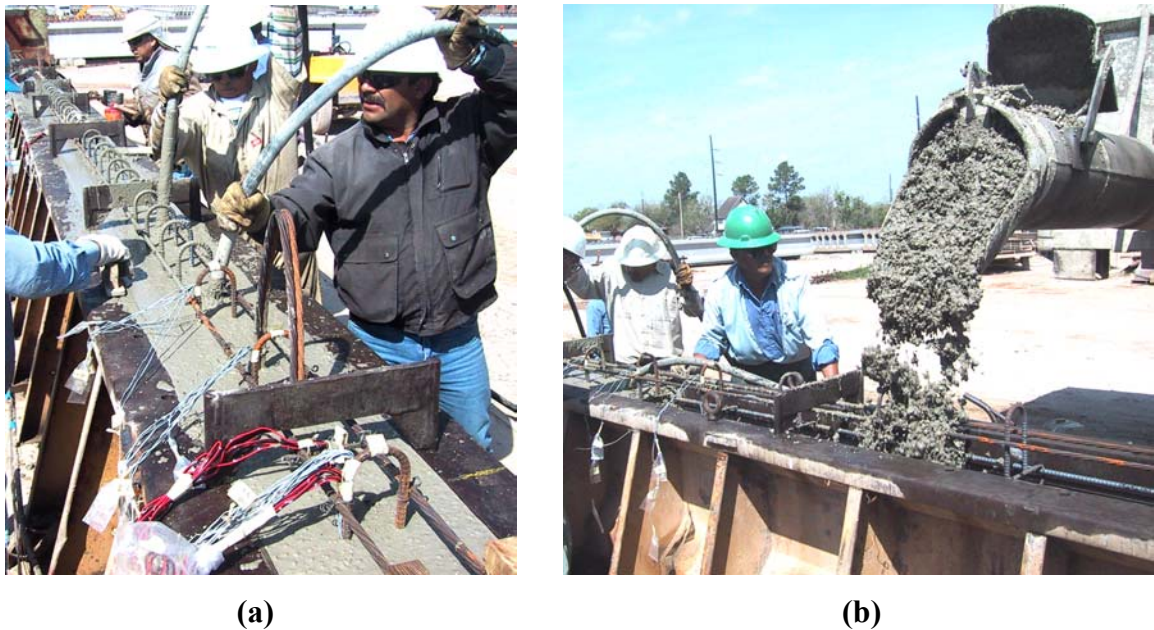


**Fig. 4.3.1 Casting of Beams: (a) Compaction Using Vibrators in Beam B1 (b) Concrete Placed in Beam B2 by a Hopper**

The SCFRC1 mix (0.5 % by volume of long fibers) in Beam B4 could not flow freely without the use of partial vibration. One vibrator was used to dislodge bulks of fibers caught around the top rebar (U-rebar). Casting rate of SCFRC1 mix was too fast, thus causing the

blocking of the mix at the top rebars and the air-pockets to form at the north ends and the center span of beam B4. This restricted filling ability problem of SCFRC1 mix could be avoided if the traditional transverse reinforcement was absent or the casting rate was reduced.

A similar problem was met with the flow of SCFRC3 mix (1 % by volume of short fibers) in beam B5 without using vibrators. The accelerated casting rate for this beam was also too high near the center span, which caused air-pocket formation in this portion of the beam. The two ends of the beam B5 were solid without any air-pockets since SCFRC3 was cast at a slower rate near the beam ends. No vibrator was used in casting beam B5.

The air pockets in beams B4 and B5 were repaired with a special high strength repair grout-‘EMACO S88.’

#### **4.4 Instrumentations for Early Age Measurements**

The beam testing plan was divided into two stages based on the objectives sought from the testing. The first stage is reported in this chapter, consisting of monitoring the beams continuously during casting, curing and release of prestress. The second stage of the research, dealing with the load testing of the beams until failure, will be reported in [Chapter 5](#).

Beams were cast in two groups at the precast plant of Texas Concrete Company in Victoria, Texas, on two different days as recorded in Table 4.1.1. Beams B1, B2, B3 and B0 with TTC1/TTFRC mixes were cast first on a single prestressing bed. A total of eighty strain gauges were installed on the rebars in these beams. The strains were continuously monitored and recorded using data acquisition system during the casting stage, the curing stage and the release of prestress. Along with the strain measurements, the concrete temperatures were recorded continuously. The temperature data not only provided an insight into the thermal loading of a beam, but also tracked the variations in temperature of different types of concrete mixes.

The concrete temperatures were measured using *IntelliRock*<sup>TM</sup> temperature loggers attached to the reinforcing bars inside the beam. The *IntelliRock*<sup>TM</sup> system consisted of three major components: loggers, readers, and windows software. The loggers are a totally self-contained measurement and computing system that had a precision temperature measurement system, microprocessor, memory and a battery. The reader was used to communicate with the logger (i.e. start loggers, download data, etc.) as well as “shuttle” data from the loggers in the field to a PC. A software was used to download logger data from the hand-held reader to a PC.

There were two types of loggers, namely, TPL-02-5M7D Temperature Logger which logged data every 5 minutes for 7 days, and MAT-02-1H28D Maturity Logger which logged data every 1 hour for 28 days.

The number and type of temperature loggers used in each beam are shown in [Table 4.4.1](#). [Fig. 4.4.1](#) shows the location of the temperature loggers inside the beam. [Fig. 4.4.1 \(a\)](#) shows the locations of the temperature loggers at the south ends of beams B1, B2, B3 and B5, and [Fig. 4.4.1 \(b\)](#) shows the locations of the temperature loggers at the center of beam B1 and south end of beams B4 and B6 (except logger #11 was not installed for B6-South). Loggers were placed at critical locations where maximum temperature would be expected and in the vicinity of the probable locations of the end zone cracking.

**Table 4.4.1 Temperature Loggers Installed in the Beams**

<b>Beam/Location</b>	<b>Number of Loggers</b>	<b>Type of Loggers</b>
B1-South	10	TPL-02-5M7D
B1-Center	5	TPL-02-5M7D
B2-South	10	TPL-02-5M7D
B3-South	10	TPL-02-5M7D
B4-South	5	TPL-02-5M7D
B5-South	10	TPL-02-5M7D
B6-South	4	MAT-02-1H28D
External	1	MAT-02-1H28D
Total	55	



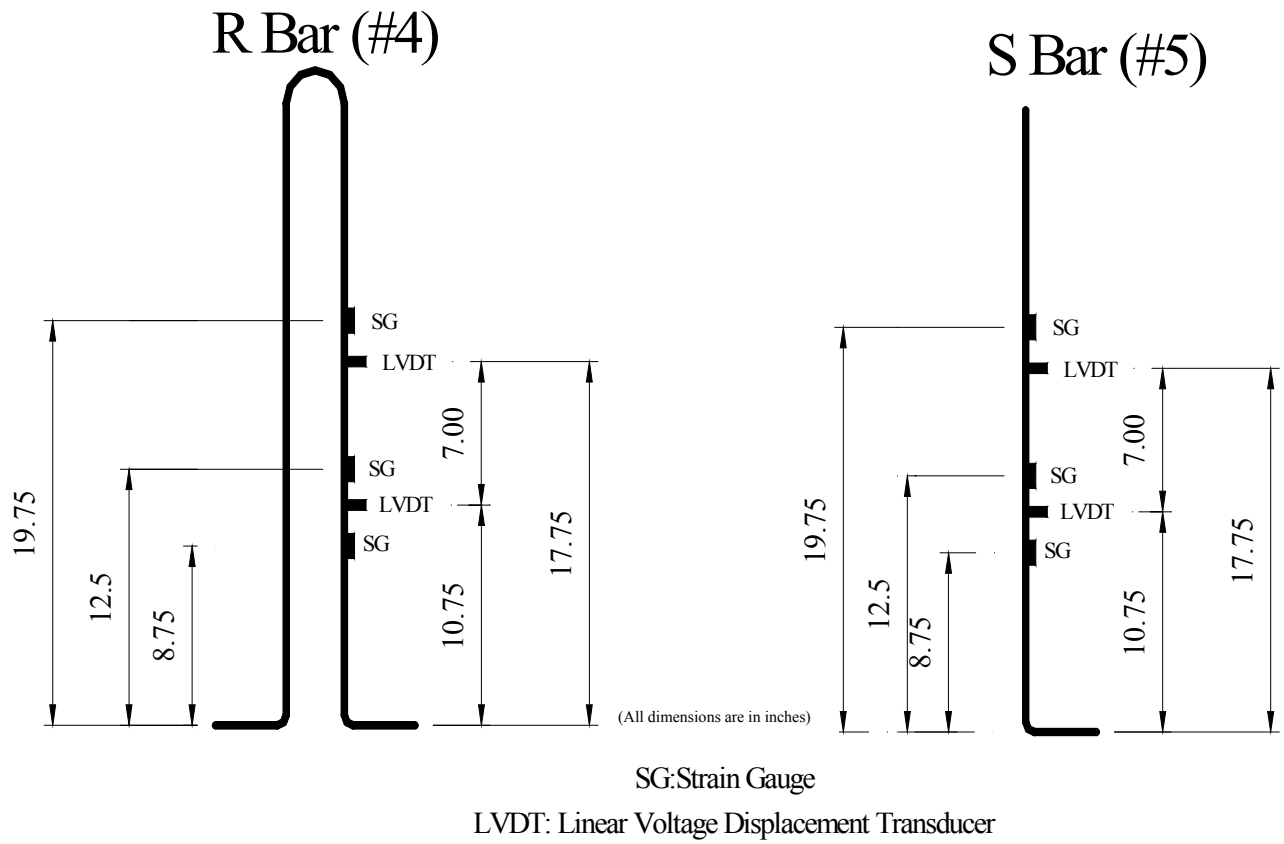


**Fig. 4.4.2 Positions of Strain Gauges and LVDT Studs on R and S Rebars**

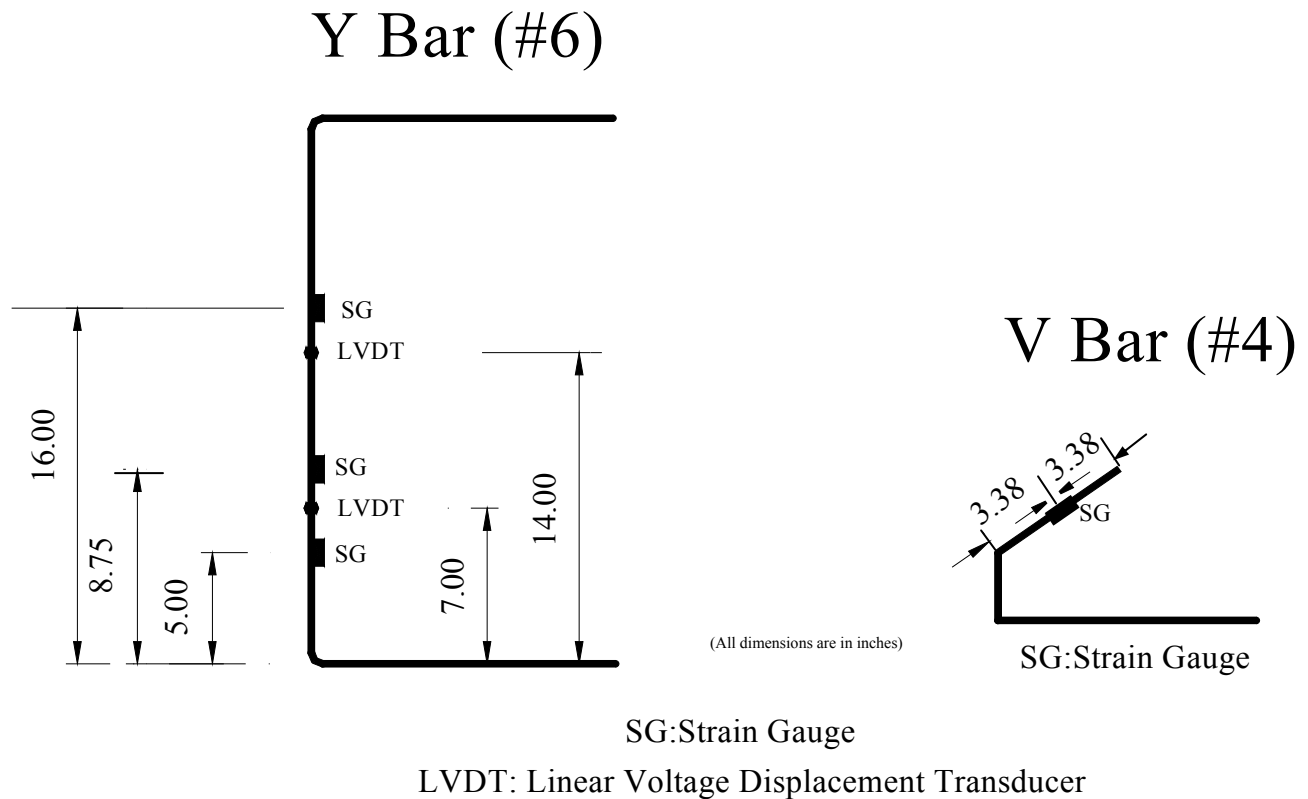


**Fig. 4.4.3 Positions of Strain Gauges and LVDT Studs on Y and V Rebar**

The purpose of installing the strain gauges, as can be observed in [Fig. 4.4.2](#) and [Fig. 4.4.3](#), was:

- (a) To measure the strains developed in the rebars during casting, curing and release of the prestressing tendons.
- (b) To track the strains in rebars at the expected initial crack locations at the end zone of the beams.
- (c) To measure rebar strains during the load tests (see [Chapter 5](#), Sections [5.3.3](#) and [5.3.4](#)).

The purpose of positioning the temperature loggers at specific locations was to determine the correlation between the strains and the temperatures developed during various stages.

[Fig. 4.4.2](#) and [Fig.4.4.3](#) also show the positions of Linear Voltage Displacement Transducer (LVDT) studs on the rebars. The studs were welded on the rebars at important

locations to mount the LVDTs on the beam web. LVDTs were used to record the displacements (strains) of the rebars during the load testing as mentioned in [Chapter 5](#). It is noteworthy to observe that the strains recorded by the strain gauges were the local strains on the rebars, whereas the strains recorded by the LVDTs were the average strains in the rebars within the web of the beam. LVDT studs could not be installed in Beam B6, since it was decided to cast the beam at the last moment.

The researchers had the opportunity to install LVDT studs, which ran the whole length of the web inside Beam B0, at the same positions as the other beams. Since there were no rebars in Beam B0, the LVDT studs were cast and embedded in concrete. Hence, unlike the LVDT studs in other beams that measured the average strains in the rebars, the LVDT studs in Beam B0 measured the average strains in the concrete.

End zone cracks were observed continuously during the curing process of the beams. Visible cracks were not developed during curing, during the demolding process, during the release of the prestressing strands, and throughout the early age of the beams. Most of the end zone cracks were found 90 days after the beams were cast.

#### **4.5 Results of Early Age Measurements**

The maximum and average strains measured by the strain gauges installed on rebars at the end zone for all the beams are shown in [Table 4.5.1](#). Typical plots of strain gauge readings and corresponding time for beam B1-North (TTC1), B2-North (TTFRC1), B3-South (TTFRC3) and B5-South (SCFRC3) are shown in [Fig. 4.5.1](#) to [4.5.4](#), respectively.

**Table 4.5.1 Tensile Strains Measured by Strain Gauges Installed on Rebars  
for Various Beams in Phase Two**

Beam-End	Tensile Strain During Curing		Tensile Strain At Prestress Release (x 10 <sup>-2</sup> in/in)		Residual Tensile Strain 10-hrs after Prestress Release # (x 10 <sup>-2</sup> in/in)
	Max.	Avg.	Max.	Avg.	
B1-North	Max.	0.80	Max.	1.16	0.13
	Avg.	0.08	Avg.	0.76	
B1- South	Max.	0.95	Max.	1.80	0.90
	Avg.	0.10	Avg.	0.14	
B2- North	Max.	0.70	Max.	1.28	0.11
	Avg.	0.10	Avg.	0.10	
B2- South	Max.	0.04	Max.	1.90	0.10
	Avg.	0.01	Avg.	0.15	
B3- North	Max.	0.06	Max.	1.15	0.03
	Avg.	0.01	Avg.	0.16	
B3- South	Max.	0.12	Max.	1.3	0.06
	Avg.	0.10	Avg.	0.35	
B4- North	Max.	0.25	Max.	0.40	0.05
	Avg.	0.05	Avg.	0.33	
B4- South	Max.	- *	Max.	- *	0.03
	Avg.	- *	Avg.	- *	
B5- North	Max.	0.30	Max.	0.80	0.50
	Avg.	0.01	Avg.	0.10	
B5- South	Max.	0.10	Max.	0.55	0.10
	Avg.	0.015	Avg.	0.25	

**Note: #** - In general all rebars recovered strains to the original level.

**\*** - No data available due to instrumentation malfunction.

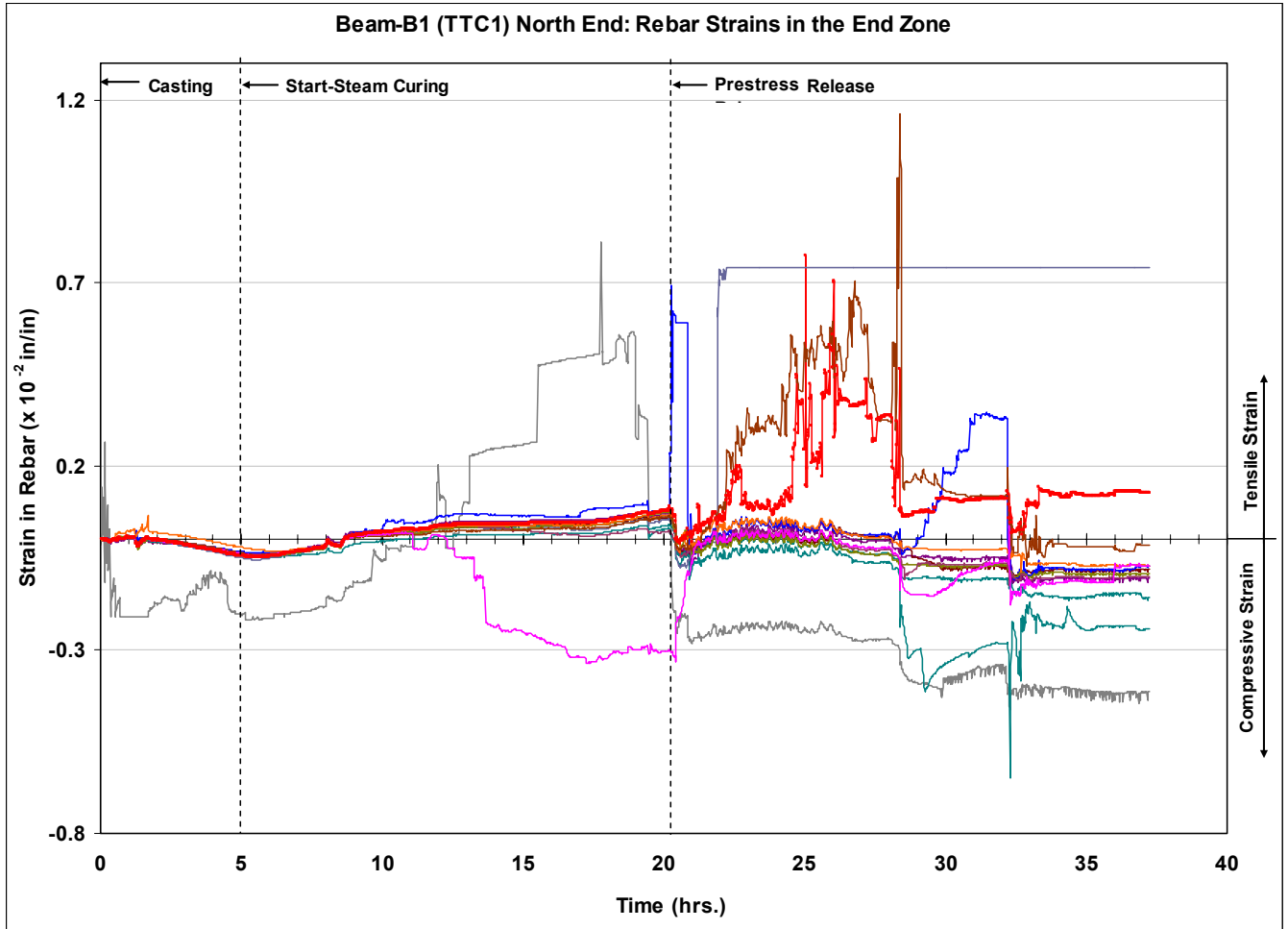


**Fig. 4.5.1 Variation of Rebar Strains Measured by Strain Gauges with Time at the End Zone for Beam B1-North**

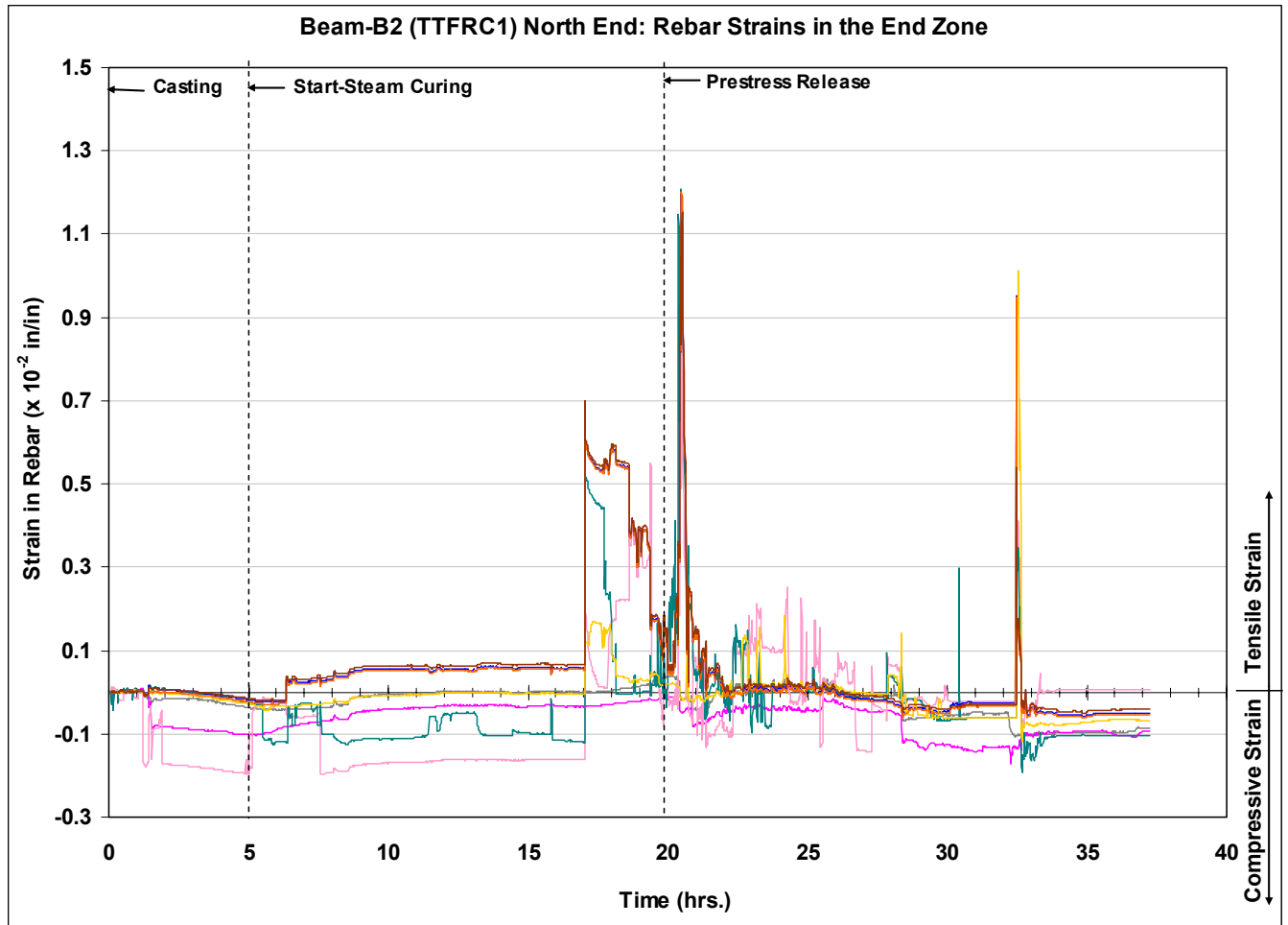


**Fig. 4.5.2 Variation of Rebar Strains Measured by Strain Gauges with Time at the End Zone for Beam B2-North**

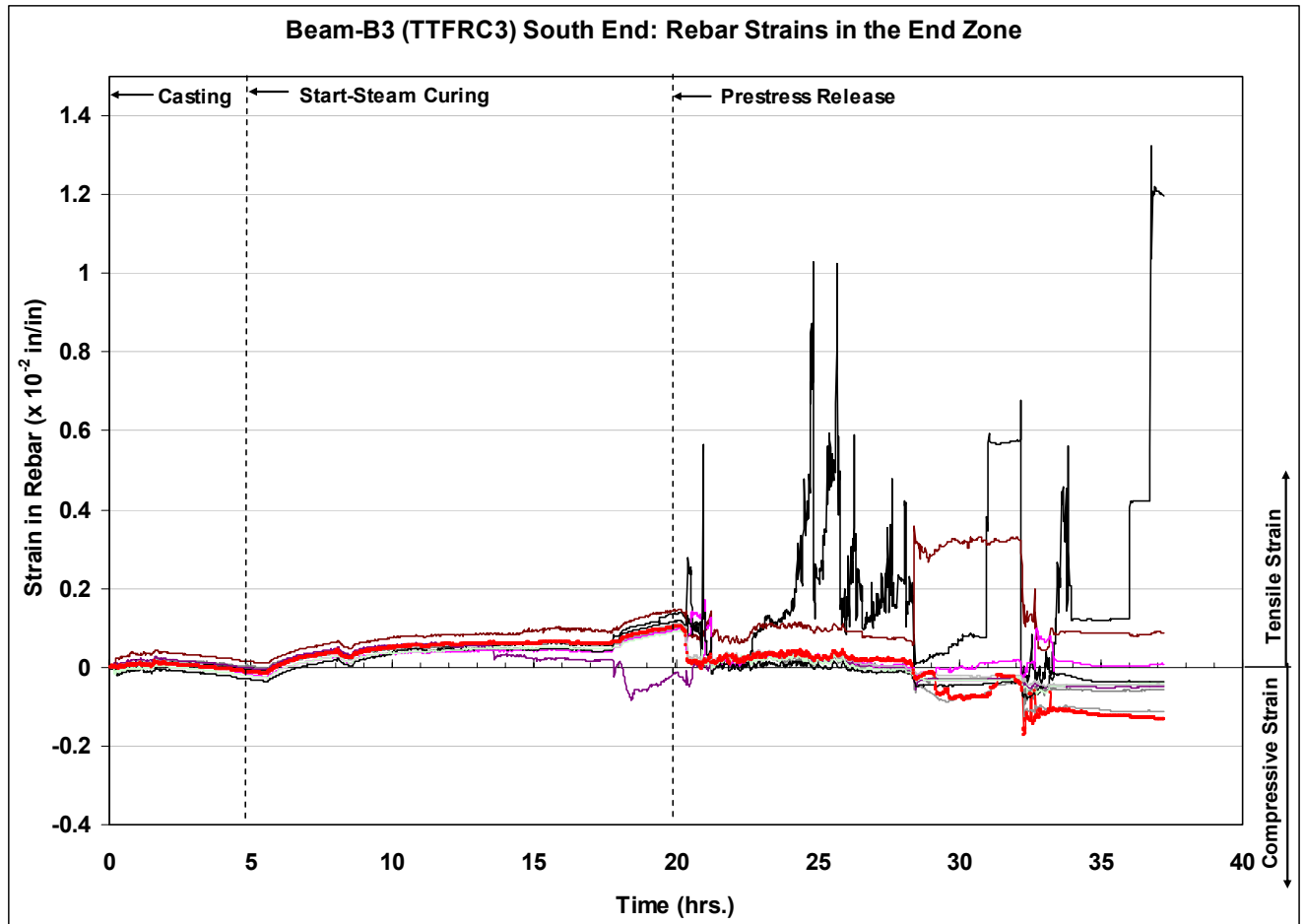


**Fig. 4.5.3 Variation of Rebar Strains Measured by Strain Gauges with Time at the End Zone for Beam B3-South**

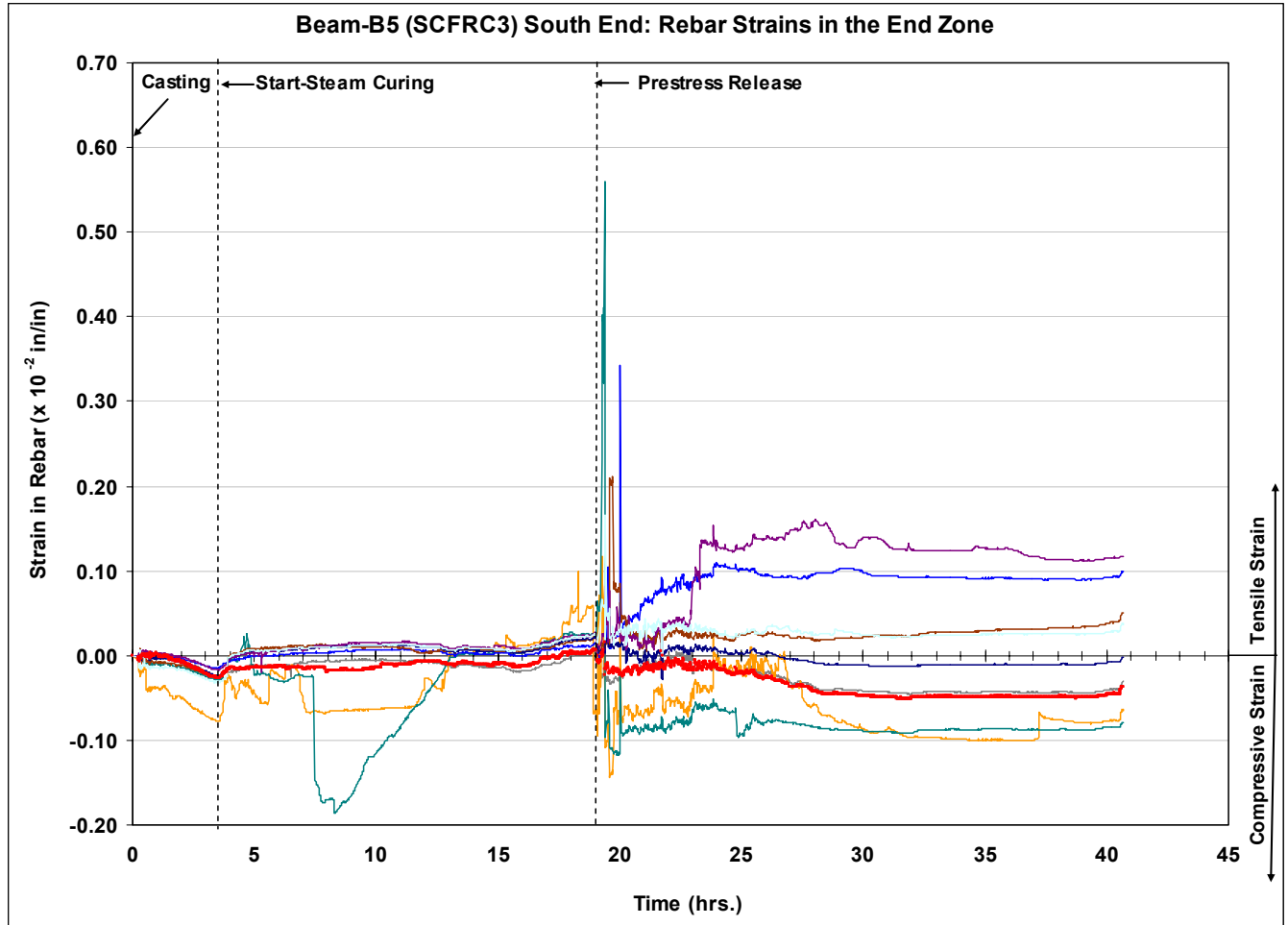


**Fig. 4.5.4 Variation of Rebar Strains Measured by Strain Gauges with Time at the End Zone for Beam B5-South**

The maximum tensile strains during curing were much pronounced in beam B1, while the average tensile strains developed in the rebars of fiber reinforced beams, B2 to B5, and were considerably smaller than that in beam B1. Hence, fibers effectively reduced the tensile strains due to thermal loading in the concrete matrix.

Similarly, the average tensile strains developed during the release of prestress in fiber reinforced beams are considerably less than that in beam B1. In other words, fibers have contributed substantially towards enhancing not only the tensile strength but also the end zone stress redistribution. Long fibers (RC80/60BN) have structurally performed slightly better than the short fibers (ZP305) in the end region of the beams. It can also be noted that fibers have

shown a little more effectiveness in beams with SCFRC than in TTFRC mixes with regard to its performance in the end region.

As observed from Fig. 4.5.1 to 4.5.4, the strain gauge data also revealed a very interesting finding. About 10-hours after release of prestress, when the rebar strains gradually recovered to the original level, very few rebars showed residual tensile strains at this point. As shown in Table 4.5.1, the average residual strains of  $0.90 \times 10^{-2}$  recorded in beam B1-South end were much higher than the residual strains of  $(0.03 \text{ to } 0.5) \times 10^{-2}$  in the North ends of all the fiber reinforced beams. Hence, fibers were very effective as end zone reinforcement - much better than the traditional transverse reinforcement.

Figs. 4.5.5 through Fig. 4.5.8 show the typical graphs of the variation of concrete temperature with concrete age for beams with different types of concrete mixes. Thermal loading of concrete for the beams, i.e. the difference between maximum temperature and minimum temperature in concrete, could be calculated from the above mentioned figures. The average maximum temperature loading for TxDOT traditional concrete was 84.15 °F, while the average maximum thermal loading for SCC was 102.6 °F. This result shows that SCC has higher thermal loading than traditional concrete. This is due to the higher cement contents of SCC when compared to the traditional concrete. The maximum thermal loading from all beams was 120.6 °F at the south end of beam B5.

The measured temperature data also revealed that the traditionally assumed thermal loading for concrete, i.e. 60 °F, was much lower than the actually measured thermal loading of 84 °F in case of traditional concrete and 120 °F for SCC. This may be the reason for the discrepancy between the analytical results and the actual observations in the beams. While no cracks may be predicted in the beams from the analytical results in Chapter 3, cracks actually did occur in the beams at a later date, i.e. at the end of three months from casting. The regions of critical stresses from the analysis always coincide with the regions of crack development in the actual beams.

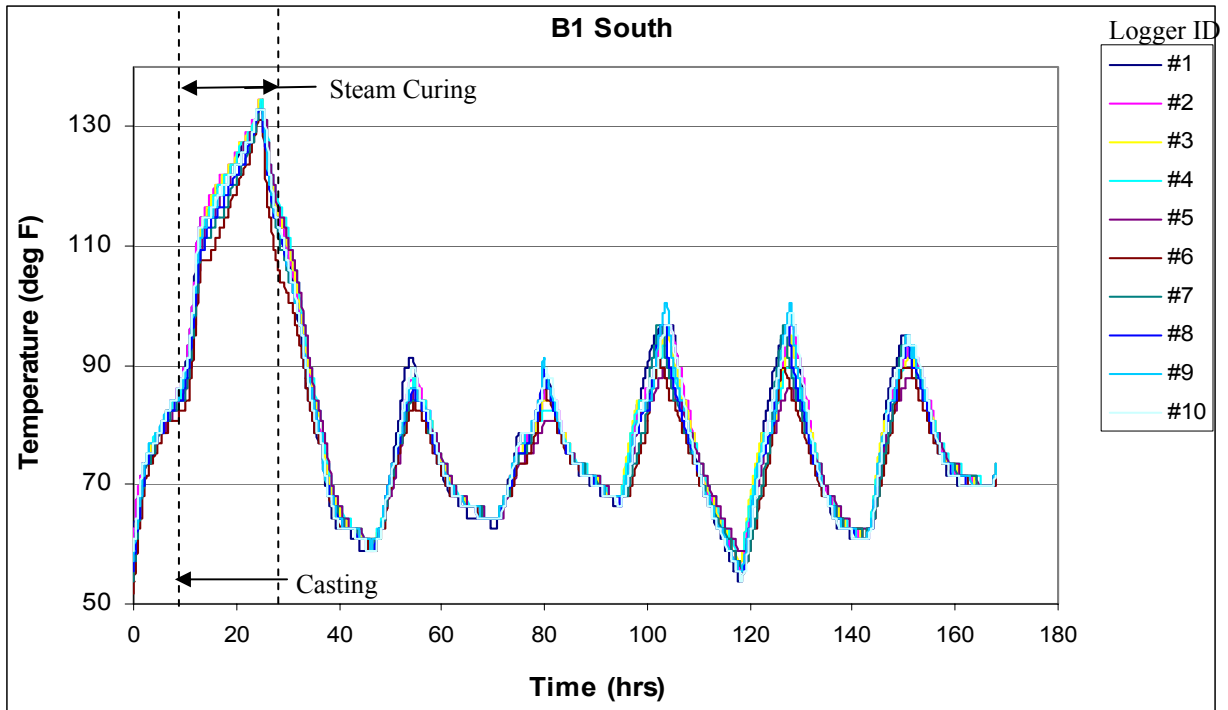


**Fig. 4.5.5** Variation of Concrete Temperature with Age at Beam B1-South (TTC1)

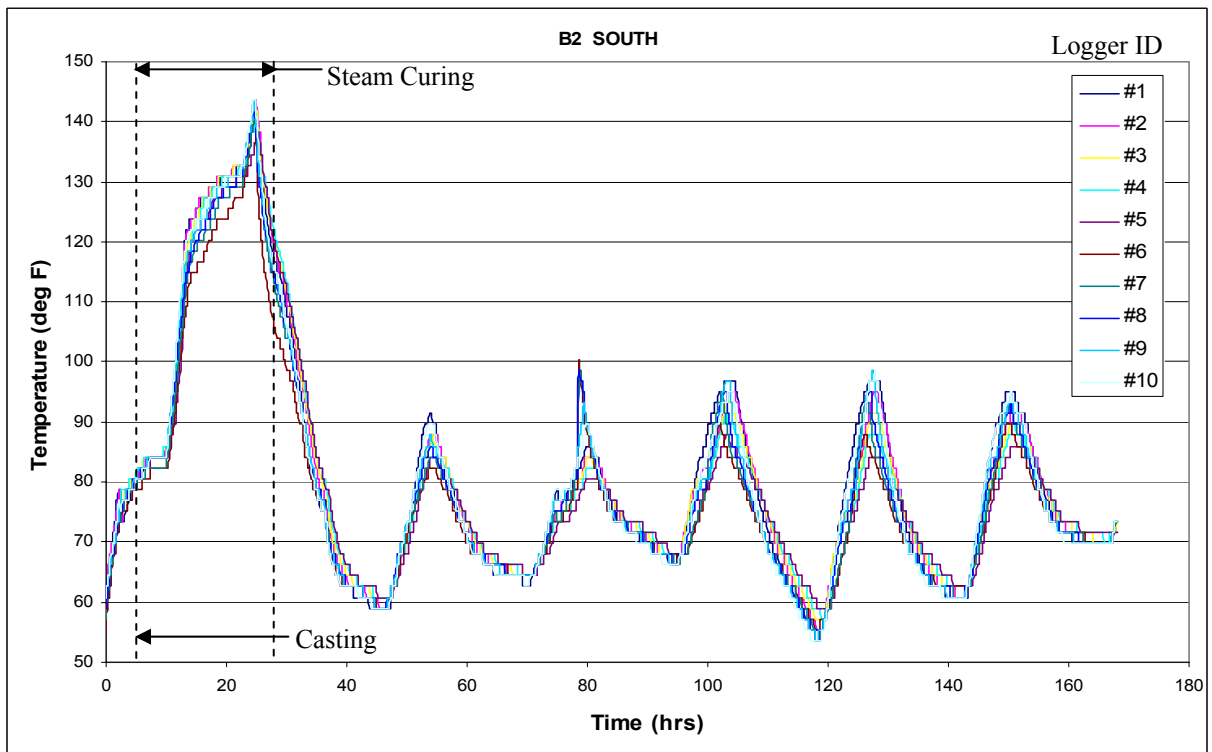


**Fig. 4.5.6** Variation of Concrete Temperature with Age at Beam B2-South (TTFRC1)

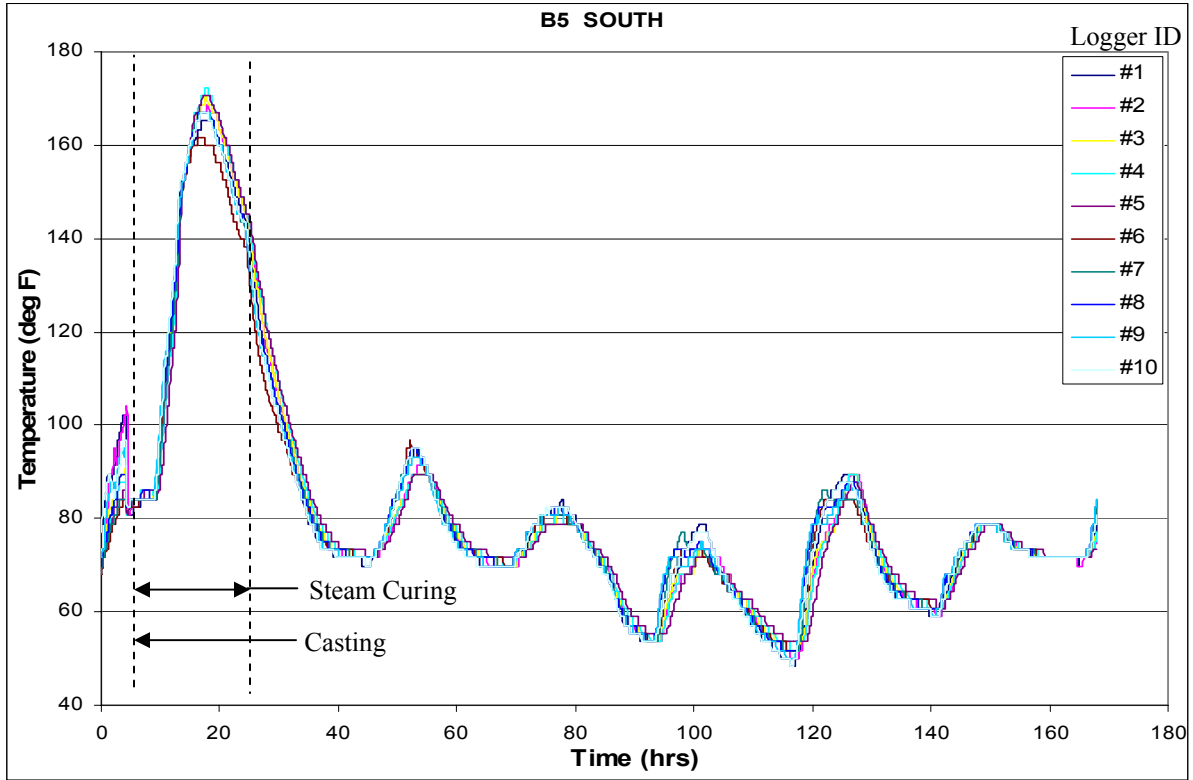


**Fig. 4.5.7** Variation of Concrete Temperature with Age at Beam B5-South (SCFRC3)

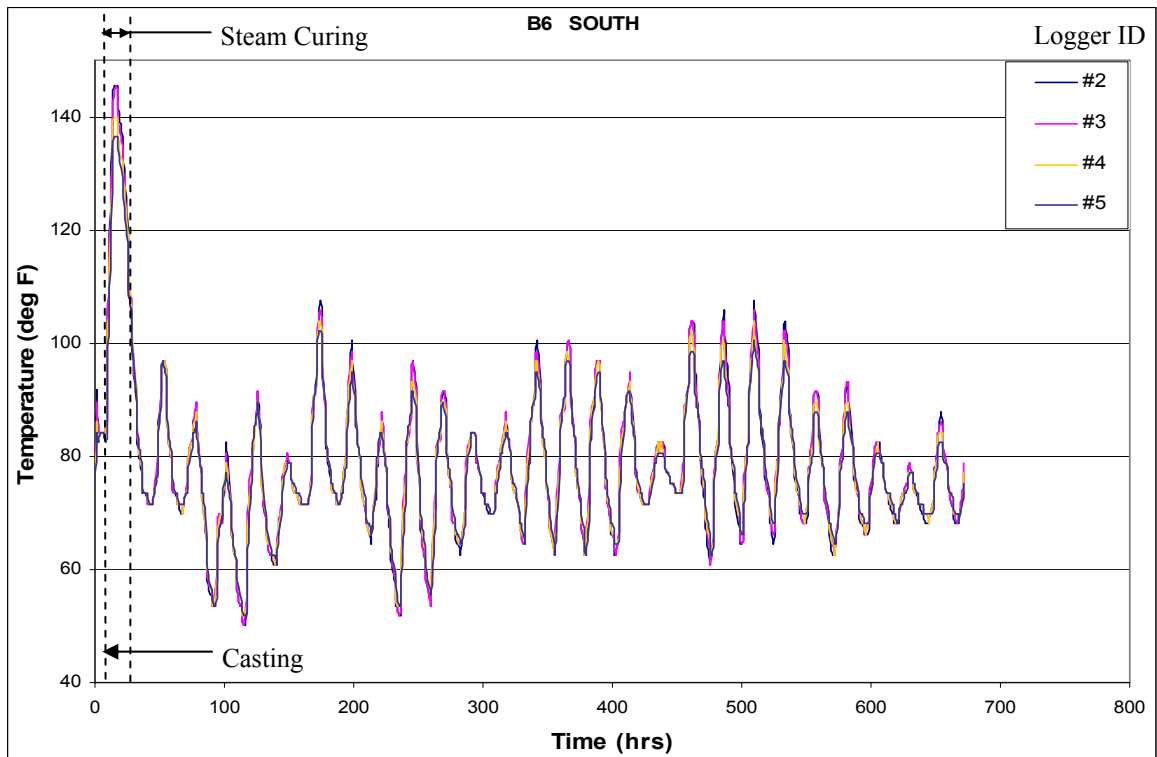


**Fig. 4.5.8** Variation of Concrete Temperature with Age at Beam B6-South (SCC)

This page replaces an intentionally blank page in the original.

-- TxDOT Research Library Digitization Team

## CHAPTER 5

### LOAD TESTS OF PRESTRESSED CONCRETE BEAMS

#### 5.1 Load Test Set-Up

In the load tests, the beams were subjected to vertical loading up to their maximum shear or moment capacity in a specially built steel loading frame as shown in Fig. 5.1.1. Four actuators, attached to the steel frame, were used to provide vertical loads on the beams. Actuators A, B, C and D each has a capacity of 220 kips, 320 kips, 320 kips and 146 kips, respectively.

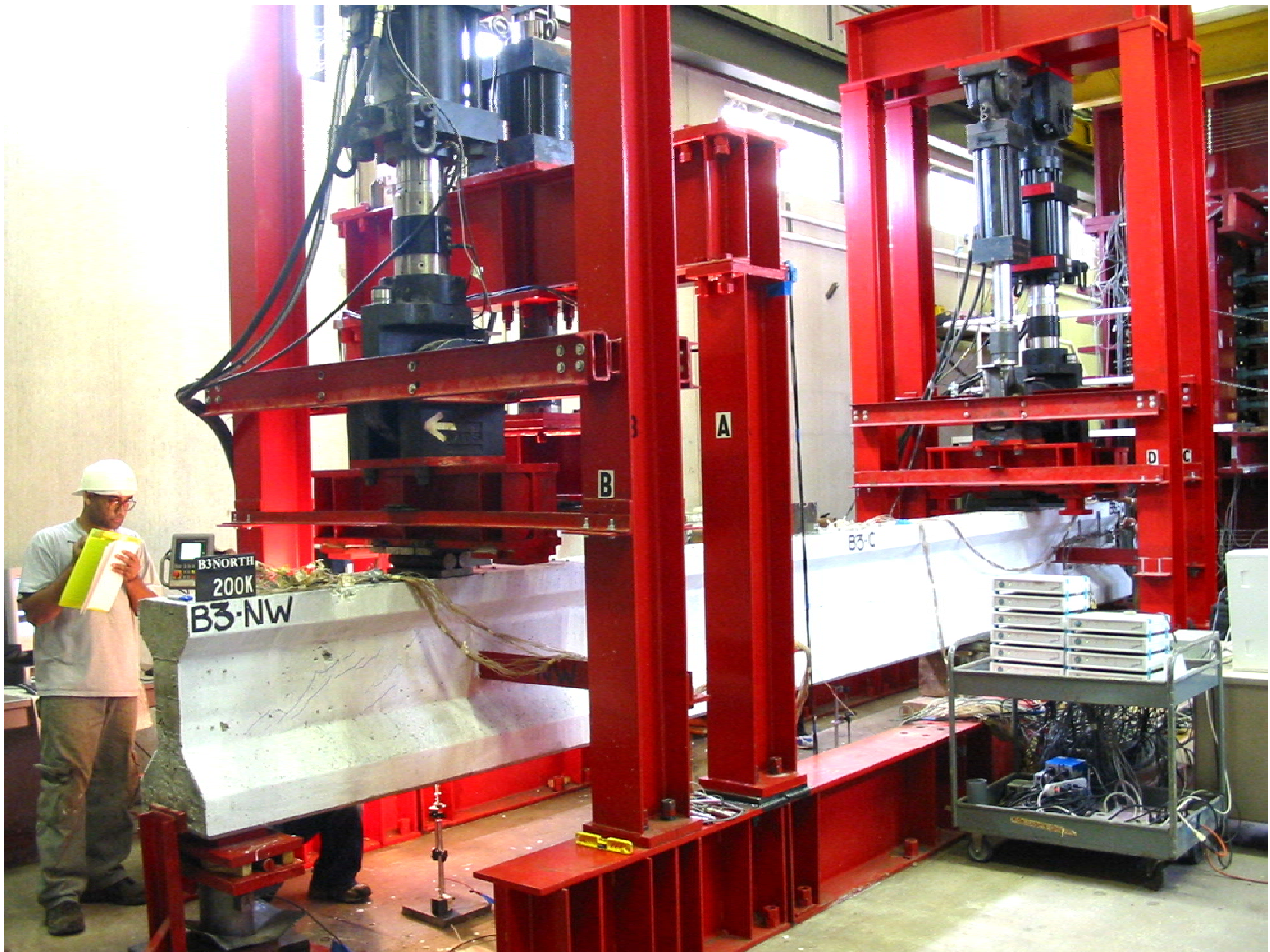


**Fig. 5.1.1 Load Test Setup**



top of two WF18 X 97 beams with a length of 20 feet. The spacing between the two WF18 X 97 beams was 87 inches center to center. The beam specimen was positioned in the middle of this spacing width on top of two load cells placed at each end. The load cells were sitting on top of the steel pedestals fixed to the strong floor. Each load cell was of 500 kips capacity. On top of the load cells, bearing plates to support the beams were placed with a roller on North end and fixed roller on South end. Thus, a beam was simply supported on a roller at North end and a hinge on the South end; allowing the beam to rotate freely and translate horizontally. Lateral bracings were provided on the actuators for their lateral stability.

The position of vertical loadings on the beam together with the support positions is shown in [Fig. 5.1.3](#). The loads from actuators B and C were positioned at 3 feet from the north support and south support, respectively. The loads from actuators A and D were positioned at 2 feet to the right of actuator B and to the left of actuator C, respectively. Actuator loads were applied through two 6 in. x 12 in. x 2 in. bearing plates and a roller assembly, so as to ensure uniform and frictionless load transfer from actuators on to the beam surface. Lead sheets were also used between the load bearing plates and beam surface. All the bearing plates and rollers were hardened to maximum possible hardness, in order to minimize local deformations.

Actuators were precisely controlled by the MTS 'MultiFlex' System. The first step of the loading procedure was to load the beam at point B and C (3 feet from support) with the same load at the same time. Actuators B and C were first programmed with a load control of 5 kips/min. This step was followed by changing the program to a displacement control of 0.2 inch/hour when the slope of the load-displacement curve approached to horizontal, i.e. the yielding of the beam. This displacement control was applied to actuator C at south end while the load from actuator B was kept constant under a very small displacement control rate. This step continued until the shear failure at the south end of the beam occurred. Some of the beams which had a higher capacity than the load capacity of actuator C had to be additionally loaded with actuator D (2 feet apart from actuator C) with the same displacement-control as actuator C. The displacement control allowed us to trace the post-peak load-deflection curve of the beams. This feature was essential in grasping the ductility/brittleness behavior of the beam reinforced with steel fibers.

After the south end failed, the south end support was moved 5 feet towards the north in order to avoid the failure zone at the south end and to provide a fixed support for testing the

north end to failure. Fig. 5.1.3 shows the position of the moved south support by the dashed arrow. The north end of the beam was then loaded by actuator B, programmed with a load control of 5 kips/min. Then, when the slope of load deflection curve approached the horizontal, the loading program was switched to a displacement control of 0.2 inches/hour. When the capacity of the north end of the beam was higher than the load capacity of actuator B, actuator A (2 feet from actuator B) was activated with the same displacement control procedure. The testing was stopped when the north end failed.

During the load testing, Linear Voltage Displacement Transducers (LVDTs) were used to measure displacements at several critical points on the web in the end zone of the beam, as shown in Fig. 5.1.4. Several LVDTs were also placed under the beam at the point of loading to measure the actual total and net displacements of the beam. Strain gauges installed on the rebars inside the beams (used previously in the early-age measurements) were also used to monitor the rebar strains during the load test. On an average, each beam was instrumented by about 30 LVDTs and 25 strain gauges to record the structural behavior of the beam. Data from these sensors were continuously monitored and stored by the HBM ‘Spider-8’ Data Acquisition System. Shear cracks formed on the beam web during the load test were regularly marked on the grid as shown in Fig. 5.1.5. The crack widths were measured using a hand-held microscope having a 0.001 in. measuring precision.

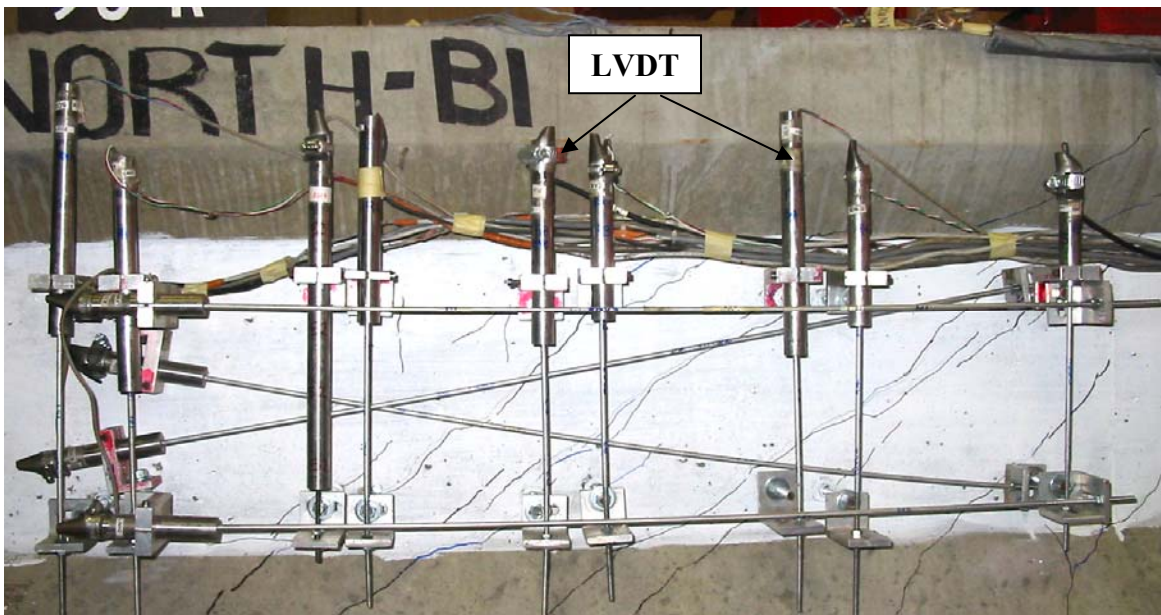


**Fig. 5.1.4 Position of LVDTs on the Web of Test Beam**

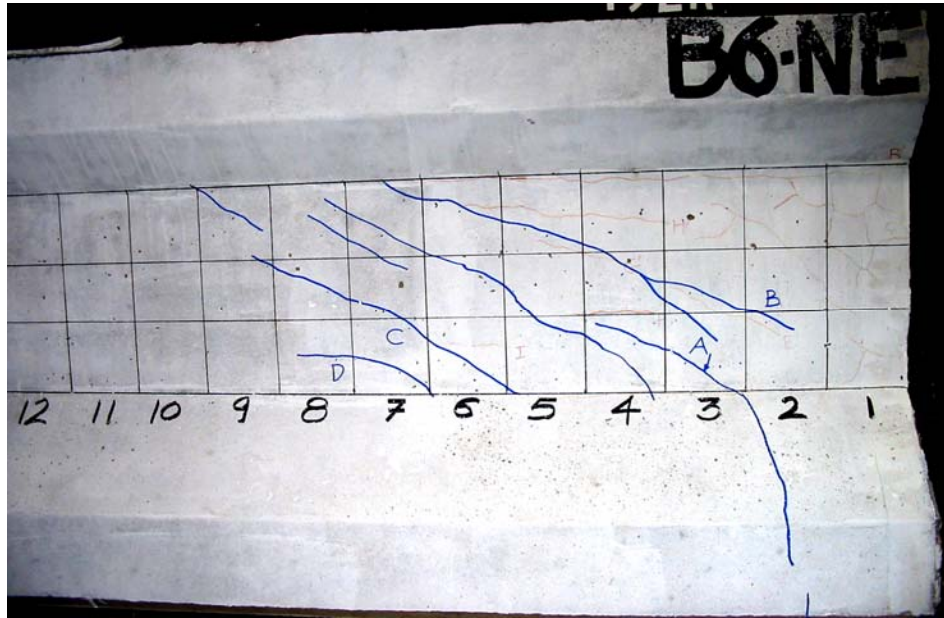


**Fig. 5.1.5 Tracking and Measuring Shear Cracks on the Web of Test Beam**

## **5.2 Load Test Variables**

The seven test specimens, B0 to B6, involve five variables: type of concrete mixes, type and volume of steel fibers (short fiber or long fiber), and transverse steel (at north end and at south end). These variables are listed in [Table 5.2.1](#). The cylinder strengths of the concrete used in the test beams are also recorded. It should be noted that the strengths indicated in this table are not measured at 28 days but on the day of the beam test. It can be seen from the table that the compressive strengths of the concrete varied between 9 ksi and 14.5 ksi. This variation in the concrete strengths may be useful in explaining the variation of behavior of different beams to be reported hereafter.

**Table 5.2.1 Variables in Test Beams B0 to B6**

<b>Beams</b>	<b>Concrete Mixes</b>	<b>Steel Fibers</b>	<b>Transverse Steel North End</b>	<b>Transverse Steel South End</b>	<b>Concrete Cylinder Strength (ksi)</b>
<b>B0</b>	TTFRC4	1.5 % SF	-0-	-0-	14.5
<b>B1</b>	TTC1	-0-	4.2 %	1 %	12.2
<b>B2</b>	TTFRC1	1 % SF	1 %	0.42 %	10.3
<b>B3</b>	TTFRC3	0.5 % LF	1 %	0.42 %	11.2
<b>B4</b>	SCFRC1	0.5 % LF	1 %	0.42 %	10.9
<b>B5</b>	SCFRC3	1 % SF	1 %	0.42 %	8.9
<b>B6</b>	SCC2-3	-0-	4.2 %	1 %	10.6

**NOTE:**

**TTC**-TxDOT Traditional Concrete Mix    **TTFRC**-TTC + Fibers Mix    **SCC** -Self-Consolidating Concrete Mix  
**SCFRC**- SCC + Fibers Mix    **SF**-Short Fiber ZP305    **LF**-Long Fiber RC80/60BN    **TS** - Transverse Steel

**5.3 Load Test Results**

Table 5.3.2 shows the ultimate strengths at failure for each of the two ends of the beam specimens. It can be seen that only the north ends of Beams B1 and B6 failed in flexure. This is due to the fact that the beam ends had a high percentage of shear reinforcement (4.2 %) contributing to the high shear capacities. Thus, these beams reached their flexure capacities before reaching their shear capacities. For all other end regions, the ultimate shear capacity governed the failure.

**5.3.1 Ultimate Shear Strengths**

The effect of steel fibers on the shear strength of test beams can be observed by examining [Table 5.3.1](#). First, the shear strength of the south ends of Beams B1 made of TTC was

294 kips, while that of B6, made of SCC was 290 kips. It can be seen that the concrete mixes (TTC vs. SCC) has negligible effect on the shear capacity of the beams. Second, the comparison of the south end shear strength of Beam B1 with those of Beams B2 and B3 shows that the shear capacity of the beams can be significantly increased due to the addition of steel fibers in concrete, even though the amount of shear steel in the south ends of beams B2 and B3 are lower than that in Beam B1. Third, the south end shear capacities of beams B4 and B5 with steel fibers (276 and 248 kips) were less than that of Beam B1 (294 kips). This may be due to the fact that Beams B4 and B5 had much lower concrete strength (10.9 and 8.9 ksi) in comparison to the concrete in Beam B1 (12.2 ksi). Also, the transverse steel was much less (0.42 % vs. 1 %). Finally, the south end of Beam B0 had a shear capacity of 375 kips, much higher than that of 294 kips for Beam B1, even though Beam B0 had no traditional shear reinforcement. In short, the significance of steel fibers in contributing to the shear strengths is evident.

**Table 5.3.1 Ultimate Strengths of Beams B0 to B6 at North and South Ends**

<b>Beam</b> (Mix)	<b>Steel Fibers</b> (% vol) (Type)	<b>Transverse Steel</b> (%vol)	<b>Concrete Strength</b> (ksi)	<b>Failure Type</b>	<b>Ultimate Shear Capacity at Failure</b> V (kips)	<b>Ultimate Moment Capacity at Failure</b> M (kips-ft.)	<b>Max. Shear at Ultimate Moment</b> (kips)	<b>Max. Moment at Ultimate Shear</b> (kips-ft.)
<b>B1-North</b> (TTC1)	0	4.2	12.2	Flexure	-	<b>1048</b>	<b>329</b>	-
<b>B1-South</b> (TTC1)	0	1.0	12.2	Shear	<b>294</b>	-	-	<b>882</b>
<b>B2-North</b> (TTFRC1)	1 (SF)	1.0	10.3	Shear	<b>330</b>	-	-	<b>1078</b>
<b>B2-South</b> (TTFRC1)	1 (SF)	0.42	10.3	Shear	<b>349</b>	-	-	<b>1151</b>
<b>B3-North</b> (TTFRC3)	0.5 (LF)	1.0	11.2	Shear	<b>253</b>	-	-	<b>759</b>
<b>B3-South</b> (TTFRC3)	0.5 (LF)	0.42	11.2	Shear	<b>342</b>	-	-	<b>1079</b>
<b>B4-North</b> (SCFRC1)	0.5 (LF)	1.0	10.9	Shear	<b>265</b>	-	-	<b>795</b>
<b>B4-South</b> (SCFRC1)	0.5 (LF)	0.42	10.9	Shear	<b>276</b>	-	-	<b>828</b>
<b>B5-North</b> (SCFRC3)	1 (SF)	1.0	8.9	Shear	<b>257</b>	-	-	<b>771</b>
<b>B5-South</b> (SCFRC3)	1 (SF)	0.42	8.9	Shear	<b>248</b>	-	-	<b>777</b>
<b>B6-North</b> (SCC2-3)	0	4.2	10.6	Flexure	-	<b>1077</b>	<b>325</b>	-
<b>B6-South</b> (SCC2-3)	0	1.0	10.6	Shear	<b>290</b>	-	-	<b>897</b>
<b>B0-North</b> (TTFRC4)	1.5 (SF)	0	14.5	Shear	<b>301</b>	-	-	<b>903</b>
<b>B0-South</b> (TTFRC4)	1.5 (SF)	0	14.5	Shear	<b>375</b>	-	-	<b>1243</b>

**NOTE:** **TTC**-TxDOT Traditional Concrete Mix **TTFRC**-TTC + Fibers Mix **SCC** -Self-Consolidating Concrete Mix  
**SCFRC** - SCC + Fibers Mix **SF** - Short Fiber ZP305 **LF** - Long Fiber RC80/60BN **TS** - Transverse Steel

### 5.3.2 Ductility Observed in Shear Forces vs. Deflection Curves

[Fig. 5.3.1](#) shows the plot of shear force acting on the beams against the beam deflections. The shear force plotted in this figure was obtained from the reading of the load cells placed under the end supports of the beams. The deflection was obtained from the readings of the LVDT placed under the individual beams at the location of the end actuator. From this figure, it can be seen that the behavior of the two ends of the beams can be easily distinguished. Hence for better comparison the plots for the south and north ends of the different beams have been shown separately in [Figures 5.3.2](#) and [5.3.3](#), respectively.

From [Fig 5.3.2](#), it can be seen that Beam B0 carried higher shear loads than the other beams, as stated before. The amount of inelastic deformation of this beam was also higher and was only comparable with Beam B2. This shows that replacement of shear steel with steel fibers increases the ductility of the structure. This can also be observed from the higher inelastic deformation of the north end of Beam B0 in [Fig 5.3.3](#).

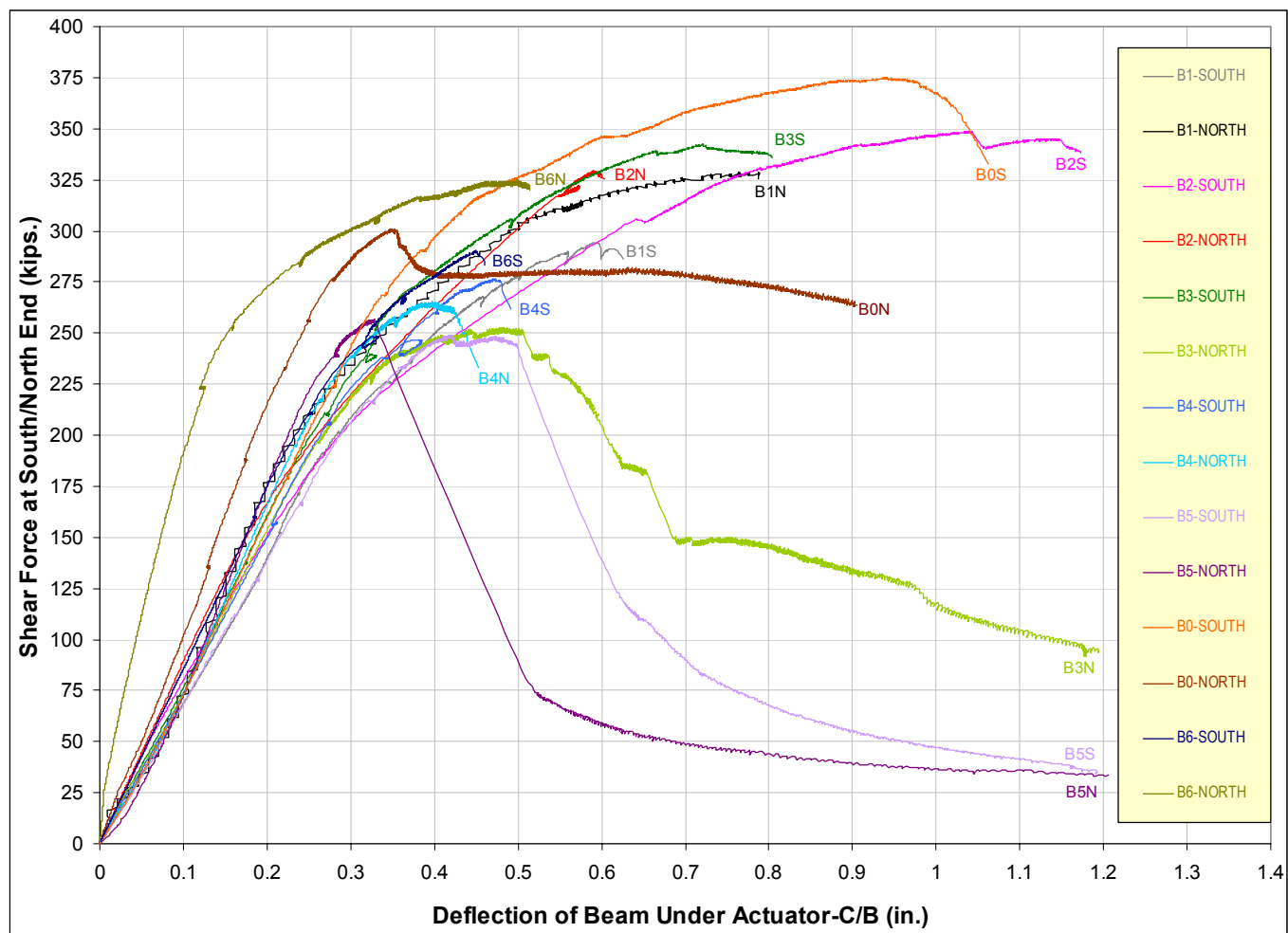


**Fig. 5.3.1 Shear Force - Deflection Curves for Beams B0 to B6**

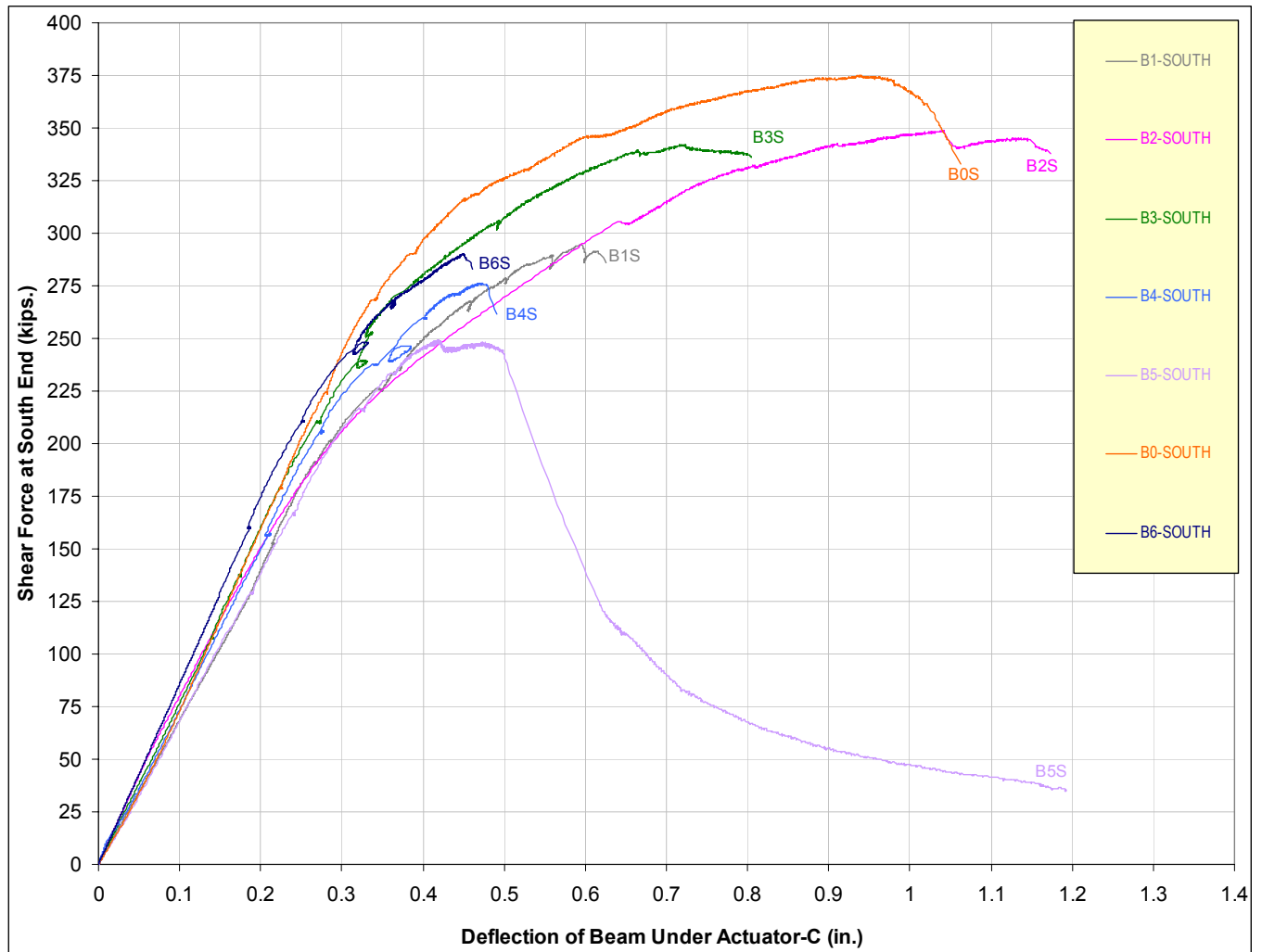


**Fig. 5.3.2 Shear Force - Deflection Curves for South Ends of Beams B0 to B6**

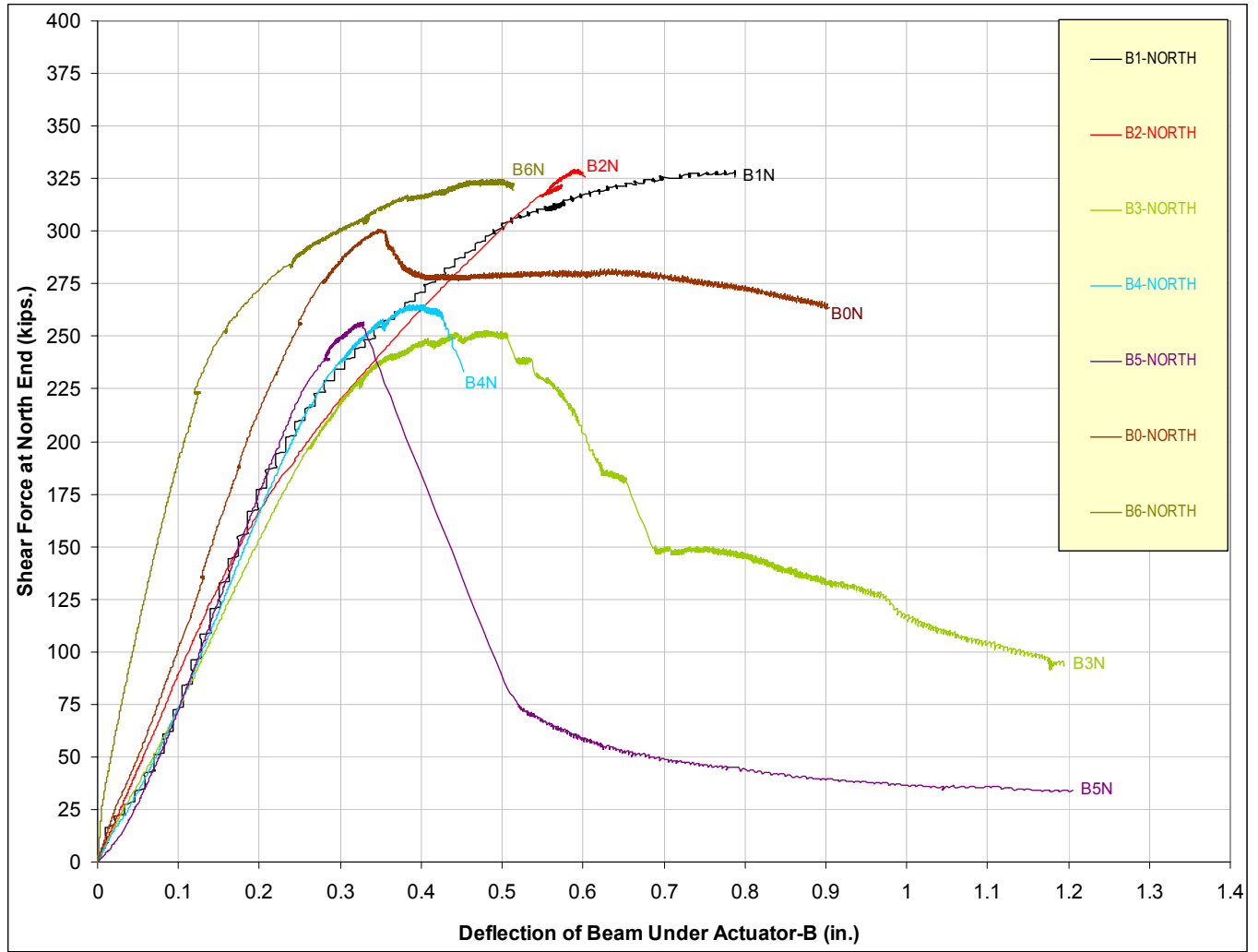


**Fig. 5.3.3 Shear Force - Deflection Curves for North Ends of Beams B0 to B6**

It could also be observed from [Fig. 5.3.2](#) and [Fig. 5.3.3](#) that the ductility of beams is enhanced with the use of steel fibers. In general, SCFRC beams have demonstrated higher ductility than the other beams with steel fibers. The failure of beams B1 and B6 were quite sudden and brittle; without any warnings even in a very low displacement control rate. On the other hands, almost all the fiber reinforced beams failed in a ductile fashion with prior warnings. From the ultimate shear capacities of all the fiber reinforced beams, it could be noted that the beams with short fibers performed better than the beams with long fibers. This was because the fiber factors for beams with short fiber were 55 and 82.5 whereas the fiber factor for the beams with long fiber was comparatively smaller, i.e. 40.

### **5.3.3 Ductility Observed in Shear Forces–Rebar Strains Curves (Strain Gauges)**

[Figure 5.3.4](#) shows the plots of shear force at the beam ends against the percentage tensile strains. The tensile strains plotted in this figure have been obtained from strain gauges attached to shear reinforcements at critical sections. Like the previous case, the plots for the south and north ends of the different beams are shown separately in [Figures 5.3.5](#) and [5.3.6](#), respectively, to facilitate better comparison of the results. It should be noted that Beams B0 and B6 could not be included in this comparative study. This was due to the fact that Beam B0 did not have any shear reinforcement to which strain gauges could be instrumented and Beam B6 did not have any strain gauges instrumented before hand on its reinforcement, as the decision to fabricate this specimen was taken on-site.

From [Figures 5.3.5](#) and [5.3.6](#) it can be seen that the amount of inelastic shear deformation was higher for Beams B2 and B3 with steel fiber reinforced traditional concrete. The shear strengths for Beams B2 and B3 were also comparatively higher than the other beams. It can be seen from [Fig. 5.3.6](#) that the strain developed in rebars of beam B1 at north end are the least. This means that the steel has not yielded even when the shear load was over the service limit, suggesting that the 4.2 % steel is quite excessive and hence uneconomical.

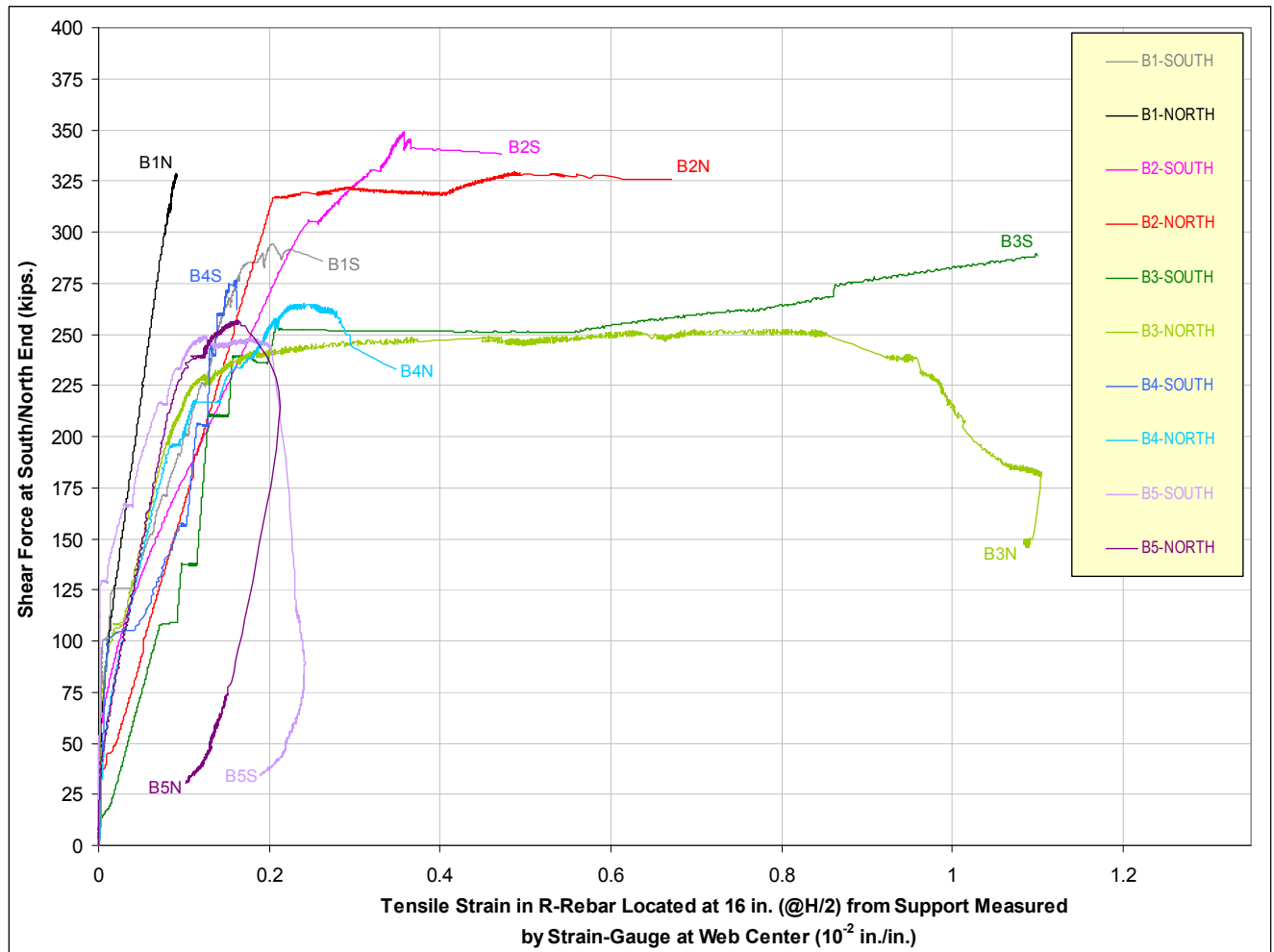


**Fig. 5.3.4 Shear Force Vs. Rebar Tensile Strains Measured by Strain Gauge for Beams B1 to B5 at a Distance of H/2 from Support**

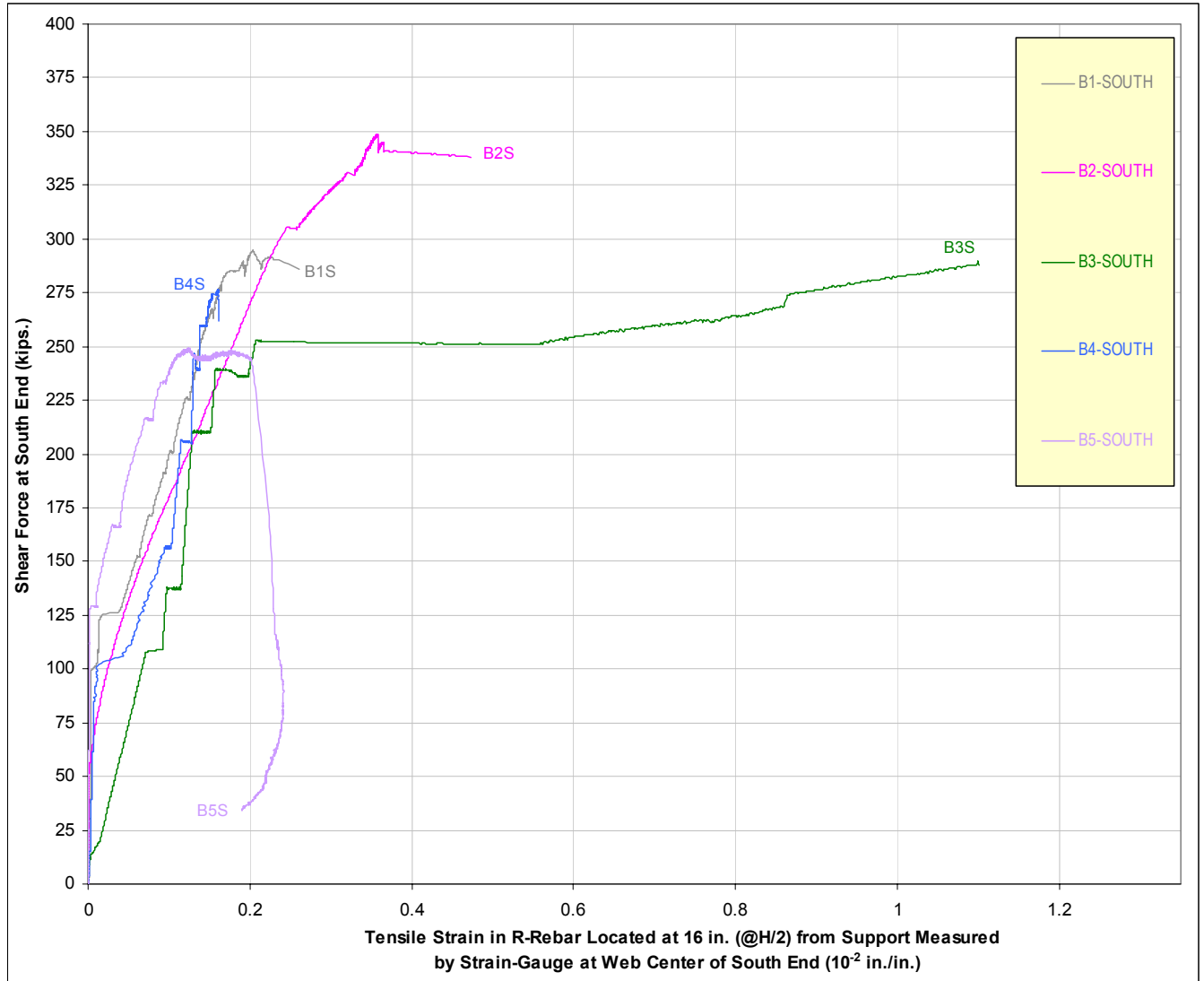


**Fig. 5.3.5 Shear Force Vs. Rebar Tensile Strains Measured by Strain Gauge for South Ends of Beams B1 to B5 at a Distance of H/2 from Support**

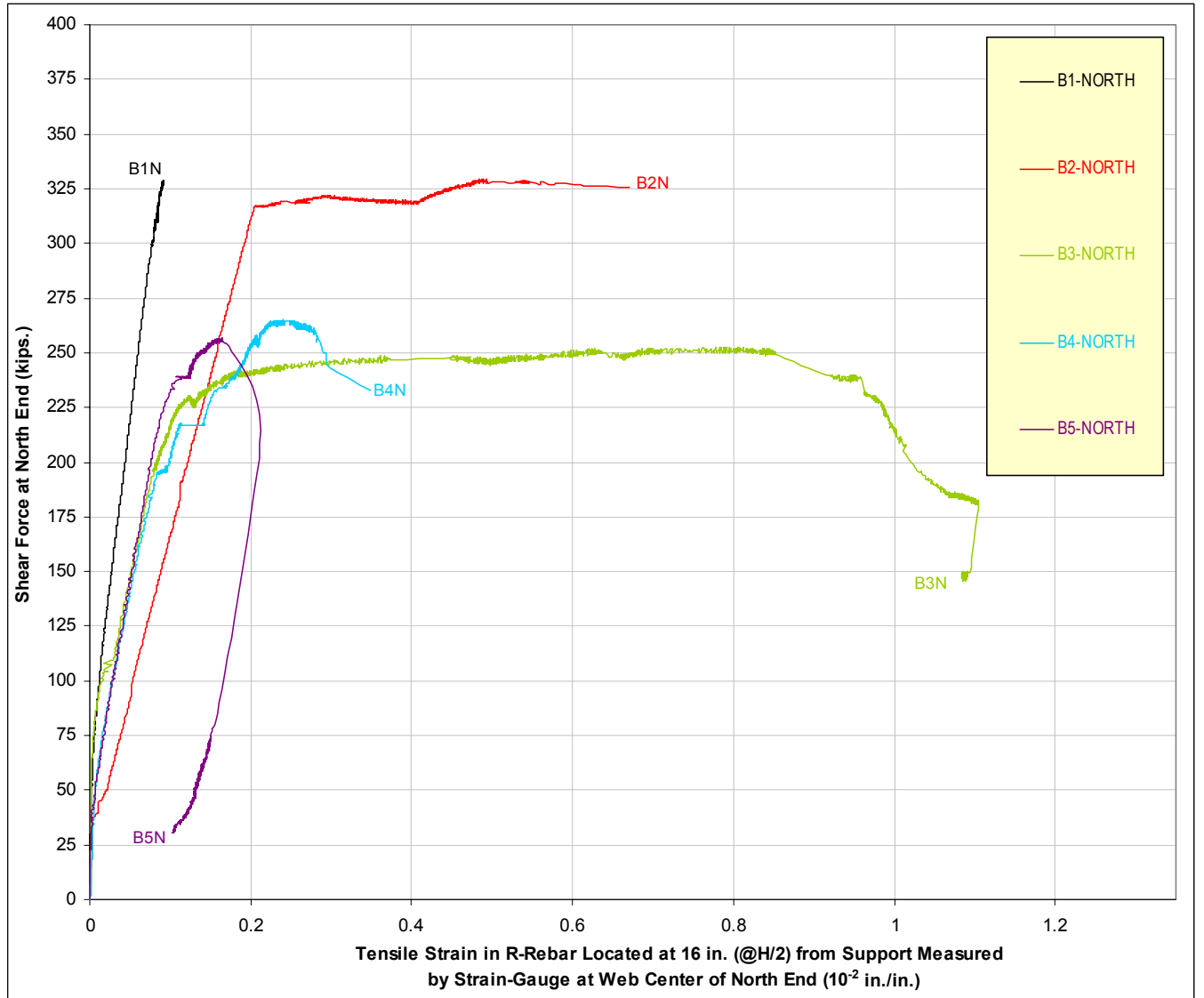
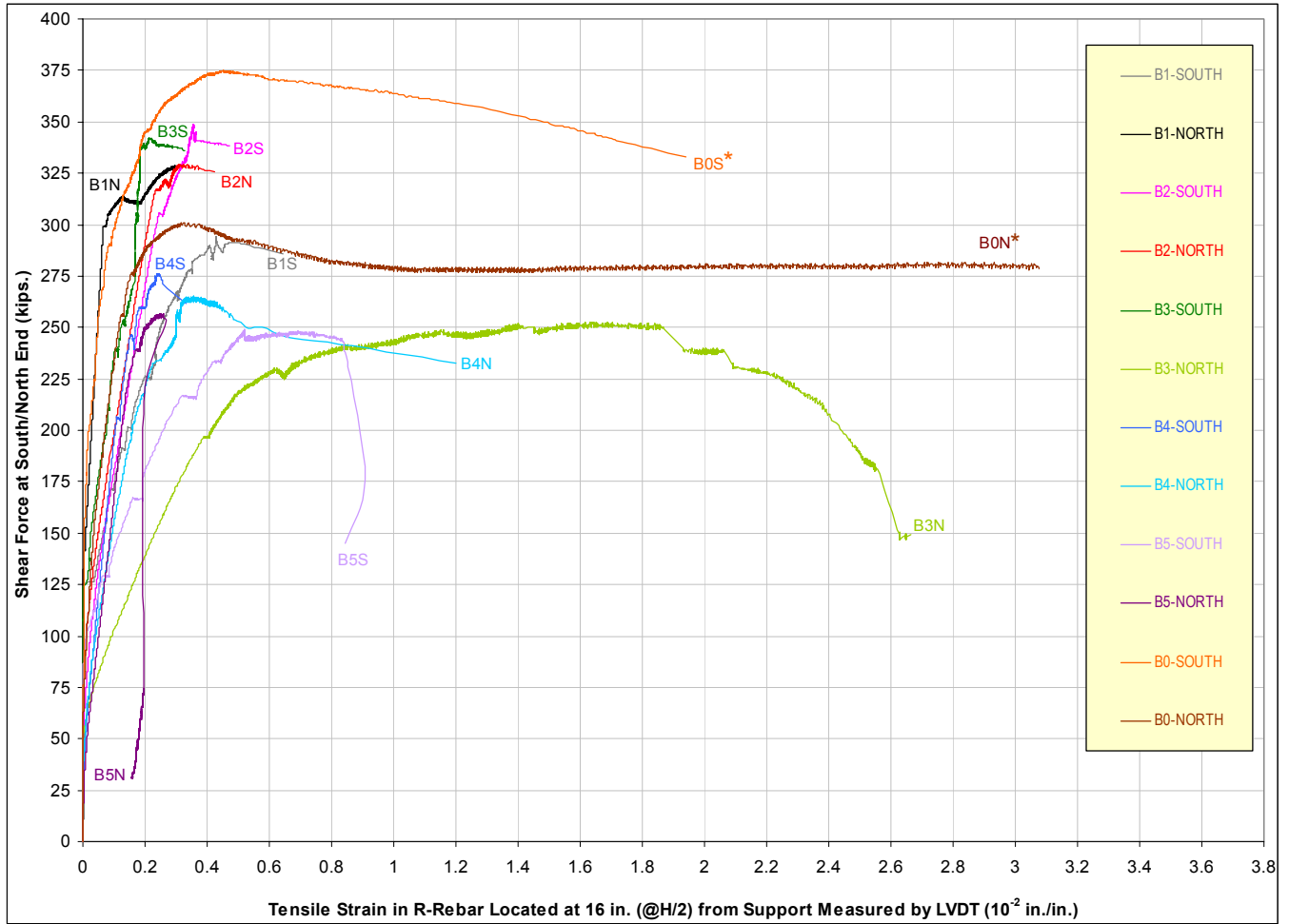


**Fig. 5.3.6 Shear Force Vs. Rebar Tensile Strains Measured by Strain Gauge for North Ends of Beams B1 to B5 at a Distance of H/2 from Support**

#### 5.3.4 Ductility Observed in Shear Forces-Rebar Strain Curves (LVDTs)

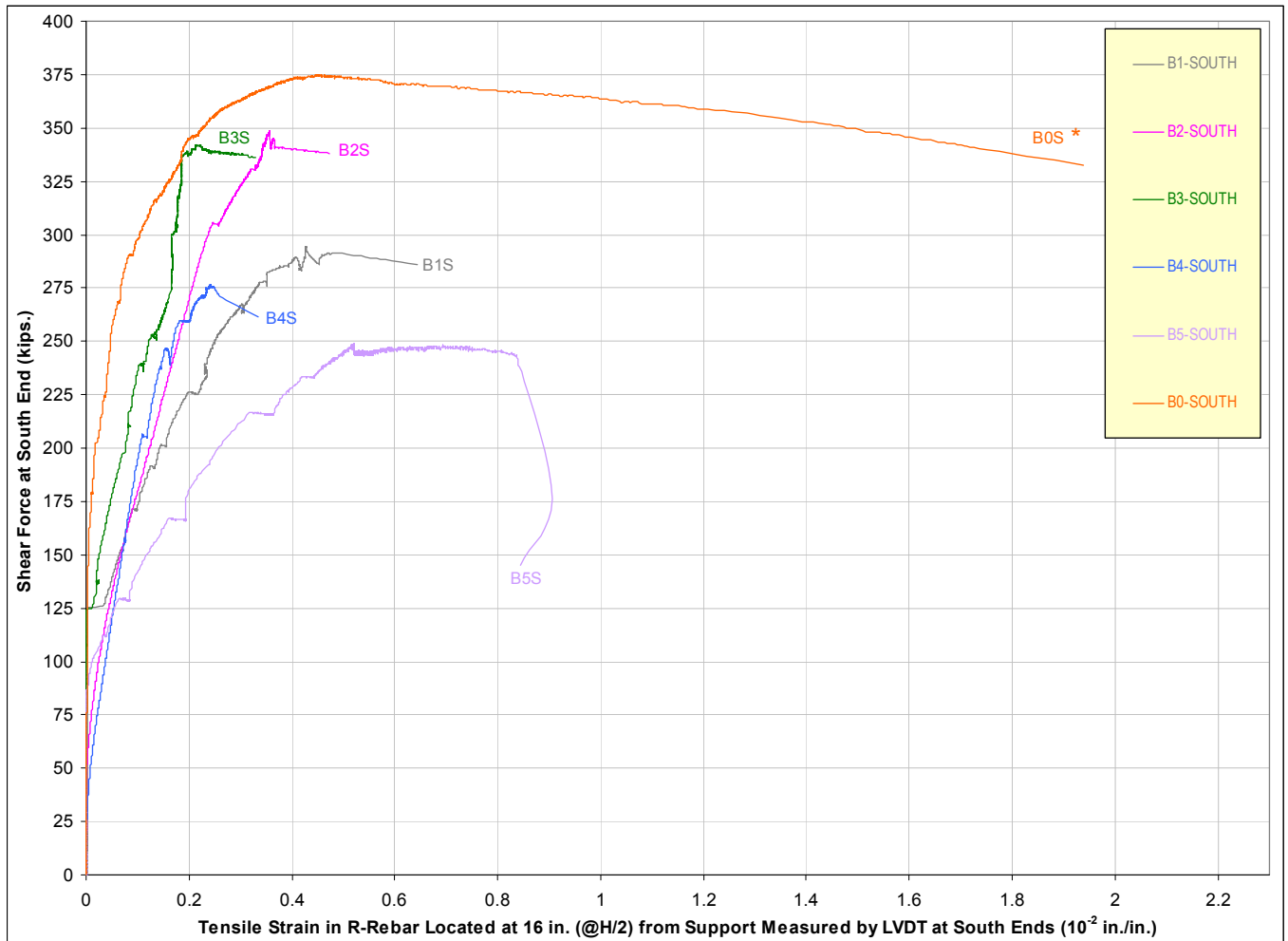
Figure 5.3.7 also shows the plots of shear force at the beam ends against the percentage tensile strains. However the tensile strains plotted in this figure have been obtained from LVDTs attached to the shear reinforcement at critical sections. Here also the plots for the south and north ends of the different beams have been shown separately in Figures 5.3.8 and 5.3.9, respectively, to facilitate better comparison of the results. It should be noted that Beam B0 and B6 could not be included in this comparative study. This was due to the fact that Beam B0 did not have any shear reinforcement to which LVDTs could be attached, and B6 was not instrumented.

From Figures 5.3.8 it can be seen that the shear strength and amount of inelastic shear deformation was much higher for Beam B0 in comparison to the others. Figure 5.3.9 also shows higher amounts of inelastic deformation in Beam B0. Although the shear strength of the beam at this end was not the largest, it compared well to those beams with higher strengths.



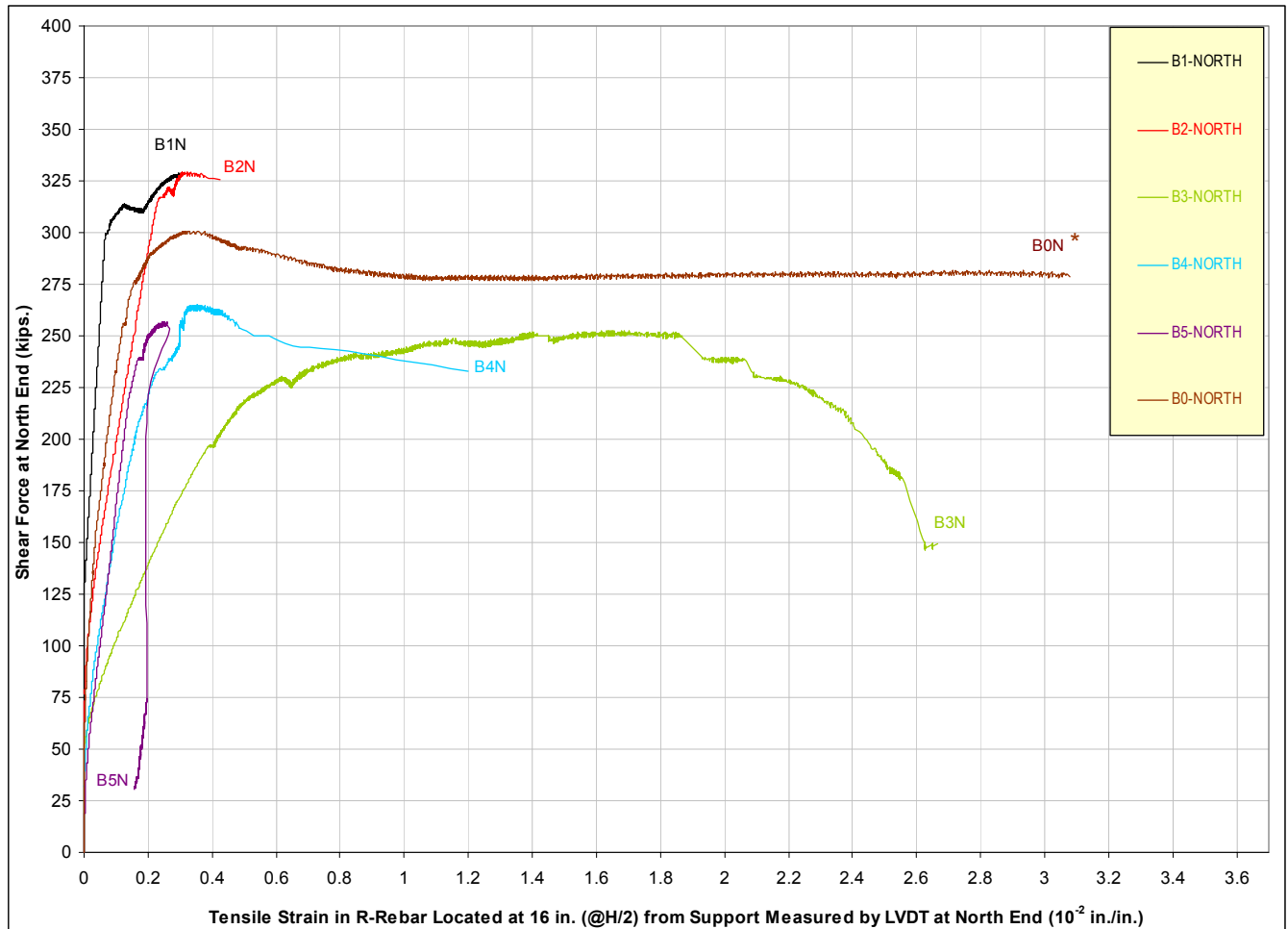
\* - Represents measured average tensile strains in concrete

**Fig. 5.3.7 Shear Force Vs. Rebar Tensile Strains Measured by LVDT for Beams B0 to B5 at a Distance of H/2 from Support**



\* - Represents measured average tensile strains in concrete

**Fig. 5.3.8 Shear Force Vs. Rebar Tensile Strains Measured by LVDT for South End of Beams B0 to B5 at a Distance of H/2 from Support**



\* - Represents measured average tensile strains in concrete

**Fig. 5.3.9 Shear Force Vs. Rebar Tensile Strains Measured by LVDT for North End of Beams B0 to B5 at a Distance of H/2 from Support**

### 5.3.5 Cracking, Crack Widths and Failures of Beams

Table 5.3.3 compares the shear forces at both ends of each of all the different beams at the onset of cracking. Cracking has been considered to initiate when the crack width reaches 0.001 inch (i.e. the minimum reading possible with the microscope used for measuring crack width). It can be seen that in this case cracking for Beam B0 initiates at the maximum shear force. The cracking at the south ends of all the fiber reinforced beams were found to be at higher shear forces than that in Beam B1, which did not contain fibers. This indicates that the addition of steel fibers in beams is notably helpful in preventing the development of initial cracks. Also, the results of Beam B0 indicate that the replacement of steel reinforcement with steel fibers greatly increases the resistance of the beams to initial cracks. Fibers have effectively delayed the onset of cracks in fiber reinforced beams.

Table 5.3.4 shows the width of shear cracks in different beams at a shear force of 250 kips. It also shows the maximum shear crack widths at shear forces close to the failure of the different beams. Comparing the shear crack widths at the south ends of all the beams, for a shear force of 250 k, it can be seen that the shear crack width was minimum for Beam B0. This emphasizes the previously stated capability of steel fibers to control the development of cracks. For most beams, the cracks at the north ends were found to be wider than the south ends. However, in Beams B1 and B6, the case was just the opposite. This may be due to the fact that the shear reinforcement at the north ends of these two beams was too high (4.2 %).

**Table 5.3.3 Comparison of Shear Force at the Onset of Shear Crack for Various Beams**

<b>Beam</b> (Mix)	<b>Steel</b> <b>Fibers</b> (% vol) (Type)	<b>Transverse</b> <b>Steel</b> (% vol)	<b>Concrete</b> <b>Strength</b> (ksi)	<b>Shear Force at Onset of Shear Crack</b> (Crack Width = 0.001 in.) (kips.)
<b>B1-North</b> (TTC1)	0	4.2	12.2	140
<b>B1-South</b> (TTC1)	0	1.0	12.2	100
<b>B2-North</b> (TTFRC1)	1 (SF)	1.0	10.3	160
<b>B2-South</b> (TTFRC1)	1 (SF)	0.42	10.3	150
<b>B3-North</b> (TTFRC3)	0.5 (LF)	1.0	11.2	115
<b>B3-South</b> (TTFRC3)	0.5 (LF)	0.42	11.2	130
<b>B4-North</b> (SCFRC1)	0.5 (LF)	1.0	10.9	145
<b>B4-South</b> (SCFRC1)	0.5 (LF)	0.42	10.9	145
<b>B5-North</b> (SCFRC3)	1 (SF)	1.0	8.9	125
<b>B5-South</b> (SCFRC3)	1 (SF)	0.42	8.9	125
<b>B6-North</b> (SCC2-3)	0	4.2	10.6	115
<b>B6-South</b> (SCC2-3)	0	1.0	10.6	120
<b>B0-North</b> (TTFRC4)	1.5 (SF)	0	14.5	160
<b>B0-South</b> (TTFRC4)	1.5 (SF)	0	14.5	175

**NOTE:**

**TTC**-TxDOT Traditional Concrete Mix    **TTFRC**-TTC + Fibers Mix    **SCC** -Self-Consolidating Concrete Mix  
**SCFRC**- SCC + Fibers Mix    **SF**-Short Fiber ZP305    **LF**-Long Fiber RC80/60BN    **TS** - Transverse Steel

**Table 5.3.4 Comparison of Shear Crack Width of Various Beams Measured Using Hand Held Microscope**

<b>Beam</b>  (Mix)	<b>Steel Fibers</b> (% vol)  (Type)	<b>Transverse Steel</b>  (%vol)	<b>Concrete Strength</b>  (ksi)	<b>Shear Crack Width at Shear Force = 250 kips.</b>  (in.)	<b>Maximum Shear Crack Width</b>  (in.)	<b>Shear Force Corresponding to Maximum Crack Width</b>  (kips)
<b>B1-North</b> (TTC1)	0	4.2	12.2	0.0040	0.010	320
<b>B1-South</b> (TTC1)	0	1.0	12.2	0.0142	0.023	290
<b>B2-North</b> (TTFRC1)	1 (SF)	1.0	10.3	0.0045	0.015	320
<b>B2-South</b> (TTFRC1)	1 (SF)	0.42	10.3	0.0032	0.027	345
<b>B3-North</b> (TTFRC3)	0.5 (LF)	1.0	11.2	0.0140	0.014	240
<b>B3-South</b> (TTFRC3)	0.5 (LF)	0.42	11.2	0.0115	0.021	330
<b>B4-North</b> (SCFRC1)	0.5 (LF)	1.0	10.9	0.0150	0.018	260
<b>B4-South</b> (SCFRC1)	0.5 (LF)	0.42	10.9	0.0140	0.015	260
<b>B5-North</b> (SCFRC3)	1 (SF)	1.0	8.9	0.0100	0.010	245
<b>B5-South</b> (SCFRC3)	1 (SF)	0.42	8.9	0.0120	0.012	245
<b>B6-North</b> (SCC2-3)	0	4.2	10.6	0.0063	0.015	320
<b>B6-South</b> (SCC2-3)	0	1.0	10.6	0.0120	0.014	270
<b>B0-North</b> (TTFRC4)	1.5 (SF)	0	14.5	0.0140	0.025	305
<b>B0-South</b> (TTFRC4)	1.5 (SF)	0	14.5	0.0030	0.010	350

**NOTE:**

**TTC**-TxDOT Traditional Concrete Mix    **TTFRC**-TTC + Fibers Mix    **SCC** -Self-Consolidating Concrete Mix  
**SCFRC**- SCC + Fibers Mix    **SF**-Short Fiber ZP305    **LF**-Long Fiber RC80/60BN    **TS** - Transverse Steel

The maximum shear crack widths recorded before failure of the beams were also low for the south end of Beam B0. However, the crack width at the north end of this beam before failure was higher in comparison to other beams. This may be due to the fact that the beam was loaded to such a high level while failing the south end, and then reloaded again for failing the north end. Beams with short fibers seemed to have performed a more effectively than the beams with long fibers in controlling the shear crack width. This was expected as the beams with short fibers had a higher fiber factor (55 and 82.5) than that of the beams with long fibers (40).

Fig. 5.3.10 shows the development of shear cracks with applied shear force for each of the two ends of the different beams. The crack width for Beam B0 has been found to be lowest throughout the loading stage. Most of the fiber reinforced beams have performed better in controlling shear crack widths than the south end of beam B1. All the above studies clearly indicate that the replacement of shear reinforcement with steel fibers plays an important role in the crack control of the beams.

Table 5.3.5 shows number, width and lengths of cracks developed at each of the two end regions of the different beams, 90 days after casting. These cracks occurred far later than expected. Hence, prestress and thermal loading may not be the only causes of the end zone cracking; secondary time dependent effects such as drying shrinkage, creep etc. might have contributed to the development of these cracks. Beam B0 did not show any crack development at the end region. The cracks in Beams B3, B4 and B5 were of very small widths. The cracks developed in Beams B1, B2 and B6 during this period were found to be comparatively more prominent.

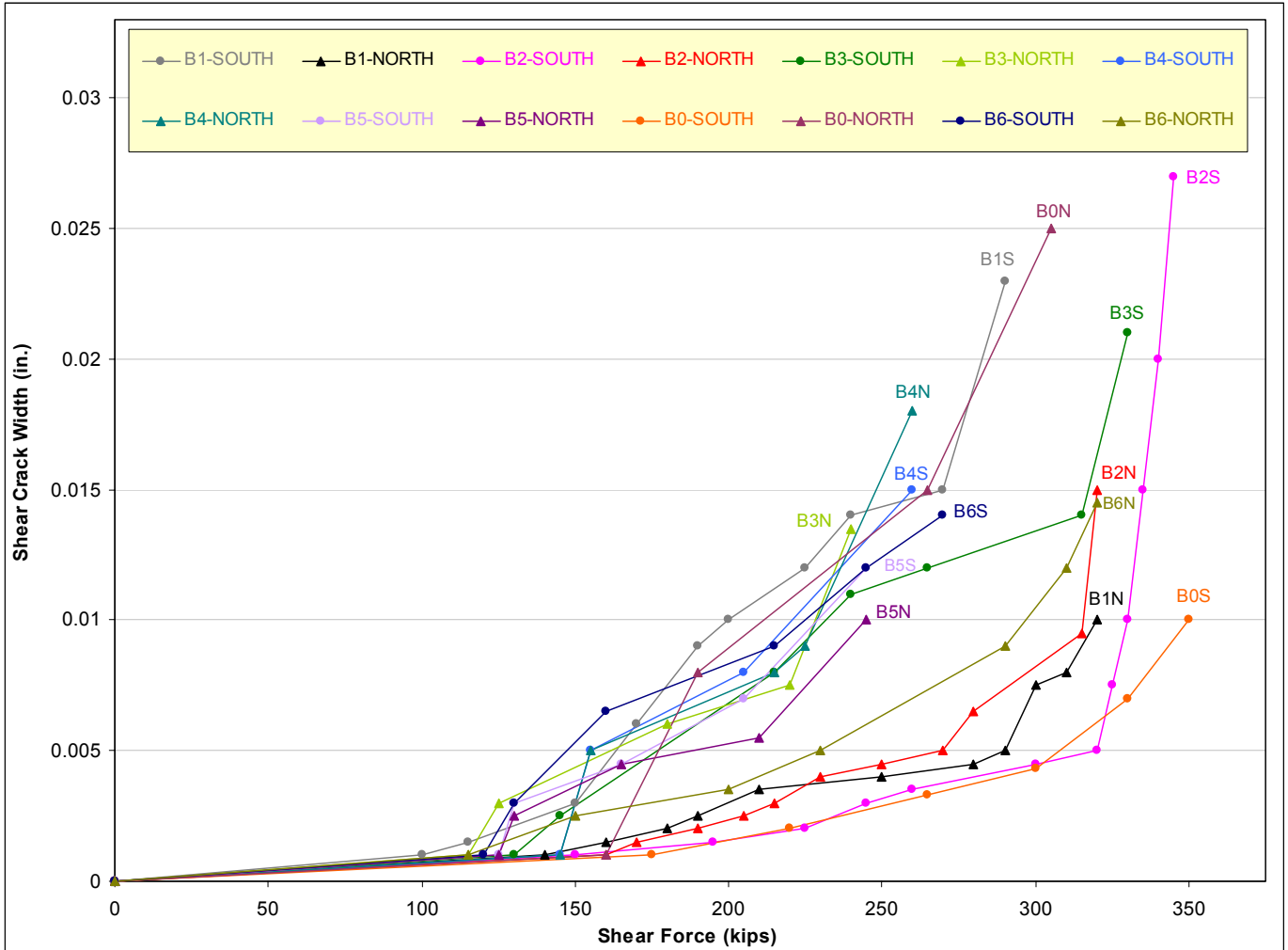


**Fig. 5.3.10 Variation of Shear Crack Width with Shear Force Measured Using Microscope for Beams B0 to B6**

Considering the north and south ends of B1, it can be found that the width of crack was not influenced by the amount of end region reinforcement. The transverse steel has only helped in reducing the number of cracks. It seems that long fibers are more efficient in controlling the end zone cracks than the short fibers.

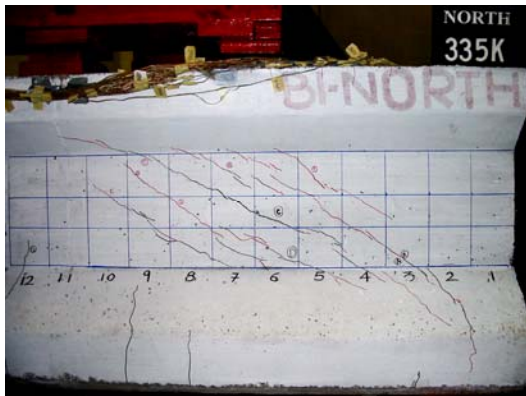
Fig. 5.3.11 to Fig. 5.3.17 shows the photographs of the crack patterns developed during loading of various beams and also shows the photographs of failed beam specimens.

**Table 5.3.5 Comparison of End Zone Crack Width of Various Beams Measured Using Hand Held Microscope**

<b>Beam (Mix)</b>	<b>Steel Fibers (% vol) (Type)</b>	<b>Transverse Steel (% vol)</b>	<b>Concrete Strength (ksi)</b>	<b>Number of Cracks</b>	<b>Maximum End Zone Crack Width at 90 Days after Casting (in.)</b>	<b>Maximum Crack Length (in.)</b>
<b>B1-North (TTC1)</b>	0	4.2	12.2	1	0.001	5
<b>B1-South (TTC1)</b>	0	1.0	12.2	1	0.001	10
<b>B2-North (TTFRC1)</b>	1 (SF)	1.0	10.3	1	0.001	12
<b>B2-South (TTFRC1)</b>	1 (SF)	0.42	10.3	3	0.003	11
<b>B3-North (TTFRC3)</b>	0.5 (LF)	1.0	11.2	<b>0</b>	<b>No Crack</b>	-
<b>B3-South (TTFRC3)</b>	0.5 (LF)	0.42	11.2	2	< 0.001	10
<b>B4-North (SCFRC1)</b>	0.5 (LF)	1.0	10.9	5	< 0.001	17
<b>B4-South (SCFRC1)</b>	0.5 (LF)	0.42	10.9	2	< 0.001	10
<b>B5-North (SCFRC3)</b>	1 (SF)	1.0	8.9	2	< 0.001	3
<b>B5-South (SCFRC3)</b>	1 (SF)	0.42	8.9	1	< 0.001	1.5
<b>B6-North (SCC2-3)</b>	0	4.2	10.6	9	0.005	25
<b>B6-South (SCC2-3)</b>	0	1.0	10.6	3	0.001	10
<b>B0-North (TTFRC4)</b>	1.5 (SF)	0	14.5	<b>0</b>	<b>No Crack</b>	-
<b>B0-South (TTFRC4)</b>	1.5 (SF)	0	14.5	<b>0</b>	<b>No Crack</b>	-

**NOTE:**

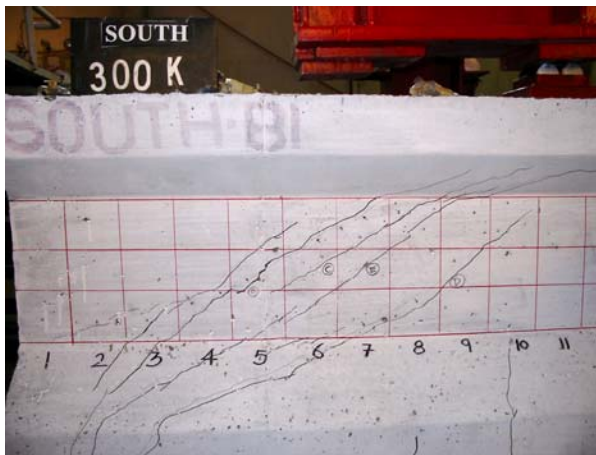
**TTC**-TxDOT Traditional Concrete Mix    **TTFRC**-TTC + Fibers Mix    **SCC** -Self-Consolidating Concrete Mix  
**SCFRC**- SCC + Fibers Mix    **SF**-Short Fiber ZP305    **LF**-Long Fiber RC80/60BN    **TS** - Transverse Steel



(a) Cracking of Beam B1-North End



(b) Flexure Failure of Beam B1-North End



(c) Cracking of Beam B1-South End



(d) Shear Failure of Beam B1-South End

**Fig. 5.3.11 Load Test Photographs of North and South Ends of Beam B1**



(a) Cracking of Beam B2-North End



(b) Shear Failure of Beam B2-North End

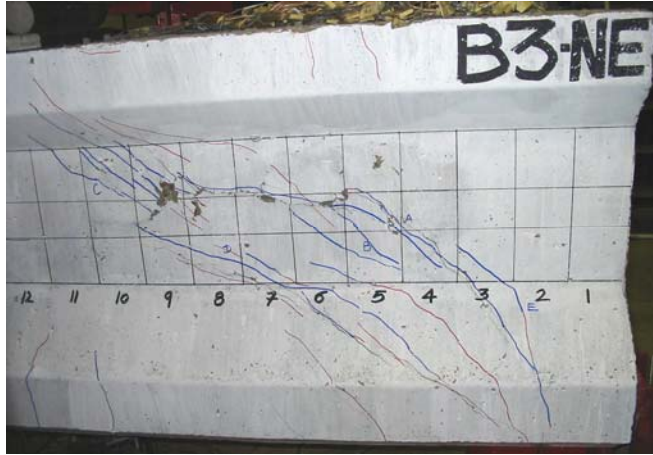


(a) Cracking of Beam B2-South End



(b) Shear Failure of Beam B2-South End

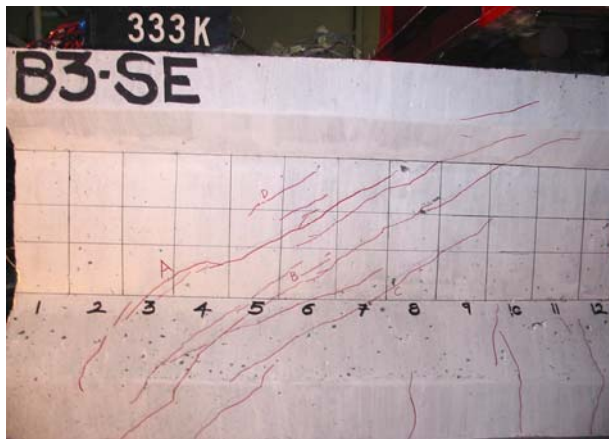
**Fig. 5.3.12 Load Test Photographs of North and South Ends of Beam B2**



(a) Cracking of Beam B3-North End



(b) Shear Failure of Beam B3-North End

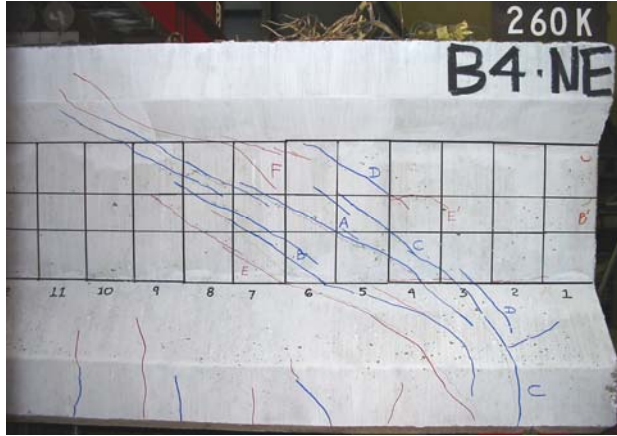


(a) Cracking of Beam B3-South End



(b) Shear Failure of Beam B3-South End

**Fig. 5.3.13 Load Test Photographs of North and South Ends of Beam B3**



(a) Cracking of Beam B4-North End



(b) Shear Failure of Beam B4-North End



(a) Cracking of Beam B4-South End



(b) Shear Failure of Beam B4-South End

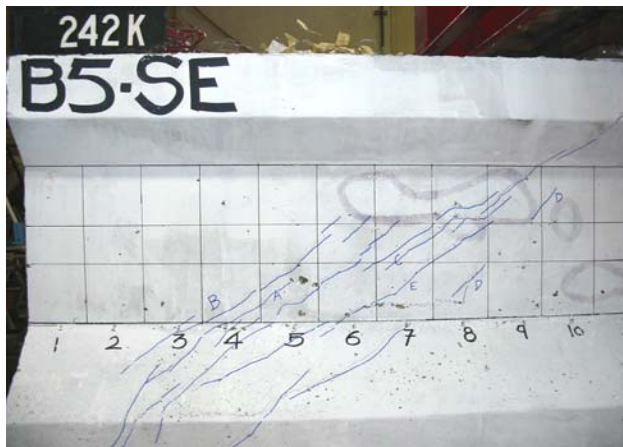
**Fig. 5.3.14 Load Test Photographs of North and South Ends of Beam B4**



(a) Cracking of Beam B5-North End



(b) Shear Failure of Beam B5-North End



(a) Cracking of Beam B5-South End



(b) Shear Failure of Beam B5-South End

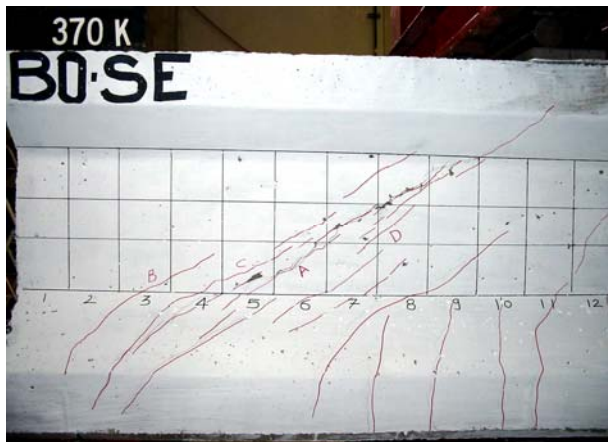
**Fig. 5.3.15 Load Test Photographs of North and South Ends of Beam B5**



(a) Cracking of Beam B0-North End



(b) Shear Failure of Beam B0-North End



(a) Cracking of Beam B0-South End



(b) Shear Failure of Beam B0-South End

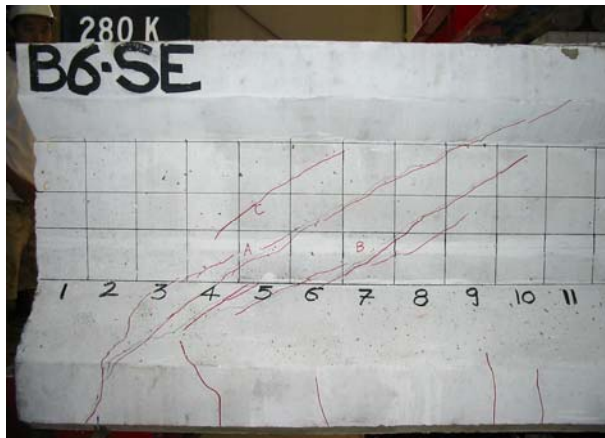
**Fig. 5.3.16 Load Test Photographs of North and South Ends of Beam B0**



(a) Cracking of Beam B6-North End



(b) Flexure Failure of Beam B6-North End



(a) Cracking of Beam B6-South End



(b) Shear Failure of Beam B6-South End

**Fig. 5.3.17 Load Test Photographs of North and South Ends of Beam B6**

### 5.3.6 Comparison of Experimental and Analytical Shear Capacities

Table 5.3.6 presents the comparison of the experimental shear capacities of beams B0 to B6 with analytical provisions. In this table, the code shear capacities contributed by concrete ( $V_c$ ) and steel ( $V_s$ ) are estimated by AASHTO LRFD 2000 and the ultimate shear strengths of fiber reinforced beams are calculated by the Fracture-Based Design method (Casanova *et al* 1997) for an average concrete strength ( $f'_c$ ) of 12 ksi. It can be seen that the experimental results are greater than the analytical capacities. It is also observed that beam B0–South end has the greatest shear capacity even though it has no transverse reinforcement. This indicates that steel fibers are very effective in resisting shear force.

**Table 5.3.6 Comparison of Theoretical and Experimental Shear Strengths**

<b>Beam</b> (Mix)	<b>Steel Fibers</b> (% vol) (Type)	<b>Transverse Steel</b> (%vol)	<b>Concrete Strength</b> (ksi)	<b>V<sub>c</sub></b> (kips)	<b>V<sub>s</sub></b> (kips)	<b>Theoretical Ultimate Shear Capacity</b> (kips)	<b>Experimental Ultimate Shear Capacity</b> (kips)
<b>B1-North</b> (TTC1)	0	4.2	12.2	124	336	460 <sup>#</sup>	-
<b>B1-South</b> (TTC1)	0	1.0	12.2	124	81	205 <sup>#</sup>	294
<b>B2-North</b> (TTFRC1)	1 (SF)	1.0	10.3	124	81	232 <sup>*</sup>	330
<b>B2-South</b> (TTFRC1)	1 (SF)	0.42	10.3	124	33	184 <sup>*</sup>	349
<b>B3-North</b> (TTFRC3)	0.5 (LF)	1.0	11.2	124	81	225 <sup>*</sup>	253
<b>B3-South</b> (TTFRC3)	0.5 (LF)	0.42	11.2	124	33	177 <sup>*</sup>	242
<b>B4-North</b> (SCFRC1)	0.5 (LF)	1.0	10.9	124	81	225 <sup>*</sup>	265
<b>B4-South</b> (SCFRC1)	0.5 (LF)	0.42	10.9	124	33	177 <sup>*</sup>	276
<b>B5-North</b> (SCFRC3)	1 (SF)	1.0	8.9	124	81	232 <sup>*</sup>	257
<b>B5-South</b> (SCFRC3)	1 (SF)	0.42	8.9	124	33	184 <sup>*</sup>	248
<b>B6-North</b> (SCC2-3)	0	4.2	10.6	124	336	460 <sup>#</sup>	-
<b>B6-South</b> (SCC2-3)	0	1.0	10.6	124	81	294 <sup>#</sup>	290
<b>B0-North</b> (TTFRC4)	1.5 (SF)	0	14.5	124	0	-	301
<b>B0-South</b> (TTFRC4)	1.5 (SF)	0	14.5	124	0	-	375

**NOTE:** **TTC**-TxDOT Traditional Concrete Mix    **TTFRC**-TTC + Fibers Mix    **SCC** - Self-Consolidating Concrete  
**SCFRC**- SCC + Fibers Mix    **SF** - Short Fiber ZP305    **LF** - Long Fiber RC80/60BN    **TS** -Transverse Steel  
**V<sub>c</sub>** – Concrete Shear Strength (AASHTO LRFD 2000)    **V<sub>s</sub>** – Steel Shear Strength (AASHTO LRFD 2000)

<sup>#</sup> – AASHTO LRFD 2000    \* - Casanova 1997

This page replaces an intentionally blank page in the original.

-- TxDOT Research Library Digitization Team

## CHAPTER 6

### CONCLUSIONS AND GUIDELINES

#### 6.1 Conclusions

The following conclusions can be drawn from this research work:

(1) TxDOT Traditional Fiber Reinforced Concrete (TTFRC) was developed in this research work. In general, all the TTFRC mixes had satisfactory workability and stability, suitable to be used in the casting of end zones of prestressed I-beams.

(2) Highly workable and stable Self-Consolidating Fiber Reinforced Concrete (SCFRC) can be made from locally available construction materials. Most of the workability tests for the SCFRC are easy to perform on site. The SCFRC mixes tested during this research had satisfactory workability and were found suitable for application to the end regions of I-beams.

(3) Preliminary test results of hardened properties of TTFRC and SCFRC mixes have confirmed the effectiveness of steel fibers in enhancing the tensile strength, flexural strength, and ductility of the concrete. The mechanical performance of SCFRC mixes was much better than that of the corresponding TTFRC mixes. On average, fibers increased the tensile strength of the concrete mix by about 50 % in case of SCFRC mixes and about 25 % in case of TTFRC mixes.

(4) Optimum fiber contents for SCFRC mixes to be used in casting the end regions of the I-beam were: 1 % by volume of short fibers (ZP305) and 0.5 % by volume of long fibers (RC80/60BN). The optimum fiber content was based on the workability requirements.

(5) Casting was relatively easy in the case of SCFRC mixes. The SCFRC mixes were highly workable without any signs of fiber blocking when placed in the beam form. SCFRC was observed to flow from one end of the beam to the other without losing its stability. The rate of casting for an SCFRC mix should be less than that for traditional concrete to avoid the formation of air-pockets in the beam. Another solution to avert the formation of air-pockets while casting SCFRC mixes is to completely eliminate the transverse reinforcement in the beam. This would not only facilitate the unrestricted filling of SCFRC in the beam, but also increase the workability performance of SCFRC.

(6) End zone cracking did not occur during the initial period of curing and prestress release. The end region cracks appeared in most of the beams about three months after casting. Hence, end zone cracking could be caused not only by the thermal and prestress forces, but also by the time-dependent secondary effects of shrinkage and temperature variation. Most of the TTFRC and SCFRC beams had end zone crack widths much smaller than the control traditional beam. Moreover, beam B0 with TTFRC4 mix (1.5 % by volume short fibers) had no end region cracks, even when the beam had absolutely zero traditional transverse steel reinforcement. Additionally, TTFRC3 mix with 0.5 % by volume of long steel fibers (RC80/60BN, fiber factor of 40) along with 1 % traditional transverse steel reinforcement was successful in averting the end zone cracking.

(7) Rebar strains measured by strain gauges in the end zones during the initial period of curing and release of prestress point out the advantageous utility of steel fibers in the end zone. Results show that steel fibers have considerably reduced the tensile strains (i.e. also the stresses) in the rebars during the initial stage of concrete curing and prestress release. This means that the steel fibers were able to take up the tensile stress developed in the concrete due to thermal and prestress loading, causing less tensile strains in the rebars.

(8) Temperature logger data revealed that the maximum thermal loading for the traditional beam was about 84 °F, much more than the conventionally known value given in literature of 60 °F. SCC produced more thermal loading (120 °F) due to a higher cement content. Hence, it is prudent to incorporate steel fibers in SCC mixes to counteract the enhanced thermal load in the matrix.

(9) Load tests of beams have shown that steel fibers were quite effective in increasing the shear strength, crack resistance, and ductility of the beams. The tests proved the ability of steel fibers to partially or completely replace traditional transverse steel reinforcement in the end region of the beams. Steel fibers were also helpful in increasing the flexural capacity of the beams. Most of the beams with steel fiber reinforced concrete were stiffer than the control beams with non-fibrous mix. Furthermore, steel fiber reinforced beams demonstrated higher ductility and energy absorption than the non-fibrous beams.

(10) Research findings of this project clearly show that the use of steel fibers in normal slump concrete and self-consolidating concrete are effective to replace the traditional transverse steel reinforcement, to control end zone cracking, to augment the shear strength, and to enhance

the ductility. The researchers would like to suggest for future research work the testing of 0.75 % (RC80/60BN, fiber factor of 60) instead of 0.5 % by volume of long steel fibers in the traditional concrete, which may result in complete elimination of the traditional transverse steel as well as the end zone cracks. The absence of transverse rebars in the beam would ensure ease of placement and better compaction of the TTFRC mix, thereby enhancing its workability and mechanical performance.

## **6.2 Guidelines**

The researchers have put forth the following tentative design guidelines for engineers to aid them in designing, producing, testing and casting satisfactory steel fiber reinforced concrete mixes for the application in the end zones of the prestressed concrete I-beams.

### **6.2.1 End Zone Crack Control**

Present research has found out that both TxDOT Traditional steel Fiber Reinforced Concrete (TTFRC) and Self-Consolidating Steel Fiber Reinforced Concrete (SCFRC) were successful in either the reduction or complete elimination of the end zone cracking in the prestressed concrete Type-A I-beam. TTFRC mix with satisfactory workability can be prepared by adding the required amount and type of steel fibers to the traditional TxDOT concrete mix, without modifying the prevalent mix design. Concrete mix proportions for TTFRC and SCFRC mixes can be selected from [Table 2.5.4](#) and [Table 2.5.5](#) of this report, respectively.

Based on the results of the experimental work in [Chapter 4](#) and [Chapter 5](#), the investigators advocate the use of TTFRC4 mix, i.e. TxDOT traditional concrete with 1.5 % by volume of short steel fibers (ZP305, fiber factor of 82.5), at the end regions of prestressed I-girders. TTFRC4 mix has the potential to completely eliminate the end zone cracks. Another option would be the use of TTFRC3 mix with 0.5 % by volume of long steel fibers (RC80/60BN, fiber factor of 40) along with 1 % traditional transverse steel reinforcement to avert the end zone cracking.

Present research work has revealed that the maximum amount of steel fibers that could be used in SCFRC mix is primarily governed by the workability criteria such as the stability and

passing ability of the mix. Based on their findings, the researchers would recommend the use of SCFRC3 mix with 1 % by volume of short steel fibers (ZP305, fiber factor of 55) in the end regions of the prestressed I-beams under the following conditions:

- (a) The traditional transverse steel reinforcement should be completely eliminated if SCFRC mix is to be used. The absence of traditional transverse steel reinforcement would provide an unrestricted space for the SCFRC mix to flow and fill more efficiently.
- (b) Rate of casting/delivering the SCFRC mix should be comparatively lower than that of the traditional concrete mix. Usually, the rate of casting a traditional TxDOT beam is 5 ft<sup>3</sup> of concrete per minute. The researchers suggest that this rate be about 3 ft<sup>3</sup> per minute for SCFRC mixes. Self-consolidation properties of SCFRC mix would be improved and occurrence of air pockets would be avoided if SCFRC mix were cast at a slower pace.

SCFRC3 mix with 1 % by volume of short steel fibers (ZP305, fiber factor of 55) might not be enough to eliminate the end zone cracks, but it would reduce the crack width to a minimum. It was found that steel fibers were more effective in controlling/eliminating the end zone cracks than the traditional transverse steel in the prestressed concrete I-beams.

### **6.2.2 Structural Performance of Beams**

Load testing of various TTFRC and SCFRC prestressed I-beams has proved the advantageous effects of steel fibers on the shear strength, flexural strength and ductility of the beams. Steel fibers were capable of changing the shear failure mode from brittle (traditional beam) to ductile (TTFRC and SCFRC beams). Based on these test results, the investigators advocate the use of TTFRC4 mix, i.e. TxDOT traditional concrete with 1.5 % by volume of short steel fibers (ZP305, fiber factor of 82.5), which would completely replace the traditional transverse steel in the prestressed concrete Type-A I-beam.

Another option recommended by the researchers considering the workability and structural performance of the mixes would be the use of SCFRC3 mix with 1 % by volume of

short steel fibers (ZP305, fiber factor of 55) along with 0.5 % of transverse steel reinforcement. Future tests may show that SCFRC mix with 1.5 % by volume of short steel fiber could completely replace the traditional transverse steel.

### **6.2.3 Overall Performance of Beams**

Considering the overall performance of the fiber reinforced concrete mixes such as the workability of the mix, ease of casting, potential to eliminate the end zone cracks and structural performance under loading, TTFRC4 mix, i.e. TxDOT traditional concrete with 1.5 % by volume of short steel fibers (ZP305, fiber factor of 82.5) used in Beam B0 is highly recommended. Being easy to cast, TTFRC4 mix has the potential to completely eliminate the end zone cracks and totally replace the traditional transverse shear reinforcement in the prestressed beam.

This page replaces an intentionally blank page in the original.

-- TxDOT Research Library Digitization Team

**Draft Specifications for Using  
TxDOT Traditional  
Fiber Reinforced Concrete  
in Prestressed Concrete Beams**

This page replaces an intentionally blank page in the original.

-- TxDOT Research Library Digitization Team

## Draft Specifications for Using TxDOT Traditional Fiber Reinforced Concrete in Prestressed Concrete Beams

Based on the research findings, the draft specifications for using TxDOT Traditional Fiber Reinforced Concrete (TTFRC) in prestressed concrete beams are presented as follows:

### 1 Materials for TTFRC

As shown below, traditionally available construction materials that are currently being used to manufacture the beams could be utilized to produce the TTFRC mixes.

Components	Description	Reference Code
<b>Portland Cement</b>	Type-III	ASTM C150
<b>Fly Ash</b>	Type-C	ASTM C618
<b>Coarse Aggregates</b>	$\frac{3}{4}$ in. Rounded River-bed gravel	AASHTO T 27
<b>Fine Aggregates</b>	FM = 2.55, Well Graded, River-bed	ASHTO M 43
<b>Superplastizer</b> Rheobuild1000	Type-F	ASTM- C494
<b>Retarder</b>	Type-B	ASTM- C494
<b>Steel Fibers</b> * Bekaert Dramix® * Hooked Ends 	<b>ZP305</b> Short Fiber ↓ L = 1.2 in., D = 0.022 in. L/D = 55	-

## 2 Optimized TTFRC Mixes and Mix Proportions

The optimized TTFRC mix that would be suitable to be used in the prestressed concrete beams is:

- (a) **TTFRC4** mix – TxDOT Traditional Fiber Reinforced Concrete with 1.5 % by volume short steel fibers (ZP305)

The mix proportions for the above-optimized TTFRC mixes are given below:

Component (lb/yd <sup>3</sup> )	Optimized Mix
	TTFRC4
<b>Cement</b>	519
<b>Fly ash</b>	248
<b>Cementitious materials</b>	767
<b>Water/Cement ratio (w/c)</b>	0.43
<b>Water/Cementitious ratio</b>	0.3
<b>Coarse aggregate (CA)</b>	1899
<b>Fine aggregate (FA)</b>	1156
<b>CA / FA ratio</b>	1.64
<b>Superplastizer (R)</b> (fl.oz./cwt)	9.6 (R) (20)
<b>Steel Fiber - RC80/60BN (% vol.)</b> Long Fiber	0
<b>Steel Fiber - ZP305 (% vol.)</b> Short Fiber	198 (1.5 %) <b>V<sub>f</sub> = 82.5</b>
<b>Retarder</b> (fl.oz./cwt)	1.0 (3)

**NOTE:** R = Rheobuild1000 Superplasticizer

V<sub>f</sub> = Fiber Factor = (Vol. of fiber) x (Aspect ratio of fiber)

### 3 **Mixing Procedure for TTFRC**

The mixing procedure for TTFRC mixes is as follows:

- a. Fine and coarse aggregates are first to be fed into the mixer-drum. Fibers in the form of bundles are to be added uniformly along with the fine and coarse aggregates.
- b. Cement and fly ash are then to be added to the aggregates inside the drum and initial dry mixing is to be carried out for 30 seconds.
- c. Premixed water with Superplastizer is then to be introduced into the mixture and mixed for another 120 seconds.

It is to be noted that the mixing procedures will be dependent on the producer's plant capabilities and mixer efficiency.

### 4 **Workability and Hardened Properties Tests for TTFRC**

Workability tests should be carried out, preferably near the mixer, to ascertain the satisfactory performance of TTFRC mix:

<b>Workability Test</b>	<b>Workability Parameter</b>	<b>Recommended Value</b>	<b>Reference Section in this Report</b>
<b>Slump Test</b> ASTM C143/C143-2003	Slump	7 to 8 inches	2.7

Hardened properties of TTFRC mix are to be determined in accordance with the **Section 2.9** of this research report. Most of the hardened properties tests for TTFRC mix are the same as those used for normal slump concrete and fiber reinforced concrete.

### 5 **Casting Technique for TTFRC Mix**

Traditional concrete casting tools and equipment can be used to cast TTFRC mixes. TTFRC mixes can be easily transported from the mixer and delivered into the beam form by means of a conventionally used mobile-hopper. External mechanical vibration is required for TTFRC mixes similar to the traditional normal-slump concrete. TTFRC mixes can be cast at the same rate as the traditional normal-slump concrete, i.e. about 5 ft<sup>3</sup> per minute. The traditional

transverse steel reinforcement in the beam should preferably be eliminated or reduced if TTFRC mix is to be used. The absence of traditional transverse steel reinforcement would provide an unrestricted space for the TTFRC mix to compact more efficiently with comparatively less compaction energy.

The above specifications would be helpful in producing, testing and casting satisfactory TxDOT Traditional Fiber Reinforced Concrete (TTFRC) for its application in the prestressed concrete beams.

**Draft Specifications for Using  
Self-Consolidating  
Fiber Reinforced Concrete  
in Prestressed Concrete Beams**

This page replaces an intentionally blank page in the original.

-- TxDOT Research Library Digitization Team

## Draft Specifications for Using Self-Consolidating Fiber Reinforced Concrete in Prestressed Concrete Beams

Based on the research findings, the draft specifications for using Self-Consolidating Fiber Reinforced Concrete (SCFRC) in prestressed concrete beams are presented as follows:

### 1. Materials for SCFRC

As shown below, traditionally available construction materials that are currently being used to manufacture the beams could be utilized to produce the SCFRC mixes.

Components	Description	Reference Code
<b>Portland Cement</b>	Type-III	ASTM C150
<b>Fly Ash</b>	Type-C	ASTM C618
<b>Coarse Aggregates</b>	$\frac{3}{4}$ in. Rounded River-bed gravel	AASHTO T-27
<b>Fine Aggregates</b>	FM = 2.55, Well Graded, River-bed	ASHTO M 43
<b>Superplasticizer/HRWR</b> Glenium3200HES	Type-F (Polycarboxylate based)	ASTM - C494
<b>Retarder</b>	Type-B	ASTM - C494
<b>Steel Fibers</b> * Bekaert Dramix® * Hooked Ends 	<b>ZP305</b> Short Fiber ↓ L = 1.2 in., D = 0.022 in. L/D = 55	-

## 2 Optimized SCFRC Mixes and Mix Proportions

The optimized SCFRC mix that would be suitable to be used in the prestressed concrete beams is:

- (a) **SCFRC3** mix – Self-Consolidating Fiber Reinforced Concrete with 1.0 % by volume short steel fibers (ZP305)

The mix proportions for the above-optimized SCFRC mixes are given below:

Component  (lb/yd <sup>3</sup> )	Optimized Mix
	SCFRC3
<b>Cement</b>	587
<b>Fly ash</b>	250
<b>Cementitious materials</b>	837
<b>Water/Cement ratio (w/c)</b>	0.43
<b>Water/Cementitious ratio</b>	0.3
<b>Coarse aggregate (CA)</b>	1540
<b>Fine aggregate (FA)</b>	1580
<b>CA / FA ratio</b>	0.97
<b>HRWR / Superplastizer (GL)</b> (fl.oz./cwt)	10.5 (20)
<b>Steel Fiber - RC 80/60 BN (% vol.)</b> Long Fiber	0
<b>Steel Fiber - ZP305 (% vol.)</b> Short Fiber	132 (1 %) $V_f = 55$
<b>Retarder</b> (fl.oz./cwt)	1.6 (4.4)

**NOTE:** GL = Glenium 3200 HES Superplasticizer

$V_f$  = Fiber Factor = (Vol. of fiber) x (Aspect ratio of fiber)

### 3 **Mixing Procedure for SCFRC**

The mixing procedure for SCFRC mixes is as follows:

- a. Fine and coarse aggregates are first to be fed into the mixer-drum. Fibers in the form of bundles are to be added uniformly along with the fine and coarse aggregates.
- b. Cement and fly ash are then to be added to the aggregates inside the drum and initial dry mixing is to be carried out for 30 seconds.
- c. Premixed water with HRWR is then to be introduced into the mixture and mixed for another 120 seconds.

It is to be noted that the mixing procedures will be dependent on the producer's plant capabilities and mixer efficiency. SCC/SCFRC is sensitive to mixing procedure, time of mixing and type of mixer.

### 4 **Workability and Hardened Properties Tests for SCFRC**

Workability tests should be carried out, preferably near the mixer, to ascertain the satisfactory performance of SCFRC mix:

<b>Workability Test</b>	<b>Workability Parameter</b>	<b>Recommended Value</b>	<b>Reference Section in this Report</b>
<b>Slump Flow Test</b>	Flowability	> 25 inches	2.3 (a)
<b>Visual Stability Index (VSI) Rating</b>	Stability	'Zero' Rating	2.3 (a)
<b>T-20in Time</b>	Filling Ability	3 to 7 seconds	2.3 (a)
<b>J-ring Value</b>	Passing Ability	< 3 inches	2.3 (b)

Hardened properties of SCFRC mix are to be determined in accordance with the **Section 2.9** of this research report. Most of the hardened properties tests for SCFRC mix are the same as those used for normal slump concrete and fiber reinforced concrete.

## **5 Casting Technique for SCFRC Mix**

Traditional concrete casting tools and equipment can be used to cast SCFRC mixes. SCFRC mixes can be easily transported from the mixer and delivered into the beam form by means of a conventionally used mobile-hopper. External mechanical vibration is not required for SCFRC mixes.

Following measures should be taken while casting SCFRC mixes:

- (a) Rate of casting should not be more than 3 ft<sup>3</sup> per minute for SCFRC mixes to enhance its restricted filling ability. Self-consolidation properties of SCFRC mix would be improved and occurrence of air pockets would be avoided if SCFRC mix is cast at a slower pace.
- (b) The traditional transverse steel reinforcement in the beam should preferably be eliminated if SCFRC mix is to be used. The absence of traditional transverse steel reinforcement would provide an unrestricted space for the SCFRC mix to flow and fill more efficiently. Hence, self-consolidation of SCFRC mix would best be achieved by complete elimination of the traditional transverse steel reinforcement.

The above specifications would be helpful in producing, testing and casting satisfactory Self-Consolidating Fiber Reinforced Concrete (SCFRC) for its application in the prestressed concrete beams.

## References

AASHTO LRFD (2000), American Association of State Highway Transportation Officials “Bridge Design Specifications-U.S. Units,” Washington D.C.

AASHTO T27 (1996), American Association of State Highway Transportation Officials “Sieve Analysis of Fine and Coarse Aggregates,” Washington D.C.

AASHTO M43 (1998), American Association of State Highway Transportation Officials “Sizes of Aggregates for Road and Bridge Construction,” Washington D.C.

ACI 318-95 (1996), “Building Code Requirements for Structural Concrete,” American Concrete Institute, Farmington Hills, Michigan.

ACI 544.1R (1996), “State-of-the-Art Report on Fiber Reinforced Concrete,” American Concrete Institute, Farmington Hills, Michigan.

Akihiro, H., Kida, T., Tamaki, T., and Hagiwara, H. (1998), “Study on Self-Compacting Concrete with Expansive Adhesive,” International Workshop on Self-Compacting Concrete, pp 218-227.

Ambroise, J., Rols, S., and Pera, J. (2001), “Properties of Self-Levelling Concrete Reinforced by Steel Fibers,” IBRACON, Brazilian Concrete Institute, Brazil.

Ashour, S.A., Hasanain, G.S., and Wafa, F.F. (1992), “Shear Behavior of High-Strength Fiber Reinforced Concrete Beams,” ACI Structural Journal, Vol. 89, No. 2, pp 176-184.

ASTM C1399 (1999), “Test Methods for Obtaining Average Residual Strength of Fiber-Reinforced Concrete,” Annual Book of American Standards for Testing of Materials, Vol. 04.02, ASTM International, West Conshohocken, PA, USA.

ASTM C496 (1996), “Standard Test Method for Splitting Tensile Strength of Cylindrical Concrete Specimens,” ASTM International, West Conshohocken, PA, USA.

ASTM C494/C494M (1999), “Standard Specification for Chemical Admixtures for Concrete,” ASTM International, West Conshohocken, PA, USA.

ASTM C150 (2002), “Standard Specification for Portland Cement,” ASTM International, West Conshohocken, PA, USA.

ASTM C78 (2002), “Standard Test Method for Flexural Strength of Concrete (Using Simple Beam with Third-Point Loading),” ASTM International, West Conshohocken, PA, USA.

ASTM C469 (2002), “Standard Test Method for Static Modulus of Elasticity and Poisson’s Ratio of Concrete in Compression,” ASTM International, West Conshohocken, PA, USA.

ASTM C618 (2003), “Standard Specification for Coal Fly Ash and Raw or Calcined Natural Pozzolan for Use as a Mineral Admixture in Concrete,” ASTM International, West Conshohocken, PA, USA.

ASTM C39/39M (2003), “Standard Test Method for Compressive Strength of Cylindrical Concrete Specimens,” ASTM International, West Conshohocken, PA, USA.

ASTM C143/143M (2003), “Standard Test Method for Slump of Hydraulic Cement Concrete,” ASTM International, West Conshohocken, PA, USA.

Barr, B. (1987), “Fracture Characteristics of FRC Materials in Shear,” Fiber Reinforced Concrete Properties and Applications, ACI SP-105, American Concrete Institute, Farmington Hills, Michigan.

Beaudoin, J.J. (1990), “Handbook of Fiber Reinforced Concrete. Principles, Properties, Developments and Applications,” Noyes Publications, Park Ridge, NJ, pp 332.

Breen, J.E., Burdet, O., Roberts, C., Sanders, D., and Wollmann G. (1994), “Anchorage Zone Reinforcement for Post-Tensioned Concrete Girders,” National Cooperative Highway Research Program Report 356, Washington D.C.

Bury, M.A., and Buhler, E. (2002), “Methods and Techniques for Placing Self-Consolidating Concrete – An Overview of Field Experiences in North American Applications,” Proceedings, First North American Conference on the Design and Use of Self-Consolidating Concrete, Rosemont, Illinois, USA.

Casanova, P. (1996), “Betrans renforces de fibres metalliques du materiau a la structure,” PhD thesis, Laboratoire Central de Ponts et Chaussees, Paris (in French).

Casanova, P., Rossi, P., and Schaller, I. (1997), “Can Steel Fibers Replace Transverse Reinforcements in Reinforced Concrete Beams?” ACI Materials Journal, Vol. 94, No. 5, pp 341-354.

Daczko, J.A. (2002), “Stability of Self-Consolidating Concrete, Assumed or Ensured?” Proceedings, First North American Conference on the Design and Use of Self-Consolidating Concrete, Rosemont, Illinois, USA.

Dixon, J., and Mayfield, B. (1971), "Concrete Reinforced with Fibrous Wire," *Journal of the Concrete Society, Concrete*, Vol. 5, No. 3, pp 73-76.

Earney, T.P. (2000), "Cracking in Prestressed I-Girder Bridges," Master's Thesis, University of Missouri – Columbia.

Edamatsu, Y., Kobayashi, T., and Nagaoka, S. (1997), "Influence of Powder Properties on Self-Compactibility of Fresh Concrete," *JCA Proceedings of Cement and Concrete*, No. 51, pp 394-399 (in Japanese).

EFNARC, (2002), "Specification and Guidelines for Self-Compacting Concrete," European Federation for Specialist Construction Chemicals and Concrete Systems, Surrey, UK.

Fenves, G. L. (2001). Annual workshop on Open System for earthquake engineering Simulation. Pacific Earthquake Engineering Research Center, UC Berkeley, California, USA.

Gaimster, R., and Foord, C. (2000), "Self-compacting concrete," *Concrete*, 34, pp 23-25.

Gopalaratnam, V.S., and Shah, S. (1987), "Failure Mechanisms and Fracture of Fiber Reinforced Concrete," *Fiber Reinforced Concrete – Properties and Applications*, SP 105, ACI, Detroit, Michigan, pp 1-25.

Gopalaratnam, V.S., Earney, T.P., Myers, J., Nani, A., and Stone, D. (2001), "Precast I-Girder Cracking: Phase II - Causes and Design Details," Missouri Department of Transportation Report No RDT 01-008.

Grünewald, S., and Walraven, J.C. (2001), "Parameter-Study on the Influence of Steel Fibers and Coarse Aggregate Content on the Fresh Properties of Self-Compacting Concrete," *Cement and Concrete Research*, 31, pp 1793-1798.

Grzybowski, M. (1989), "Determination of Crack Arresting Properties of Fiber Reinforced Cementitious Composites," Chapter 12, Royal Institute of Technology, Stockholm, Sweden.

Grzybowski, M., and Shah, S.P. (1990), "Shrinkage Cracking in Fiber Reinforced Concrete," *ACI Materials Journal*, Vol. 87, No2, pp 138-148.

Hannant, D.J. (1978), "Fiber Cements and Fiber Concrete," John Wiley and Sons Ltd., Chichester, UK, pp 53.

Hoff, G. (1987), "Durability of Fiber Reinforced Concrete in a Severe Marine Environment," *Fiber Reinforced Concrete Properties and Applications*, SP-105, ACI, Detroit, Michigan, pp 997-1041.

Holschemacher, K., and Klug, Y. (2002), "A Database for the Evaluation of Hardened Properties of SCC," LACER, No. 7, pp. 123-134.

Imam, M. (1995), "Shear-moment Interaction of Steel Fiber High Strength Concrete," PhD thesis, Katholieke Universiteit Leuven, Leuven, Belgium.

Johnston, C.D. (1974), "Steel Fiber Reinforced Mortar and Concrete – A Review of Mechanical Properties," Fiber Reinforced Concrete, SP-44, ACI, Detroit, Michigan, pp 127-142.

Johnston, C.D. (1980), "Properties of Steel Fiber Reinforced Mortar and Concrete – A Review of Mechanical Properties," Proceedings, International Symposium on Fibrous Concrete (C1-80), Construction Press, Lancaster, pp 29-47.

Johnston, C.D. (1989), "Effect on Flexural Performance of Sawing Plain Concrete and of Sawing and Other Methods of Altering Fiber Alignment in Fiber Reinforced Concrete," Cement, Concrete and Aggregate, ASTM, CCAGDP, Vol. 11, No. 1, pp 23-29.

JSCE Research Subcommittee on Self-Compacting Concrete (1998), "Recommendation for Construction of Self-Compacting Concrete," Japan Society of Civil Engineers (in Japanese), Japan.

Khayat, K.H., Manai, K., and Trudel, A (1997), "In-Situ Mechanical Properties of Wall Elements Cast Using Self-Consolidating Concrete," ACI Materials Journal, 94(6), pp 491-500.

Khayat, K.H., Hu, C., and Monty, H. (1999), "Stability of Self-Consolidating Concrete, Advantages, and Potential Applications," Proceedings of First International RILEM Symposium on Self-Compacting Concrete, Stockholm, Sweden, pp 143-152.

Naaman, A.E. (1985), "Fiber Reinforcement for Concrete," Concrete International: Design and Construction, Vol. 7, No. 3, pp 21-25.

Narayanan, R., and Darwish, I. (1987), "Use of Steel Fibers as Shear Reinforcement", ACI Structural Journal, Vol. 84, No. 3, pp 216-277.

Nawa, T., Eguchi, H., and Fukaya, Y. (1989), "Effect of Alkali Sulfate on the Rheological Behavior of Cement Paste Containing a Superplasticizer," ACI SP-119, pp 405-424.

Nawa, T. et al.(1993), "A Study on the Super Workable, High Strength Concrete with Belite Rich Cement," Proceedings of the Japan Concrete Institute, Vol. 15, No. 1, pp 143-148 (in Japanese).

Noghabai, K. (1998), "Effect of Tensioning Softening on the Performance of Concrete Structures: Experimental, Computational and Analytical Studies," PhD thesis, Lulea University of Technology, Lulea, Sweden.

Noghabai, K. (2000), "Beams of Fibrous Concrete in Shear and Bending: Experiment and Model," *Journal of Structural Engineering*, ASCE, Vol. 126, No. 2, pp 243-251.

Oh, S.G., Noguchi, T., and Tomosawa, F. (1999), "Evaluation of Rheological Constants of High-Fluidity Concrete by Using the Thickness of Excess Paste," *Journal of the Society of Materials Science*, Aug., Japan.

Okamura, H., and Ozawa, K. (1995), "Mix-Design for Self-Compacting Concrete," *Concrete Library of the Japanese Society of Civil Engineers*, pp 107-120.

Padmarajaiah, S.K., and Ramaswamy, A. (2002), "Comparative Study on Flexural Response of Full and Partial Depth Fiber-Reinforced High-Strength Concrete," *Journal of Materials in Civil Engineering*, Vol. 14, No. 2, pp 130-136.

PCI (1999), "PCI Design Handbook," *Precast/Prestressed Concrete Institute*, 5<sup>th</sup> Edition, Chicago, Illinois.

PCI, TR-6-03 (2003), "Interim Guidelines for the Use of Self-Consolidating Concrete in Precast/Prestressed Concrete Institute Member Plants," *Precast/Prestressed Concrete Institute*, Chicago, Illinois.

Petersson, O. (1998), "SCC Task 9 Research Report," *Swedish Cement and Concrete Research Institute*, Stockholm, Sweden.

Rapoport, J., Aldea, C., Shah, S.P., Ankenman, B., and Karr, A.F. (2001), "Permeability of Cracked Steel Fiber-Reinforced Concrete," *Technical Report No. 115*, National Institute of Statistical Sciences (NISS), Research Triangle Park, NC, USA.

Romualdi, J.P., and Batson, G.B. (1963), "Mechanics of Crack Arrest in Concrete," *Journal of Engineering Mechanics Division*, ASCE, Vol. 89, No. EM3, pp 147-168.

Schupack, M. (1985), "Durability of Steel Fiber Reinforced Concrete Exposed to Severe Environments," *Steel Fiber Concrete*, US-Sweden Joint Seminar (NSF-STU), Stockholm, Sweden

Shah, S.P. (1991), "Do Fibers Increase the Tensile Strength of Cement-Based Matrixes?," *ACI Materials Journal*, Vol. 88, No. 6, pp 595-602.

Snyder, M.L., and Lankard, D.R. (1972), "Factors Affecting the Strength of Steel Fibrous Concrete," *ACI Journal Proceedings*, Vol. 69, No. 2, pp 96-100.

Sonebi, M., and Bartos, P.J.M. (2002), "Filling Ability and Plastic Settlement of Self-Compacting Concrete," *Materials and Structures*, 35 (252), pp 462-469.

Toyoharu, N., Tatsuo, I., and Yoshinobu, E. (1998), "State-of-the-art Report on Materials and Design of Self-Compacting Concrete," *International Workshop on Self-Compacting Concrete*, Japan, pp 160-189.

Waterhouse, B.L., and Luke, C.E. (1972), "Steel Fiber Optimization," *Conference Proceedings M-28, Fibrous Concrete – Construction Materials for the Seventies*, pp 630-681.

Williamson, G.R. (1974), "The Effect of Steel Fibers on Compressive Strength of Concrete," *Fiber Reinforced Concrete, SP-44*, ACI, Detroit, Michigan, pp 195-207.

Williamson, G.R. (1978), "Steel Fibers as Reinforcement in Reinforced Concrete," *Proceedings, US Army Science Conference, West Point, Vol. 3*, pp 363-377.

Zhong, J. (2005). "Model-Based Simulation of Reinforced-Concrete Plane Stress Structures," Ph.D. Dissertation, Department of Civil and Environmental Engineering, University of Houston, Houston, TX.